EFFECT OF BEARING CONSTRAINTS ON THE WHIRLING CHARACTERISTICS OF A MULTI-ROTOR SYSTEM.

by

R.BOSWORTH Dip.Tech.(Hons.) G.I.Mech.E.

Submitted in fulfilment of the requirements for the degree of Doctor of Philosophy.

University of Aston in Birmingham.

October, 1966.

Faculty of Engineering.
Dept. of Mech. Eng.

Head of Department,
Prof. A.C. Walshaw.

Supervisor,
Prof. E. Downham.

Synopsis.

The thesis describes an investigation of the behaviour of a symmetrical two-rotor shaft system supported in journal bearings. The rotors are of appreciable diametral inertia and overhung from the bearings. Oil is gravity fed to the bearings from a header tank.

The thesis is divided into two parts.

Part one describes a phenomenon in which the system exhibits sub-shaft speed resonances while part two describes a phenomenon in which the system becomes unstable and whirls in contact with the bearings, at half the shaft rotational speed.

To the authors knowledge these phenomena have not been reported previously.

The source of the phenomenon of sub-shaft speed resonances is attributed to a rubber flexible drive coupling. Treating the coupling as a non-linear spring, a theory is propounded which explains the shaft behaviour. Agreement between theory and experiment is quite good.

The phenomenon of the unstable half shaft rotational speed motion described in part two is also attributed, though indirectly to the drive coupling. The coupling causes the rotors to move in antiphase so that gyroscopic couples, arising out of this

movement, are able to control the shaft motion. The appearance of instability is given because the amplitude of the motion is beyond that limited by the bearings. Neglecting external forces, a theory is propounded which, provided the lubricant viscosity is known accurately, predicts the shaft speed at the onset of "instability".

Acknowledgements

The author wishes to express his gratitude and appreciation to

Prof. A.C. Walshaw who allowed the work to be carried out in the department of Mechanical Engineering at the University of Aston.

Prof. E. Downham for his assistance and guidance.

The numerous Technicians who helped in building the experimental rig.

Also he wishes to thank his wife who typed the thesis.

Introduction.

Vibrations in rotating machinery have attracted the interest of research workers since the middle of the last century. Although many vibration characteristics have been satisfactorily explained, the increased complexity and increase in running speed has given rise to additional phenomena which require further investigation. It has not been uncommon for machines which have been tested and approved in the manufactures development laboratory to have failed due to fatigue produced by some vibration phenemonon not encountered under test, when put into service.

An insight into the behaviour of rotating machinery can, to some extent, be obtained from models. A vast amount of experimental work has been so performed to obtain an understanding of the basic principles involved in the vibration of rotating shafts and empirical and theoretical formulae have been developed to predict the occurence of some vibration phenomenon. Usually these formulae can seldon predict the behaviour of full scale systems with the same degree of accuracy. This is to be expected, because in a model the physical significance of some properties in the full size system e.g. friction, due to relative movement between parts and hystersis, flexibility of bearing and bearing structure, coupling effects etc. can be so reduced as to

have a negligible effect on the vibration characteristics of the model. Troubles can arise particularly in the case of two machines being coupled, e.g. a diesel-electric set, when each machine is tested separately. It is practically impossible to subject one machine to the same type of loading it incurs when coupled to another

A large proportion of rotors are supported in journal bearings lubricated with oil. Recent investigations by other workers have shown that forces generated within the bearing, due to the inherent build up of an oil film are capable of producing a condition of instability. These oil forces are complex insomuch as they can be expressed by a summation of non-linear displacement and velocity dependent terms and analytical and experimental work has been carried out to determine their role in shaft vibrations. Most of the experimental work has been performed on models and little work has been carried out on full scale rigs. Consequently the results have been of limited value to manufacturers.

This thesis describes the work carried out in an investigation of the vibration characteristics of a two-rotor shaft system supported in two journal bearings. The system is analogous to the rotor of a turbo-charger with the exception that the rotor blade-hub assemblies have been represented by two symmetrical disks. The disks are overhung from the bearings and of appreciable

diametral inertia so that the shaft experiences gyroscopic couples when rotating.

A turbo-charger experiences an appreciable temperature difference between the compressor and turbine stages. This anomaly has been neglected in the investigation although its effect is commented on. Also no external stimulas has been applied to the disks i.e. gas force excitation has been neglected.

Table of Contents.

Table of Contents (Contd.)

Table of Contents(contd.)

Historical and Technical Review

The literature on the vibrations of rotating shafts is extensive and to present a historical and technical review of all the literature would be a major undertaking. The historical and technical review presented here is a review of the more important papers, relevant to the investigation. The review is composed of five sections viz.

1. Synchronous Whirl Produced by Out-of-Balance Forces.
2. Non-Synchronous Whirl Produced by Out-of-Balance Forces.
3. Effect of Gyroscopic Couples on the Motion of a Rotating Shaft.
4. Effect of Friction Forces on the Motion of a Rotating Shaft.
5. Effect of Oil-Film-Forces on a Rotating Shaft.

and is written with the intention that each section follows on from the previous one. Because of this writers mentioned are not neccessarily in chronological order. Also, some sections contain parts which, strictly speaking do not belong there, but, are put in to clarify a statement and to provide continuity.

1. Synchronous Whirl Produced by Out-of-Balance Forces.

The first rational explanation of the vibration of a rotating shaft subjected to an unbalance force was given in a paper by Jeffcott(1) published in 1919. Previous to this workers in this field, notably Greenhill, (2) Chree (3) and Dunkerley(4) had based their arguments on fallacious reasoning. Jeffcott's theory showed that the critical whirling speed of a shaft carrying a single rotor subject to unbalance, arose when the rotational speed coincided with the natural vibratory frequency of

the system and a perfectly balanced shaft could not whirl. That this state of affairs was not understood was evident from the following quotation from a paper by Chree"---- whirling is not really a case of coincidence of period between a vibrating system and disturbing forces----". Morris (5) extended the work of Jeffcott to more complex systems and showed that critical whirling speeds arose when the rotating speeds coincided with the natural vibratory frequencies of the rotating system. The emphasis here being on "natural vibratory frequencies of the rotating system", for if a shaft carried disks (rotors) of appreciable inertia the natural vibratory frequencies would be lower than the natural vibratory frequencies of the rotating system. The difference is produced by the gyroscopic couples (arising only when the shaft rotates) tending to stiffen the shaft.

It is unfortunate that for the simpler cases of shaft whirling (negligible rotor inertia and symmetric stiffness etc.) the critical whirling speeds occur at the same frequency as the natural vibratory frequency of the system.

The works of Dunkerley, Chree etc. all arrived at this conclusion and conseqently the calculated critical whirling speeds were numerically correct.

In 1894, Dunkerley reported his classical experiments. In order to cope with a pulley mounted on a

heavy shaft Dunkerley first calculated the critical speed for the loaded shaft, in which the mass of the shaft itself was neglected. Calling the frequency thus obtained N_2 and that found for the unloaded shaft N_1, Dunkerley deduced a final value N for the frequency of the complete system from the equation

$$\frac{1}{N^2} = \frac{1}{N_1^2} + \frac{1}{N_2^2}$$

which is an empirical method still widely used at present. It can be shown by extending Jeffcott's theory to include a shaft carrying more than one load, say two, that the frequency obtained by Dunkerley's empirical formula for the two loads in combination is lower than either of the two actual frequencies of the system.

Downham (6) in 1957 carried out extensive experimental work using a cantilever shaft carrying a rotor of appreciable inertia supported in a symmetric and asymmetric flexible bearing. Using theory based on that of Jeffcott and extended by Morris, Downham obtained good correlation with experimental results. Also he showed that with an asymmetric flexible bearing the shaft would, when running at speeds between the two critical speeds (the two critical whirling speeds arising because of the different support stiffness in the horizontal and vertical directions) whirl in a reverse direction to that of rotation and at rotational speed. Hull (7) using a similar apparatus

as Downham investigated the phase-angle relationship of an unbalanced shaft-rotor system supported in an asymmetric bearing. He consluded that to fulfill the neccessary phase-angle requirements, the shaft would either whirl in a forward direction at a third shaft speed or in a backward direction at shaft speed, when running at speeds between the two critical whirling speeds. Neither Downham nor Tull observed a forward whirl when the shaft ran at these speeds. It is interesting to note here that a sub-shaft speed forward whirl is theoretically possible.

2. Non-synchronous Whirl Produced by Out-of-Balance Forces.

In 1933 Baker (8) explained how a shaft subjected to unbalance forces can whirl at a frequency which is exactly half or third shaft speed. By sufficiently good rotor balancing this phenomenon could be corrected for. Tudeke (9) performed work using an electromechanical analogue to study the phenomenon of sub-harmonic resonance showed that sub-harmonic resonances could be generated by an unbalance force acting on a non-linear spring. The order of the sub-harmonics depended on the non-linear spring characteristics.

Unlike the effect obtained by Baker which, as already mentioned could be corrected for by good balancing, Tudeke showed that the generation of sub-harmonic resonances could only be eliminated by perfect balancing.

The theory propounded by Ludeke was based on a small out of balance force exciting a non-linear system and therefore could have a practical application to rotating shafts supported in flexible bearings and /or driven from a flexible coupling. The "jump" phenomenon, described by Stoker,(10) which is characteristic of all non-linear systems was also apparent with the generation of sub-harmonics, see Fig 1. Ludeke pointed out that because of the unstable condition during a "jump" the frequency of vibration e.g. of a shaft, may jump from that of shaft speed to third shaft speed i.e. omit the sub-harmonic resonance of order half.

3. Effect of Gyroscopic Couples on the Motion of a Rotating Shaft.

The gyroscopic effects on shaft whirling have been recognised for many years. Stodola (11) described both forward and backward synchronous precession. Den Hartog (12) indicated possible nonsynchronous precessions and Green (13) in a paper titled "Gyroscopic Effects on the Critical Speeds of Flexible Rotor" published in 1948 showed theoretically that a shaft carrying a thin balanced disk was capable of nonsynchronous presession. The operative word being precession, for Jeffcott had shown that a perfectly balanced shaft was not capable of whirling. Schulte and Riester (14) observed both forward and backward whirl in tests carried

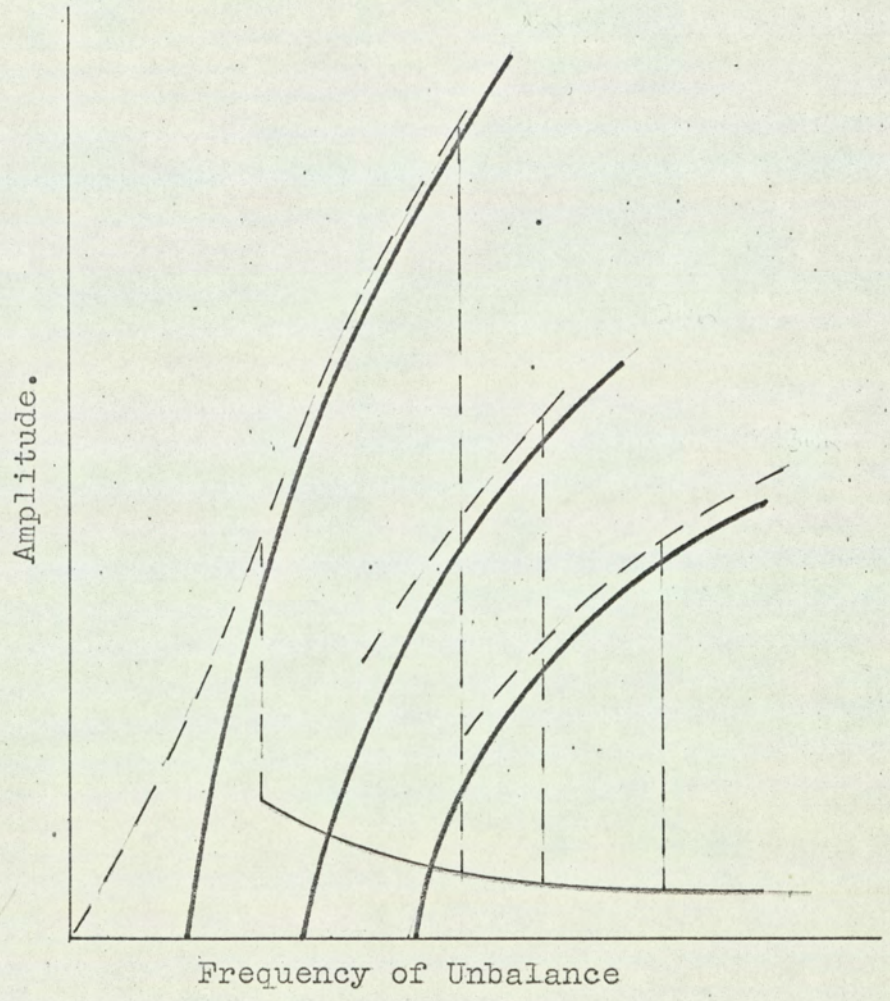

A Diagram of Subharmonic Transitions by Ludeke.

FIG.1

out with a shaft supported in two bearings and carrying a rotor overhung from the bearings. They investigated the effect of mass distribution and used rotors which

1. the diametral inertia was less than the polar inertia.
2. the diametral inertia was equal to the polar inertia.
3. the diametral inertia was greater than the polar inertia.

and in all cases observed the resonant condition for forward synchronous whirl but only in six tests out of the nine tests performed did they detect the backward synchronous whirl. The only exciting force used to promote the resonant conditions was that due to unbalance.

4. Effect of Friction Forces on the Motion of a Rotating Shaft.

In 1924 Kimball (15) described a phenomenon in which a shaft whirled at its natural frequency whilst running at speeds greater than this. He ascribed this phenomenon to the internal friction forces of the shaft set up by the hysteretic behaviour of the shaft material.

Kimball thought of hysteresis as a viscous action, and gave a mathematical theory based on the assumption that it followed the viscous law. However, when he performed tests to measure internal friction he showed that

this assumption was hopelessly wrong. A quote from Kimball's (16) paper reads as follows"----. It is a remarkable fact that the internal friction is nearly independent of the speed of rotation, contrary to the very common assumption that internal friction in metals is proportional to velocity of strain, like fluid friction.----" It is unfortunate that many writers today choose to ignore this evidence, and still treat friction forces as being viscous in nature. Robertson(17) gives a full explanation of this phenomenon in a paper titled "Hysteretic Influences on the Whirling of Rotors". He showed how a transient vibreation in a rotating shaft would be sustained by hysteretic forces, if of sufficient magnitude, when the shaft was running above its critical speed and damped out if the shaft was running below its critical speed. Robertson included friction forces between components of the system e.g. a disk shrunk onto a shaft, as well as internal friction forces, in his definition of hysteretic forces. Newkirk (18) showed that friction forces(produced by relative movement between components of a system) were more likely to produce a sustained transient whirl than internal friction forces as they were usually much greater in magnitude. Downham (19) produced evidence in favour of Newkirk's work when he observed this phenomenon whilst driving a cantilever shaft through a split collet. When the shaft was given a

slight disturbance, friction forces, produced by relative movement between the shaft and the collect, were sufficient to drive a transient whirl into a steady whirl. Downham also noted that the instability was a function of the magnitude of the disturbing force i.e. the initial amplitude of the shaft disturbance; this was also in agreement with the views of Robertson and Newkirk.

5. Effect of Oil-Film-Forces on a Rotating Shaft.

In 1924, Newkirk described experiments made with two compressors and various models. The compressors ran on journal bearings and the models on ball bearings. Newkirk found that in all cases the rotors whirled, and that the whirl frequencies were equal to the natural frequencies of transverse vibration of the rotors. It was thought at that time the phenomena were identical, but later Newkirk and Taylor (2) showed the whirling of the compressors was due to action of the oil film and that of the models was due to a hysteretic condition of the shaft due to shrink fits of the rotors. The distinguishing feature of the two phenomena was that the hystertic whirl became resonant at speeds above the critical speed while the oil-film whirl, or whip, did not become resonant at speeds below twice critical speed. Newkirk and Taylor obtained the first indication of the cause of this oil-whirl phenomenon when they discovered accidentally

that the whipping was stopped immediately by shutting off the oil supply to the bearings and could be brought back by turning the oil on again. A theory propounded by Newkirk gave a qualitative explanation of the phenomenon based on the fact that the average velocity of the oil film was half the velocity of the shaft due to its rotation. However the theory does not explain why the shaft should persist to whip with large amplitude at speeds greater than twice the critical speed. Newkirk and Taylor investigated the effect of bearing length and bearing load and found that whipping could be prevented by

1. using a sufficiently short bearing.

and 2. increasing the bearing load.

A first attempt to relate this form of instability in the hydrodynamic behaviour of journal bearings was made by Robertson.(21) Robertson showed by means of hydrodynamic theory that, neglecting friction forces, that resultant film force due to journal rotation in an ideal bearing was at right angles to the eccentricity (of the journal in relation to the bearing) and was just balanced by the resultant force due to whirling when the whirling frequency was half the rotational frequency. Simons (22) indicated that this was true for lightly loaded bearings only.

Hagg,(23) when investigating the behaviour of a

a vertical pump motor, came to the conclusion that with the ideal case of oil-film whirl i.e. with no load, the motion of the journal was unstable for all speeds and would whirl at approximately half the rotational speed of the journal. The pump motor, with a self aligning ball bearing at the top and a full (360°) journal bearing at the bottom was observed to whirl"---- in the manner of a pendulum, and from a few revolutions to 1200 revolutions per minute the whirling frequency held to slightly less than half the rotational frequency----"

It would appear, from the forementioned literature that there were two cases of whirl instability instigated by oil-film forces; first the case as observed by Newkirk in which instability only arose when the shaft was running above twice its critical speed and secondly, that observed by Hagg in which the shaft whirled at all speeds. It is important to note that Newkirk performed work, in the main, with a horizontal rotor whilst Hagg used a vertical rotor; the bearing load in each case differed appreciably. The work of Hagg agreed with the theory propounded by Robertson.

Hagg carried out tests with different types of bearings and found that with a plain journal bearing the journal motion was unstable (oil whip occurring, the

journal whirling at approximately half rotational speed) whereas with the tilting pad type of journal bearing the journal motion was quite stable, even when the shaft was struck a blow. A condition for stability arrived at by Hagg was

$$\omega_n > \frac{\Omega}{2}$$

where Ω = journal speed

ω_n = natural frequency of vibration of the journal.

He suggested that the factor half might be replaced by a smaller one with heavily loaded bearings because "----. Whirling frequency is reduced by the increased side leakage which accompanies high film pressures.----" This statement, taken from Hagg's paper was in disagreement with the findings of Newkirk and Taylor. Later, in conjunction with Warner,(24) Hagg derived the conclusions that low lubricant viscosity, low speed, large bearing clearance and high bearing pressure were in the direction of stability.

Hagg and Warner appear to have been the first investigators to have treated the oil-film forces as being composed of stiffness and damping forces, though they do not relate how these might be determined accurately to form a criterion for instability. Attempts to measure these properties experimentally were made by Hagg and Sankey (25) in 1956. Using a 150° partial

bearing Hagg and Sankey determined the maximum and minimum oil-film elasticity and oil-film damping properties on a linear basis. It was noted these properties of the oil-film brought about a reduction in the natural frequency of vibration (as calculated assuming knife edge support). An accurate knowledge of the properties of the oil-film was therefore essential if critical speeds were to be evaluated. Using a method established by Miller, (26) Hagg and Sankey were able to predict the critical whirling speeds of a horizontal flexible rotor supported on two 150° short journal bearings with good accuracy.

Poritsky, (27) in 1953, verified the conclusion of Robertson that the theory of the long full journal bearing indicated instability at all speeds. However by the inclusion of a radial force, exerted by the oil-film on the journal Poritsky derived a criterion for stability as:

$$M\Omega^2\left[\frac{1}{k}+\frac{1}{k_1}\right] < 4$$

where M = mass of the rotor.

Ω = rotation speed.

k = elastic constant of the shaft.

k_1 = elastic constant of the oil-film.

For relatively flexible shafts ($k \ll k_1$) this criterion

was reduced to

$$\omega_n > \frac{\Omega}{2} \text{ for stability, which was}$$

the same criterion arrived at by Hagg.

Newkirk (28) in a paper titled "Varieties of Shaft Disturbances Due to Fluid Films in Journal Bearings", published in 1956 discussed some anomalies which had arisen during the course of studies previously carried out. Cases were quoted where a flexible shaft would whirl at it's natural frequency (resonant whirl) whilst rotating at speeds twice and above twice the natural frequency and a very stiff shaft which would whirl, when running at speeds below the natural frequency, at frequencies somewhat less than half the running speeds. In the latter case the half running speed whirl would usually disappear at higher speeds (still below the critical speed of the shaft) Newkirk related that this occurence was usually with lightly loaded stiff shafts and advocated for stable running large bearing clearance, moderate loading and low viscosity. Pinkus (29) on the other hand observed a case of a rotor which had developed this non-resonant whirl at speeds below twice the critical speed and then developed into a resonant whirl as the rotor had passed through twice the critical speed. He (Pinkus) added that the rotor became stable at speeds above three times the first critical speed and that more viscous oil

inhibited this disturbance.

Pinkus investigated the susceptibility of bearings of various designs to oil whirl (whip), the effect of some of the numerous design and operating variables on oil whirl and tried to obtain a characteristic pattern of oil whirl. Among the varibles tested were loading, speed, bearing tightness, viscosity, unbalance, flexibility of the shaft and external excitation. The tests included circular (two and three groove), elliptical, three lobe (symmetrical and assymetrical), tilting pad, and self energising bearings.

With tests carried out on two shaft rotor systems (weighing 187 lb_f and 64 lb_f) he reported that with an increasing shaft speed the start of whipping was usually characterized by a vibration whose frequency was approximately half the running speed. This usually covered a relatively narrow range of speeds and was soon overtaken by a vibration where the frequency was constant and equal to the first critical speed of the shaft. The transition between the two frequencies of whip occured at speeds equal to twice the value of the first critical speed. This second type of whipping (resonant whip) persisted over a wide range of speeds but whenever a speed was reached corresponding to a higher critical speed of the shaft

or other resonance of the system, resonant whip tended to be damped out and the resonant vibration with a vibration frequency equal to the running speed would prevail. As soon as this region was passed the resonant whip would return.

In addition to the change of vibration frequency at the onset of whip, Pinkus observed a sudden change in amplitude of vibration and in a number of tests an "inertia effect", inasmuch as when the shaft was stable there was a resistance to whip and an unwillingness to pull out of the whip once it had developed.

Pinkus reported that one of the most effective ways of eliminating oil whip was to increase the bearing loading,"---- with a sufficiently high load any form of whipping can be stopped.----" The conclusions drawn by Pinkus as regards the effect of bearing loading were

1. at a given speed it took a higher load to stop oil-whip than to prevent it.
2. The load neccessary to stop or prevent whip was higher when the viscosity of the oil was lower.
3. The whip eliminating load was not a constant but changed with speed and was determined by the degree or "depth" of the unstable

state of the shaft.

He also showed that higher viscosities and a reduction in oil flow tended to eliminate oil-whip. This last statement showed the complexity of oil whirl phenomena because it appeared as a contradiction; a reduction in oil flow would have caused the journal to run hotter, and would of neccessity decreased the viscosity. Unbalance load was found to have little effect on resonant whip although there was an increase in amplitude.

From tests carried out investigating the effect of different bearing designs Pinkus found the three lobe and tilting pad bearings were the most stable ones, while plain cylindrical bearings were the most susceptible to whip. Of the two three lobe bearings (symmetric and asymetric) he found the asymetric one to be the most stable. The self energising bearing was in a class by itself and when suitably loaded would prevent whipping under the most adverse conditions.

It had been mentioned by previous writers, notably Pinkus, that a shaft-rotor system would in some instances behave erratically as the rotational speed approached twice the critical speed; the shaft would be in a quasi-stable state, "jumping" in and out of a stable condition. This condition was called

"the whirl impending speed" i.e. the lowest speed at which the disturbance would build up spontaneously during the normal quiet running of a well balanced rotor. Newkirk and Lewis,(30) in order to obtain a better criterion for the safe operation of shafts carried in journal bearings, set up apparatus so that the shaft could be struck a blow (a blow could cause a severe disturbance to build up at lower speeds than the whirl-impending speed). The speed at which the shaft would recover and settle down to smooth operation after this blow (bump) was called the "bumping speed" and would give an indication of the safe operating speed.

From tests using combinations of three rotors of different weight and five bearings of different clearance and length, Newkirk and Lewis observed when a rotor ran with small eccentricty (light rotor) there was sometimes a considerable difference brtween the "quiet" whirl-impending speed and the "bumping" speed, but with large eccentricity (heavy rotor) the two speeds were identical. When the lightest rotor was used the highest ratio of whirl-impending speed to critical speed was obtained with the shortest bearing and largest clearance. In all cases with the heavier rotor, warming the oil increased the range of stabilty and in several cases it was noted that slight misalignment

of the bearings resulted in much higher whirl impending values.

Hummel,(31) who studied the 180° plain journal bearing, found that a mild instability developed with an eccentricity ratio less than 0.7. This suggested that there might have been some limiting value of eccentricity ratio beyond which operation would always be stable. Newkirk and Lewis found instability with eccentricity ratios up to 0.96, however they noted that plots of eccentricity ratio versus whirl-impending speed for any rotor-bearing combination frequently showed asymptotic approaches to definite values of eccentricity ratio; these values varying with different rotor-bearing combinations.

Hori,(32) working with a flexible shaft supported with a ball bearing at one end and a plain journal bearing at the other, found for small vibrations that if the displacement of the journal centre f the bearing centre was more than approximately 80°/$_o$ of the radial clearance of the bearing (journal), or if the vertical displacement of the journal centre from it's lowest position was less than 50°/$_o$ of the clearance, the shaft would be stable. Small vibrations were defined as "---- such vibrations of the rotor that the amplitude is sufficiently small compared with its eccentricity from the bearing centre".

Hori also established that large vibrations ("---- such that the shaft bends considerably"----") would only exist if the shaft ran above twice its critical speed. By considering both small and large vibrations, Hori was able to show that the apparent contradiction of statements made by Newkirk and Lewis and by Pinkus with regard to the effest of viscosity on oil whip, were just inconsistencies. Low viscosity gave greater stability for small vibrations and was therefore effective in preventing the occurence of oil whip, whereas high viscosity was effective in depressing whip after it had once developed.

Hori concluded that a rotor-shaft system could be stable at any speed if the journal eccentricity was large enough. This would explain why, in some instances, a shaft would not whip until a speed, in excess of twice the critical speed, was reached. Newkirk and Lewis reported a case where a shaft did not whip until a speed of five times the critical speed was reached. The "inertia" effect observed by Pinkus was also accounted for in so far as once the shaft had become unstable (at a speed greater than twice the critical speed) it would not stabilise until the speed was reduced to below trice the critical speed. Hori also observed this effect, see Fig.2.

Holmes,(33) in a paper titled "The Vibration of a

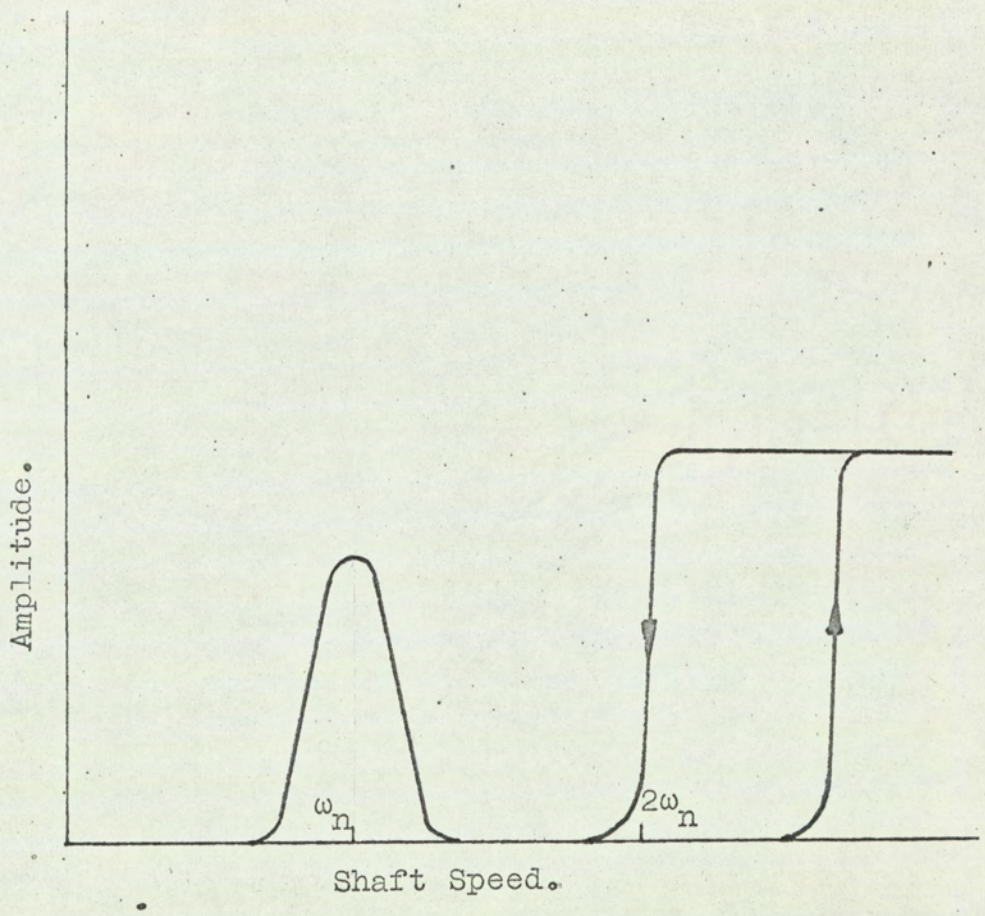

Diagram Showing "Inertia" Effect.

By Hori.

FIG. 2

Rigid Shaft on Short Sleeve Bearings" published in 1960 obtained the dynamic oil-film forces acting on a journal in two perpendicular directions in terms of linearized velocity dependent and displacement dependent terms. These displacement dependent terms are not "elastic" in the sense that $y_{12} \neq y_{21}$ and hence stability considerations arise from these terms quite apart from those introduced by the velocity terms. Holmes found for the short bearing that with eccentricity ratio less than 0.8 the shaft might whirl, either at one half or some other sub-multiple of the rotational speed, whereas the shaft would always be stable with eccentricity ratios greater than 0.8.

Morrison (34) produced evidence to show that the theoretical reasoning of the magority of previous writers was in error. A common assumption made by many of the early writers was to neglect the velocity dependent terms because it was thought their effect would be considerably less than the displacement dependent terms. This is not the case however, for Morrison showed the velocity dependent terms were not small and would in the majority of cases give rise to forces of the same order as those due to the displacement terms.

More recently, Huggins(36) showed that through linearization of the oil forces certain modes of vibration would be overlooked. By maintaining the non-linearity in

the oil force terms and using an anologue computer to solve the equations of motion, Huggins found that half shaft speed self-sustained vibrations could exist and, with an exciting force subharmonics were likely.

PART ONE.

PART ONE.

1. Summary.

An investigation of the behaviour of a two-rotor shaft system supported in two large clearance journal bearings is reported. A vibration in which the shaft exhibited sub-shaft speed resonances has been observed, which to the authors knowledge has not previously been reported. The source of the phenomenon is attributed to a rubber flexible drive coupling which prevented shaft support from one bearing. Out-of-balance forces cause the shaft to whirl as rigid body, rocking about the other bearing. The standard theoretical tratment based on Jeffcott's theory assuming the shaft to be simply supported on two bearings is found to be inadequate.

Treating the coupling as a spring, a theory is propounded, based on the work of Ludeke, which explains the phenomenon. Agreement between theory and experiment is quite good.

2. Description of System and Experimental Technique.

2.1. Description of System.

Photographs of the rotor-shaft assembly are shown in Fig.3. The shaft and rotors are of mild steel and are 1 in. diameter x 20 in. long and 7 in. diameter

x $1\frac{1}{4}$ in. thick respectively. Thus the rotors have appreciable diametral inertia. The rotors are a slide fit on the ends of the shaft, the nominal shaft diameter being reduced at each end for a length slightly less than the thickness of a rotor to form shoulders. Holes are drilled and tapped in each end of the shaft to take $\frac{5}{16}$ in. B.S.F. screws. One rotor is held firmly against the shoulder by a screw and the other by a screwed rod and locking nut. The purpose of the screwed rod is two fold in that it is also used as an attachment for the Fenner flexible drive rubber coupling.

The shaft is supported in two phosphur bronze journal bearings (1.015 in diameter nominally). The bearings are carried in mild steel bearing housings which are screwed to a $\frac{3}{8}$ in. thick mild steel plate. This plate has holes drilled and tapped so that the bearings can be set at different spans and is bolted to a cast iron table.

Oil is gravity fed from a header tank, placed 12 in. above the bearings axial centreline, through a single central oil hole drilled $\frac{1}{8}$ in. diameter vertically through the bearing housing and bearing. A longitudinal groove is chiselled in the bore of the bearings, equal distances from the oil hole for a total length of $\frac{3}{4}$ in. along with a 360° central cirumferential groove (machined $\frac{1}{8}$ in. wide x 0.080 in. deep) see Fig.4. to aid the flow of oil within

the bearings. Oil flow to the bearings is restricted by means of clamps attached to the plastic oil supply pipes.

The shaft was driven via the coupling from a drive shaft which is belt driven from a Heenan and Froude dynamometer. By means of pulleys of different diameter a speed ratio of approximately 4:1 is obtained between the experimental shaft and the dynamometer. This gives a maximum speed approaching 12000 R.P.M.

The final drive shaft was supported in ball bearings attached to the same plate as the journal bearings to aid alignment. The centre of the final drive shaft is aligned with the centres of the two journal bearings. Vertical and horizontal displacement of the rotors are detected by inductive type displacement pick-ups. These consist of a steel case inside of which is a ferrite dust core surrounded by an insulated coil. The coil is surrounded with an insulation material (Araldite) and set into the case. The steel case is attached to the spindle of a micrometer and the whole mounted close to a rotor. The purpose of the micrometer is to enable the calibration of the pick-up to be made in situ. The gap between the pick-up and the rotor is arranged so that the expected rotor movement is a small percentage of the gap. In this way the calibration is considered linear and the movement can be determined

accurately. Two pick-ups 180° apart are connected so as to form one half of a full wave bridge circuit, the other half being contained in a carrier amplifier. The bridge being balanced by means of a variable inductance and resistor in the carrier amplifier. Thus the horizontal, or vertical displacement is determined between the two pick-ups oppsite to each other. This has advantage over a similar pick-ups of greater sensitivity.

A carrier signal of high frequency is applied to the pick-ups from a carrier-amplifier. Displacement of the rotor alters the "flux" between the rotor and the pick-ups and an e.m.f. is generated. The magnitude and the frequency of e.m.f. is proportional to the rotor displacement and is superposed on the carrier frequency to form a modulated signal. This signal is then amplified and demodulated in the carrier amplifier to produce a signal which is fed to a C.R.O. to give a visual display of the rotor displacement alone.

Speed measurement is obtained from a proximity pick-up placed close to the drive shaft. Ten equally spaced chisel edges screwed into the shaft provide ten pulses per revolution of the shaft to the pick-up. The signal from the pick-up is fed into an electronic counter where a visual display of the shaft speed is shown.

A block diagram of the apparatus is shown in

Fig.5.

2.2. Experimental Technique.

The two rotor-shaft was first balanced in situ. The two rotors were designed with holes (2.B.A.) around the periphery close to the edge so that weights, in the form of screws, could be added to effect balancing. Unbalance was detected from chalk marks made on the rotors; the shaft was rotated at a constant speed and a piece of chalk advanced against each rotor. Weights were added in the appropriate places and the procedure was repeated at different speeds. Rotor displacements were monitored on the C.R.O. It was observed that as balancing was effected the shaft behaved differently. With large unbalance the shaft exhibited the normal out-of-balance resonance at the critical speed but upon reducing the unbalance the shaft exhibited several resonances below the critical speed and no resonance at the critical unbalance speed. It was decided to investigate this phenomenon and no further attemps at balancing were made.

Recordings of rotor displacements for dufferent speed settings were made by photographing the traces on the C.R.O. The amplitude and frequency analysis of the traces were then taken from the film. The double amplitude of vibration was measured from peak to peak in all cases, including the complex wave forms.

Frequency analysis was also performed manually. The complex waveforms were usually of such short duration it was considered that analysis by other methods would be fruitless. Film records were taken for increasing and decreasing shaft speeds; the procedure was to set the shaft speed constant, allow time for any transients to subside (due to acceleration from the previous speed setting) and then take a recording of the vibration waveform and the shaft speed. The procedure was repeated for different bearing spans. In all the tests the oil flow to the bearings was restricted so that drip feed lubrication was obtained. The oil flow was sufficient, according to calculations bases on a paper by Sternlicht and Fuller for an oil film to develop.

3. Theoretical Investigations.

3.1. Analytical Treatment.

3.1.1. The out of Balance Whirling Condition.

Consider first the dynamics of a shaft (Fig 6) supported in bearings of symmetrical stiffness carrying a load 'W' of mass 'm' and of appreciable moments of inertia a,a,c ('c' being the polar moment and 'a' the moment about a diameter).

In Fig.6 the line OZ is drawn through 'O' the point of attachment between the rotor and the shaft parallel to the centre line of the bearings. The point O' represents

the displaced position of 'O' having coordinates X and Y relative to the major (fixed) axes OX and OY.

The point G represents the C.G. of the rotor assumed to be displaced an amount 'h' from O' in the plane XOY. The motion of the system is considered relative to the three axes Gx, Gy and Gz drawn parallel to the major axes OX, OY and OZ.

The positions of the principal axes of the rotor in a general displacement of the system are represented by Gx", Gy" and Gz", the inertias relative to these axes being a, a, and c respectively. The position of these axes is determined by imagining first a small rotation $\dot{\theta}$ in the yz plane about the x axis, then a small rotation $\dot{\phi}$ in the x' z' plane about the displaced y axis (Gy') and finally a rotation ωt about the Gz" axis.

The rotation $\dot{\phi}$ and $\dot{\theta}$ are assumed to be small which would be the case in practice and ω is the angular speed of the shaft.

The instantaneous angular velocities about the axes Gx", Gy" and Gz" are represented by ω_1, ω_2, ω_3 respectively and are obtained by summing the components of the angular velocities $\dot{\theta}$, $\dot{\phi}$ and ω in the planes y" z" G, x" z" G and y" x" G respectively.

Thus considering only first order terms and neglecting product terms we have for a torsionally rigid system.

$$\omega_1 = \dot{\theta} \cos \omega t + \dot{\phi} \sin \omega t$$

$$\omega_2 = \dot{\phi} \cos \omega t - \dot{\theta} \sin \omega t \qquad . \; 3.1.1.(1)$$

$$\omega_3 = \omega$$

The angular momenta due to the angular velocities of equations 3.1.1.(1.) are respectively $a\omega_1$, $a\omega_2$ and $c\omega_3$ and therefore the component angular momenta in the directions y to z, and z to x are given by

$$h_x = a\omega_1 \cos \omega t - a\omega_2 \sin \omega t + c\omega\varphi$$

and $$h_y = a\omega_2 \cos \omega t + a\omega_1 \sin \omega t - c\omega\theta \qquad 3.1.1.(2)$$

substituting for ω_1, ω_2 and ω_3 from (1) in (2) gives

$$h_x = a\dot{\theta} + c\omega\varphi \qquad 3.1.1.(3)$$

$$h_y = a\dot{\phi} - c\omega\theta \qquad 3.1.1.(4)$$

The coordinates of G relative to axes OX and OY will be $X + h \sin (\omega t + \alpha)$ and $Y + h \cos (\omega t + \alpha)$ respectively where $(\omega t + \alpha)$ is the angle O'G and Gx and α is constant. Since 'h' is small it may be assumed that the following forces will act on the shaft at O'

(1) An inertia force $- m\left[\ddot{X} - \omega^2 h \sin (\omega t + \alpha)\right]$ in the direction of the X axis. 3.1.1.(5)

(2) An inertia couple $- \dot{h}_x = - (a\ddot{\theta} + c\omega\dot{\varphi})$ about an axis through O' parallel to GX in the direction z to y. 3.1.1.(6)

(3) An inertia force $- m\left[\ddot{Y} - \omega^2 h \cos (\omega t + \alpha)\right]$ in the direction of the Y axis. 3.1.1.(7)

(4) An inertia couple $- \dot{h}y = - (a\ddot{\phi} - c\omega\dot{\theta})$ about an axis through O' parallel to

Gy in the direction x to z. 3.1.1.(8)

The equations of motion are therefore

$$X = -m\left[\ddot{X} - \omega^2 h \sin(\omega t + \alpha)\right] y_{11} - (a\ddot{\varphi} - c\omega\dot{\varphi})\, z_{11}$$

3.1.1.(9)

$$\theta = -m\left[\ddot{X} - \omega^2 h \sin(\omega t + \alpha)\right] z_{11} - (a\ddot{\varphi} - c\omega\dot{\theta})\, \Phi_{11}$$

3.1.1.(10)

$$Y = -m\left[\ddot{Y} - \omega^2 h \cos(\omega t + \alpha)\right] y_{11} - (a\ddot{\theta} + c\omega\dot{\varphi})\, z_{11}$$

3.1.1.(11)

$$\varphi = -m\left[\ddot{Y} - \omega^2 h \cos(\omega t + \alpha)\right] z_{11} - (a\ddot{\theta} + c\omega\dot{\varphi})\, \Phi_{11}$$

3.1.1.(12)

Where y_{11}= linear deflection due to unit load at the point of attachment

Φ_{11}= angular deflection due to unit couple at the point of attachment

z_{11}= angular deflection due to unit load at the point of attachment

= angular deflection due to unit couple at the point of attachment

A particular solution of equations 3.1.1. (4), (10), (11) and (12) will be of the form.

$$X = X_o \cos(\omega t + \alpha) \qquad Y = X_o \sin(\omega t + \alpha)$$

$$\theta = \theta_o \cos(\omega t + \alpha) \qquad \varphi = \phi_o \sin(\omega t + \alpha)$$

and substituting for X, Y, θ and φ, in these equations gives

$$(m\, y_{11}\, \omega^2 - 1)\, X_o + (a-c)\, z_{11}\, \omega^2 \theta_o = m y_{11}\, \omega^2 h$$

$$m\, x_{11}\, \omega^2\, X_o + \left[(a-c)\, \Phi_{11}\, \omega^2 - 1\right] \theta_o = -m\, z_{11}\, \omega^2 h$$

from which

$$X_o = -m\, \omega^2 h \left[(a-c)\,(y_{11}\, \Phi_{11} - z_{11}^2)\, \omega^2 - y_{11}\right] / Q$$

and $\theta_o = m\omega^2 h\, z_{11} / \Delta$

where

$$\Delta = m\left[(a-c)\left(y_{11}\Phi_{11} - z_{11}^2\right)\right]\omega^4 - \left[(a-c)\,\Phi_{11} + m y_{11}\right]\omega^2 + 1$$

It follows therefore that O will describe a circle about the axis OZ with steady motion.

Also X_o and θ_o become infinite when $\Delta = 0$, therefore the equation

$$m\,(a-c)\left[y_{11}\Phi_{11} - z_{11}^2\right]\omega^4 - \left[(a-c)\,\Phi_{11} + m y_{11}\right]\omega^2 + 1 = 0 \qquad 3.1.1.(13)$$

will give the critical whirling speeds.

If 'c' is greater than 'a' which is usually the case, then only one value of ω^2 given by equation 3.1.1.(13) will be positive and hence there will be one critical speed only. It so happens that the particular solution chosen for equations 3.1.1. (9),(10), (11) and (12) gives the critical speed for forward whirl.

However if the particular solution is chosen of the form

$$X = X_o \sin(\omega t + \alpha) \qquad Y = X_o \cos(\omega t + \alpha)$$

$$\theta = \theta_o \sin(\omega t + \alpha) \qquad \varphi = \theta_o \cos(\omega t + \alpha)$$

then the critical whirling speed for backward whirl will be given when

$$m(a+c)\left[y_{11}\Phi_{11} - z_{11}^2\right]\omega^4 - \left[(a+c)\Phi_{11} + m y_{11}\right]\omega^2 + 1 = 0 \qquad 3.1.1.(14)$$

In this case (with 'c' greater than 'a') there will be two critial speeds. It can be seen that

the frequency equation for backward whirl can also be obtained by replacing $(a-c)$ in equation 3.1.1.(13) with $(a+c)$. Consider now a shaft carrying two symmetrical loads (m_1, a_1, a_1, c_1), (m_2, a_2, a_2, c_2) whose coordinates are respectively $(X_1, Y_1, \theta_1, \varphi_1, h_1, \alpha_1)$ and $X_2, Y_2, \theta_2, \varphi_2, \alpha_2)$.

Proceeding as before the equations of motion are

$$X_1=-m_1\left[\ddot{X}_1-\omega^2 h \sin(\omega t+\alpha_1)\right]y_{11}-m_2\left[\ddot{X}_2-\omega^2 h_2 \sin(\omega t+\alpha_2)\right]y_{12} - (a_1\ddot{\varphi}_1 - c_1\omega\dot{\theta}_1)\, z_{11}-(a_2\ddot{\varphi}_2 - c_2\omega\dot{\theta}_2)\, z_{12} \qquad 3.1.1.(15)$$

$$X_2=-m_2\left[\ddot{X}_2-\omega^2 h_2 \sin(\omega t+\alpha_2)\right]y_{22}-m_1\left[\ddot{X}_1-\omega^2 h_1 \sin(\omega t+\alpha_1)\right]y_{21} - (a_2\ddot{\varphi}_2-c_2\omega\dot{\theta}_2)\, z_{22}-(a_1\ddot{\varphi}_1-c_1\omega\dot{\theta}_1)\, z_{21} \qquad 3.1.1.(16)$$

$$Y_1=-m_1\left[\ddot{Y}_1-\omega^2 h_1 \cos(\omega t+\alpha_1)\right]y_{11}-m_2\left[\ddot{Y}_2-\omega^2 h_2 \cos(\omega t+\alpha_2)\right]y_{12} -(a_1\ddot{\theta}_1+c_1\omega\dot{\varphi}_1)\, z_{11}-(a_2\ddot{\theta}_2+c_2\omega\dot{\varphi}_2)\, z_{12} \qquad 3.1.1.(17)$$

$$Y_2=-m_2\left[\ddot{Y}_2-\omega^2 h_2 \cos(\omega t+\alpha_2)\right]y_{22}-m_1\left[\ddot{Y}_1-\omega^2 h_1 \cos(\omega t+\alpha_1)\right]y_{21} -(a_2\ddot{\theta}_2+c_2\omega\dot{\varphi}_2)\, z_{22}-(a_1\ddot{\theta}_1+c_1\omega\dot{\varphi}_1)\, z_{21} \qquad 3.1.1(18)$$

$$\Theta_1=-m_1\left[\ddot{X}_1-\omega^2 h_1 \sin(\omega t+\alpha_1)\right]z_{11}-m_2\left[\ddot{X}_2-\omega^2 h_2 \sin(\omega t+\alpha_2)\right]z_{12} -(a_1\ddot{\varphi}_1-c_1\omega\dot{\theta}_1)\, \Phi_{11}-(a_2\ddot{\varphi}_2-c_2\omega\dot{\theta}_2)\, \Phi_{12} \qquad 3.1.1(19)$$

$$\Theta_2=-m_2\left[\ddot{X}_2-\omega^2 h_2 \sin(\omega t+\alpha_2)\right]z_{22}-m_1\left[\ddot{X}_1-\omega^2 h_1 \sin(\omega t+\alpha_1)\right]z_{21} -(a_2\ddot{\varphi}_2-c_2\omega\dot{\theta}_2)\, \Phi_{22}-(a_1\ddot{\varphi}_1-c_1\omega\dot{\theta}_1)\, \Phi_{21} \qquad 3.1.1(20)$$

$$\varphi_1 = -m_1\left[\ddot{Y}_1 - \omega^2 h_1 \cos(\omega t+\alpha_1)\right] z_{11} - m_2\left[\ddot{Y}_2 - \omega^2 h_2 \cos(\omega t+\alpha_2)\right] z_{12}$$
$$-(a_1\ddot{\theta}_1 + c\omega\dot{\varphi}_1)\Phi_{11} - (a_2\ddot{\theta}_2 + c_2\omega\dot{\varphi}_1)\Phi_{12} \qquad 3.1.1.(21)$$

$$\varphi_2 = -m_2\left[\ddot{Y}_2 - \omega^2 h_2 \cos(\omega t+\alpha_2)\right] z_{22} - m_1\left[\ddot{Y}_1 - \omega^2 h_1 \cos(\omega t+\alpha_1)\right] z_{21}$$
$$-(a_2\ddot{\theta}_2 + c_2\omega\dot{\varphi}_2)\Phi_{22} - (a_1\ddot{\theta}_1 + c_1\omega\dot{\varphi}_1)\ \Phi_{21} \qquad 3.1.1(22)$$

where y_{12}= linear deflection at point (1) due to unit load at point (1)

y_{21}= linear deflection at point (2) due to unit load at point (1)

$y_{12} = y_{21}$

Φ_{12}= angular deflection at point (1) due to unit couple at point (2)

Φ_{21}= angular deflection at point (2) due to unit couple at point (1)

$\Phi_{12} = -\Phi_{21}$

z_{12}= angular deflection at point (1) due to unit load at point (2)

= linear deflection at point (1) due to unit couple at point (2)

z_{21}= angular deflection at point (2) due to unit load at point (1)

= linear deflection at point (2) due to unit couple at point (1)

$z_{12} = -z_{21}$

y_{11}, y_{22}, Φ_{11}, Φ_{22}, z_{11}, z_{22} areas described before.

A particular solution of equations 3.1.1.(15) to (22) will be of the form.

$$X_1=A_1\cos(\omega t+\alpha_1)+B_1\cos(\omega t+\alpha_2) \quad Y_1=A_1\sin(\omega t+\alpha_1)+B_1\sin(\omega t+\alpha_2)$$
$$\theta_1=D_1\cos(\omega t+\alpha_1)+E_1\cos(\omega t+\alpha_2) \quad \phi_1=D_1\sin(\omega t+\alpha_1)+E_1\sin(\omega t+\alpha_2)$$
$$X_2=A_2\cos(\omega t+\alpha_1)+B_2\cos(\omega t+\alpha_2) \quad Y_2=A_2\sin(\omega t+\alpha_1)+B_2\sin(\omega t+\alpha_2)$$
$$\theta_2=D_2\cos(\omega t+\alpha_1)+E_2\cos(\omega t+\alpha_2) \quad \phi_2=D_2\sin(\omega t+\alpha_1)+E_2\sin(\omega t+\alpha_2)$$

and substituting for these values gives four relations between A_1, A_2, D_1, D_2 and four between B_1, B_2, E_1, E_2. The former are found to be

$$(m_1y_{11}\omega^2-1)A_1+(a_1-c_1)z_{11}\omega^2D_1+m_2y_{12}\omega^2A_2+(a_2-c_2)z_{12}D_2 = -m_1y_{11}h_1\omega^2$$

$$m_1z_{11}\omega^2A_1+\left[(a_1-c_1)\Phi_{11}\omega^2-1\right]D_1+m_2z_{12}\omega^2A_2+(a_2-c_2)\Phi_{12}\omega^2D_2 = -m_1z_{11}h_1\omega^2$$

$$m_1y_{21}\omega^2A_1+(a_1-c_1)z_{21}\omega^2D_1+(m_2y_{22}\omega^2-1)A_2+(a_2-c_2)z_{22}\omega^2D_2 = -m_1y_{12}h_1\omega^2$$

$$m_1z_{21}\omega^2A_1+(a_1-c_1)\Phi_{21}\omega^2D_1+\omega_2z_{22}\omega^2A_2+\left[(a_2-c_2)\Phi_{22}-1\right]D_2 = -m_1z_{21}h_1\omega^2$$

and there will be a similar set with B_1 for A_1, E_1 for D_1, B_2 for A_2 and E_2 for D_2 on the L.H.S. of 3.1.1.(23)

while the R.H. members will be respectively $m_2 y_{12} h_2 \omega^2$, $m_2 z_{12} h_2 \omega^2$, $m_2 y_{22} h_2 \omega^2$, $m_2 z_{22} h_2 \omega^2$. From either system the whirling speeds are given by the determinental equation in ω^2.

$$\begin{vmatrix} m_1 y_{11}\omega^2 - 1 & (a-c) z_{11}\omega^2 & m_2 y_{12}\omega^2 & (a-c) z_{12}\omega^2 \\ m_1 z_{11}\omega^2 & (a-c)\Phi_{11}\omega^2 - 1 & m_2 z_{12}\omega^2 & (a-c) z_{12}\omega^2 \\ m_1 y_{21}\omega^2 & (a-c) z_{12}\omega^2 & m_2 y_{22}\omega^2 - 1 & (a-c) z_{22}\omega^2 \\ m_1 z_{21}\omega^2 & (a-c)\Phi_{21}\omega^2 & m_2 z_{22}\omega^2 & (a-c)\Phi_{22}\omega^2 - 1 \end{vmatrix} = 0$$

3.1.1.(24)

If the two loads are of equal weight and moments of inertia and if $y_{11}=y_{22}$, $\Phi_{11}=\Phi_{22}$, $z_{22}, z_{12}=-z_{21}$ which is the case when the system is symmetrical, then equation 3.1.1.(24) can be written,

$$\left[m\left\{(y_{11}+y_{12})(\Phi_{11}-\Phi_{12})-(z_{11}+z_{12})^2\right\}(a-c)\omega^4 - \left\{m(y_{11}+y_{12}) + (a-c)(\Phi_{11}-\Phi_{12})\right\}\omega^2 + 1\right] \times \left[m\left\{(y_{11}-y_{12})(\Phi_{11}+\Phi_{12})-(z_{11}-z_{12})^2\right\}(a-c)\omega^4 - \left\{m(y_{11}-y_{12}) + (a-c)(\Phi_{11}+\Phi_{12})\right\}\omega^2 + 1\right] = 0$$

3.1.1.(25)

If 'c' is greater than 'a' then only two values of ω^2 given by equation 3.1.1.(25) will be positive and hence there will be two critical speeds only.

The backward whirling speeds will be obtained by replacing (a-c) by (a+c)

3.1.2. The Natural Vibrations of the Rotating System.

The natural vibrations of the rotating system are considered appropriate to the case where the forcing due to the out of balance 'h_1', and 'h_2' is absent. For these there will be a solution of the form

$$X_1=A_1\cos(kt+\alpha) \qquad Y_1=A_1\sin(kt+\alpha)$$
$$X_2=A_2\cos(kt+\alpha) \qquad Y_2=A_2\sin(kt+\alpha)$$
$$\theta_1=D_1\cos(kt+\alpha) \qquad \varphi_1=D_1\sin(kt+\alpha)$$
$$\theta_2=D_2\cos(kt+\alpha) \qquad \varphi_2=D_2\sin(kt+\alpha)$$

which constitute circular vibrations of amplitude A_1 and D_1 and frequency $\frac{k}{2\pi}$. Inserting these in equations 3.1.1.(15) to (22) with 'h' put equal to zero gives

$$\left[m\left\{(y_{11}+y_{12})(\Phi_{11}-\Phi_{12})-(z_{11}+z_{12})^2\right\}(a-\tfrac{c\omega}{k})k^4 - \left\{m(y_{11}+y_{12})+(a-\tfrac{c\omega}{k})(\Phi_{11}-\Phi_{12})\right\}k^2+1\right]$$
$$\times\left[m\left\{(y_{11}-y_{12})(\Phi_{11}+\Phi_{12})-(z_{11}-z_{12})\right\}(a-\tfrac{c\omega}{k})k^4 - \left\{m(y_{11}-y_{12})+(a-\tfrac{c\omega}{k})(\Phi_{11}+\Phi_{12})\right\}k^2+1\right]=0 \qquad 3.1.2.(1)$$

as the frequency equation. It may be shown that there are eight real roots to this equation, four of which are positive and four negative. This means that for any value of ω there will be eight natural free vibrations which are circular. The negative roots correspond to circular vibrations in the opposite direction to the rotation of the shaft and the positive roots to circular vibrations in the same direction.

The forward whirling speeds occur when $\omega=k$ i.e. when the forced circular vibration due to out-of-balance has the same frequency as the positive natural vibrations of the rotating shaft and the backward or reverse whirling speeds occur when $\omega=-k$ i.e. when the forced circular vibration due to out-of-balance has the same frequency as the negative natural vibrations of the rotating shaft.

3.1.3. The Natural Vibrations of the Non-Rotating System.

The frequencies of the non-rotating system are obtained by substituting $\omega=0$ in equation 3.1.2.(1) which gives

$$\begin{aligned}&\Big[m\Big\{(y_{11}+y_{12})(\Phi_{11}-\Phi_{12})-(z_{11}+z_{12})^2\Big\}ak^4\\&\quad-\Big\{m(y_{11}+y_{12})+a(\Phi_{11}-\Phi_{12})\Big\}k^2+1\Big]\\&\times\Big[m\Big\{(y_{11}-y_{12})(\Phi_{11}+\Phi_{12})-(z_{11}-z_{12})^2\Big\}ak^4\\&\quad-\Big\{m(y_{11}-y_{12})+a(\Phi_{11}+\Phi_{12})\Big\}k^2+1\Big]=0\end{aligned}\qquad 3.1.3.(1)$$

3.2. Calculated Results for the Experimental System.

Using equation 3.1.3.(1) in conjunction with the flexibility coefficients obtained from Appendix I and II the natural frequencies of the non-rotating system were calculated.

The family of curves given by plotting ω against k for the rotating system was obtained, with the aid of a computer, from equation 3.1.2.(1)

By superimposing the lines $\omega=k$ and $\omega=-k$ on

these curves, the critical whirling speeds were obtained at the intersections.

3.3. Rigid Body Theory.

Consider the case where the shaft takes up the position shown in Fig 7a. In this position the shaft is supported by one bearing (furthermost from the drive end) and by the coupling represented as a spring. The shaft is induced to take up this position because of the spring stiffness i.e. it is assumed that the spring is sufficiently stiff to prevent the shaft making contact with the other bearing. Also it is assumed that the oil flow to the bearings is insufficient to build up an oil film which might have a controlling effect on any vibratory motion of the shaft i.e. the oil forces may be neglected.

Because the shaft is more rigid than the coupling, any vibratory motion of the shaft will be in a rigid body mode of vibration i.e. the shaft will vibrate, pivoting about the one bearing.

Fixed axes OXYZ are set up at the one bearing 'O' being at the centre of the shaft and OZ drawn parallel to the centreline of the coupling.

The shaft carries two symmetric rotors equally spaced from the centre of the shaft. The spring (representing the coupling) is considered as attached to the geometric centre of one end of the shaft and the spring force acts at right angles to the centreline from

the point of attachment. The point's G_1 and G_2, represent the centre of gravity of each rotor assumed to be displaced amounts 'h_1' and 'h_2' respectively from their geometric centres.

The positions of the principle axes (Fig.7b) of the rigid body in a general displacement of the system are represented by O_x, O_y and O_z. Since 'h_1', 'h_2' are small it may be assumed that the principle axes pass through the geometric centre of the rotor. The position of these axes is determined by imagining first a small rotation θ' in the yz plane about the X axis and then a small rotation φ' in the xz plane about the displaced Y axis. The shaft is then assumed to rotate about the Oz' axis with constant angular speed ω. i.e. the principle axes Ox and Oy rotate about Oz' with angular speed ω.

The component angular velocities about the axes Ox, Oy and Oz' are represented by ω_1, ω_2 and ω_3. Thus

$$\omega_1=\dot{\theta}' \cos\varphi \qquad \omega_2=\dot{\varphi}' \qquad \omega_3=-\dot{\theta}' \sin\varphi \qquad 3.3(1)$$

which for small angles θ, φ, reduce to

$$\omega_1=\dot{\theta}' \qquad \omega_2=\dot{\varphi}' \qquad \omega_3=\dot{\theta}'\varphi \qquad 3.3.(2)$$

The component angular moment about these axes, represented by h_1, h_2 and h_3, are

$$h_1=A\omega_1 \qquad h_2=A\omega_2 \qquad h_3=C(\omega_3+\omega) \qquad 3.3.(3)$$

where

A= Moment of Inertia about Ox axis

C= Polar Moment of Inertia

The external moments about 'O' are due to the out-of-balance and spring forces. About the Ox axis the moments are

(1) due to the out-of-balance

$$m\omega^2\left(h_1 \sin(\omega t+\alpha_1)\, b - h_2 \sin(\omega t+\alpha_2)\, n\right)$$

(2) due to the spring

$$-l.\, f(\theta)$$

About the Oy axis the moments are

(1) due to the out-of-balance

$$m\omega^2\left(h_1 \cos(\omega t+\alpha_1)\, b - h_2(\omega t+\alpha_2)\, n\right)$$

(2) due to the spring

$$-l.f(\varphi)$$

About the Oz axis the moments are zero. The momentum equations are thus

$$\dot{h}_1 + h_2\omega_3 - h_3\omega_2 = m\omega^2\left[(h_1 \sin(\omega t+\alpha_1)\, b - h_2 \sin(\omega t+\alpha_2)\, n\right] - l.f(\theta)$$

$$\dot{h}_2 - h_1\omega_3 + h_3\omega_1 = m\omega^2\left[h_1 \cos(\omega t+\alpha_1)\, b - h_2 \cos(\omega t+\alpha_2)\, n\right] - l.f(\varphi)$$

$\dot{h}_3 + h_1\omega_2 - h_2\omega_1 = 0$

Which on substituting the appropriate values and neglecting product and square terms becomes

$$A\ddot{\theta} - C\omega\dot{\varphi} = m\omega^2\left[h_1 \sin(\omega t+\alpha_1)\, b - h_2 \sin(\omega t+\alpha_2)\, n\right] - l.f(\theta) \qquad 3.3.(5)$$

$$A\ddot{\varphi} + C\omega\dot{\theta} = m\omega^2\left[h_1 \cos(\omega t+\alpha_1)\, b - h_2 \cos(\omega t+\alpha_2)\, n\right] - l.f(\varphi) \qquad 3.3.(6)$$

$$C\dot{\omega} = 0 \qquad 3.3.(7)$$

From (7) $\dot{\omega} = 0$ i.e. ω = constant.

The problem is simiplified if the out-of-balance forces in equations (5) and (6) are written as $m\omega^2 H \sin \omega t$ and $m\omega^2 H \cos \omega t$ respectively.

The momentum equations then become

$$A\ddot{\theta} - C\omega\dot{\varphi} + l.f(\theta) = m\omega^2 H \sin \omega t \qquad 3.3.(8)$$

$$A\ddot{\varphi} + C\omega\dot{\theta} + l.f(\varphi) = m\omega^2 H \cos \omega t \qquad 3.3.(9)$$

... the spring characteristic of the coupling are nonlinear, and are assumed to be of the form

$$f(\theta) = k_1 x + k_3 x^3 \qquad 3.3.(10)$$

$$f(\varphi) = k_1 y + k_3 y^3 \qquad 3.3.(11)$$

where $x = l\,\theta$

and $y = l\,\varphi$

Equations (8) and (9) therefore become

$$A\ddot{\theta} - C\omega\dot{\varphi} + k_1 l^2\theta + k_3 l^4\theta^3 = m\omega^2 H \sin \omega t \qquad 3.3.(12)$$

$$A\ddot{\varphi} + C\omega\theta + k_1 l^2\varphi + k_3 l^4\varphi^3 = m\omega^2 H \cos \omega t \qquad 3.3.(13)$$

Assume solutions of the form

$$\theta=\theta_o \sin\left(\frac{\omega t}{3}\right) + p\theta_o \sin \omega t$$

$$\varphi = \theta_o \cos\left(\frac{\omega t}{3}\right) + p\theta_o \cos \omega t$$

where p is small.

Upon substituting for θ and φ and neglecting terms in p^2 equations 3.3.(12) and 3.3.(13) become

$$- A\omega^2\left(\frac{1}{9} \sin \frac{\omega t}{3} + p \sin \omega t\right)\theta_o + C\omega^2\left(\frac{1}{3} \sin \frac{\omega t}{3} + p \sin \omega t\right)\theta_o$$

$$+ k_1 l^2\left(\sin \frac{\omega t}{3} + p \sin \omega t\right)\theta_o$$

$$+ \theta_o^3 k_3 l^4\left(\frac{1}{4}\left(3 \sin \frac{\omega t}{3} - \sin \omega t\right) + \frac{3p}{2}\sin \omega t\left(1-\cos \frac{2}{3}\omega t\right)\right)$$

$$= m\omega^2 H \sin \omega t \qquad 3.3.(14)$$

and

$$-A\omega^2\left(\frac{1}{9} \cos \frac{\omega t}{3} + p \cos \omega t\right)\theta_o + C\omega^2\left(\frac{1}{3} \cos \frac{\omega t}{3} + p \cos \omega t\right)\theta_o$$

$$+k_1 l^2\left(\cos \frac{\omega t}{3} + p \cos \omega t\right)\theta_o$$

$$+\theta_o^3 k_3 l^4\left(\frac{1}{4}\left(3 \cos \frac{\omega t}{3} - \cos \omega t\right) + \frac{3p}{2} \cos \omega t\left(1+\cos\frac{2}{3}\omega t\right)\right.$$

$$= m\omega^2 H \cos \omega t \qquad 3.3.(15)$$

respectively.

Use having been made of the identities

$$\cos^3 \omega t = \frac{1}{4}\left(3 \cos \omega t - \cos 3\omega t\right)$$

$$\sin^3 \omega t = \frac{1}{4}\left(3 \sin \omega t - \sin 3\omega t\right)$$

Equating terms of sin ωt, sin $\frac{\omega t}{3}$, gives

$$-\frac{A\omega^2}{9} + \frac{C\omega^2}{3} + k_1 l^2 + \frac{3}{4}k_3 l^4 \theta_o^2 = 0 \qquad 3.3.(16)$$

and

$$p(-A\omega^2 + C\omega^2 + k_1 l^2)\theta_o - k_3 l^4 (-\frac{1}{4} + \frac{3p}{2} - \frac{3p}{2}\cos\frac{2}{3}\omega t)\theta_o^3$$

$$= m\omega^2 H \qquad 3.3.(17)$$

there will also be similar equations for terms in cos ωt and cos $\frac{\omega t}{3}$. Substituting for $k_3 l^4 \theta_o^2$ from equation 3.3.(16) in 3.3.(17) gives

$$p((C-A)\omega^2 + k_1 l^2)\theta_o$$

$$+ \frac{4}{3}((3C-A)\frac{\omega^2}{9} + k_1 l^2)(-\frac{1}{4} + \frac{3p}{2} - \frac{3p}{2}\cos\frac{2}{3}\omega t)$$

$$= m\omega^2 H$$

Hence

$$p\theta_o = \frac{m\omega^2 H - X(k_1 l^2 - (A-3C)\omega^2/9)}{k_1 l^2 - (A-C)\omega^2} \qquad 3.3.(18)$$

where

$$X = \frac{4}{3}(-\frac{1}{4} + \frac{3p}{2} - \frac{3p}{2}\cos\frac{2}{3}\omega t)$$

Since 'X' is bounded in value the last part of equation 3.3.(18) can be made negligible by choosing large values of ω. Thus equation 3.3.(18) becomes

$$p\theta_o = \frac{m\omega^2 H}{k_1 l^2 - (A-C)\omega^2} \qquad 3.3.(19)$$

It can be seen that for small out-of-balance, as is assumed, neglecting terms containing p^2 and higher is justifiable.

An examination of equation 3.3.(16) and 3.3.(19) shows that the amplitude of the subharmonic follows the frequency amplitude, relationship of the free vibration starting in this case , (when $\theta_o=0$) at $\omega^2=9\ (k_1l^2/\ A-3C)$ rather that at $\omega^2=k_1l^2/\ (A-C)$, while the amplitude of the oscillation having the frequency of the out-of-balance force follows the resonance curve of a linear system. Equation 3.3.(16) also shows that the sub-harmonic vibration (in the form considered) exists only when

$$\omega^2 > \frac{9k_1l^2}{A-3C} + \frac{27k_3l^4\theta_o^2}{4(A-3C)}$$

By generalizing equations 3.3.(12) and 3.3.(13) viz

$$A\ddot{\theta} - C\omega\dot{\varphi} + k_1l^2\theta + - - - - - + k_nl^{n+1}\theta^n = m\omega^2H \sin \omega t \qquad 3.3.(20)$$

$$A\ddot{\varphi} + C\omega\dot{\theta} + k_1l^2\theta + - - - \quad + k_nl^{n+1}\varphi^n = m\omega^2H \cos \omega t \qquad 3.3.(21)$$

solutions of the form

$$\theta = \theta_o \sin \frac{\omega t}{n} + \theta_o p \sin \omega t$$

$$\varphi = \theta_o \cos \frac{\omega t}{n} + \theta_o p \cos \omega t$$

are expected.

3.3.1. Natural Vibrations of the Rotating Syatem.

The natural vibrations of a rotating system are considered appropriate to the case where the forcing due to the out of balance 'h' and 'h' are absent. The natural vibrations are determined from the following equations

$$A\ddot{\theta} - C\omega\dot{\varphi} + k_1 l^2\theta + k_3 l^4\theta^3 = 0$$

$$A\ddot{\varphi} + C\omega\dot{\theta} + k_1 l^2\varphi + k_3 l^4\varphi^3 = 0 \qquad 3.3.1.(1)$$

Equations 3.3.1.(1) may be written as

$$A\ddot{\theta} = C\omega\dot{\varphi} + k_1 l^2\theta + k_3 l^4\theta^3$$

$$A\ddot{\varphi} = -C\omega\dot{\theta} + k_1 l^2\varphi + k_3 l^4\varphi^3$$

As an approximation let

$$\theta = \theta_o \sin \Omega t$$

$$\varphi = \theta_o \cos \Omega t$$

then

$$A\ddot{\theta} = -C\omega\Omega\theta_o - k_1 l^2\theta_o - \frac{3}{4}k_3 l^4\theta_o^3 \sin \Omega t + \frac{3}{4} k_3 l^4\theta_o^3 \sin 3\Omega t$$

and

$$A\ddot{\varphi} = -C\omega\Omega\theta_o - k_1 l^2\theta_o - \frac{3}{4} k_3 l^4\theta_o^3 \cos \Omega t + \frac{3}{4} k_3 l^4\theta_o^3 \cos 3\Omega t \qquad 3.3.1.(2)$$

Intergrating equations 3.3.1.(2) twice with respect to time gives

$$\theta = \frac{1}{A\Omega^2}\left(C\omega\Omega\theta_o + k_1 l^2\theta_o + \frac{3}{4}k_3 l^4\theta_o^3\right)\sin\Omega t$$

$$- \frac{3k_3 l^4\theta_o^3}{36A\Omega^2}\sin 3\Omega t \qquad 3.3.1.(3)$$

and

$$\varphi = \frac{1}{A\Omega^2}\left(C\omega\Omega\theta_o + k_1 l^2\theta_o + \frac{3}{4}k_3 l^4\theta_o^3\right)\cos\Omega t$$

$$- \frac{3k_3 l^4\theta_o^3}{36A\Omega^2}\cos 3\Omega t \qquad 3.3.1.(4)$$

Hence if the approximation is a reasonable one then θ will be given by the coeffient of the sin Ωt term of equation 3.3.1.(2) and φ by the coeffient of the cos Ωt term of equation 3.3.1.(3) Thus the frequency amplitude relationship becomes

$$A\Omega^2 - C\omega\Omega = k_1 l^2 + \frac{3}{4}k_3 l^4\theta_o^2 \qquad 3.3.1.(5)$$

and putting $\Omega = \omega$ gives the frequency-amplitude relationship of the harmonic vibration

$$(A-C)\omega^2 = k_1 l^2 + \frac{3}{4}k_3 l^4\theta_o^2$$

or

$$\omega^2 = \frac{k_1 l^2}{(A-C)} + \frac{3k_3 l^4\theta_o^2}{4(A-C)} \qquad 3.3.1.(6)$$

for the sub-shaft speed vibration we have with $\Omega = \frac{\omega}{3}$

$$(A-3C)\frac{\omega^2}{9} = k_1 l^2 + \frac{3k_3 l^4 \theta_o^2}{4}$$

or

$$\omega^2 = \frac{9k_1 l^2}{(A-3C)} + \frac{27k_3 l^4 \theta_o^2}{4(A-3C)} \qquad 3.3.1.(7)$$

4. Discussion of Rigid Body Theory.

A theory has been developed which shows how a small out-of-balance force can produce sub-harmonic resonances as a direct consequence of the system being driven through a nonlinear coupling. An important issue arises viz. the equilibium position, which it is thought requires discussion.

Vibration may take place about a position of equilibrium or steady motion. An example of the latter is nutation of a gyroscope, where a small angular variation is impressed on a steady uniform precession. In the theory, vibration is assumed to take place about a position of equilibrium and the forces which bring the shaft to this position are neglected.

If the coupling were represented by a linear spring then the position of equilibrium would not be important. This is apparent when the curve of spring force versus displacement (Fig 8) is considered. Any displacement of the same amplitude from any equilibrium position requires the same force to displace the spring. If the coupling is represented by a non-linear spring,

as was assumed in the theory, then the position of equilibrium becomes vitally important. By considering the curve of spring force versus displacement for the nonlinear spring (Fig 8) it is apparent that any displacements, from any equilibrium position, of the same amplitude require a different force to displace the spring for each equilibrium position. Hence, for accurate theoretical predictions the spring characteristics should be known about each equilibrium position.

In the investigations, tests were performed with the bearings set at different centres (see Experimental Procedure). For each test, therefore, the equilibrium position was different. Unfortunately no measurements were made to determine the equilibrium position and consequently the theory, as presented, cannot be applied directly to the experimental system.

Even so the basic conception is thought to be fundamentally correct and an attempt has been made, by a modification (see Appendix III.) to the theory, to correlate experimental results with predicted results.

4.1. Calculated Results for the Experimental System.

The nonlinear spring coefficients were obtained by applying a curve fitting technique to the spring characteristic curve (see Appendix IV). Using these coefficients and the modified theory, natural

free harmonic and subharmonic resonance curves were calculated for each of the different bearing centres employed in the investigation.

5. Discussion of Results.

5.1. Natural Frequencies without Rotation.

Table I shows the comparison between calculated and measured natural frequencies of vibration, with no rotation, of the system when supported on knife edges. Theoretically the system has eight natural frequencies, four positive and four negative (see theory section 3.1.3.). Attempts were made only to excite the positive natural frequencies and of these only the lowest of the four theoretical frequencies showed a resonance. Tests were carried out with the span between the knife edges set at different values and in all cases agreement between the theoretical and the measured lowest or first natural frequency was very good.

Theoretical values of the natural frequencies show that the frequencies appear as pairs i.e. the two lower frequencies are relatively close to each other, as are the two higher frequencies. Each pair is separated by a considerable frequency range. It could be possible therefore for the resonance at the second natural frequency to be masked by the first and correspondingly the resonance at the fourth natural

frequency by the third. However this does not explain why only one resonance should occur. The reason is thought to be that the higher pair of natural frequencies are of such frequency values that when the system vibrates at these frequencies, the shaft looses contact with the knife edges, thereby eliminating the resonances and invalidating the theory.

Although experimental and analytical techniques exist for determining natural frequencies when they are closely spaced, see for instance papers by Kennedy and Pancu (36) and Pendered and Bishop (37), it was not considered essential to the problem in view to proceed any further along these lines, bearing in mind also that the natural frequencies of the rotating system differ from the natural frequencies of the system with no rotation because of the gyroscopic stiffening effect.

It should also be noted that results obtained with the shaft supported in the test bearings were identical with those obtained with the shaft supported on knife edges.

5.2. Critical Whirling Speeds.

Attempts to determine the critical whirling speeds met with limited success. With a "well-balanced" shaft the results were at first surprising if not bewildering. As the shaft speed was increased gradually

from zero to its "maximum" the shaft experienced several "resonant" vibrations at speeds below the calculated critical whirling speed (see,for example Fig 11). At low speeds a resonance appeared, where the frequency of vibration was the same as the shaft speed. As the speed was increased beyond this resonance the amplitude of vibration in both the horizontal and vertical directions would suddenly "jump" to a much larger value. This occured when the speed was approximately twice the first resonance and the frequency of vibration would change from that of shaft speed frequency to exactly half the shaft speed frequency.

Increasing the speed beyond the "jump" speed showed that the amplitude of this sub-shaft speed vibration decreased. However when a speed was reached which was approximately three times the first resonance the amplitude of vibration would "jump" from a small to a large vibration, and the frequency of vibration would change from half shaft speed to a third shaft speed. A further "jump" phenomenon was observed at a higher shaft speed (in excess of a speed of four times the first "resonance") In this case the frequency of vibration "jumped" from a third shaft speed to a quarter shaft speed vibration.

Within the maximum speed limitation

imposed on the system (see Appendix V) no other "jump" phenomenon was observed.

At a "jump", the shaft would sometimes be in a condition of instability e.g. as a speed of approximately twice the shaft speed or synchronous resonance was approached the shaft would sometimes jump from a shaft speed vibration to a half speed vibration of much larger amplitude and then jump back again (see Fig 9a, 9b).

The waveform under these conditions was usually complex, consisting of a shaft speed frequency wave combined with the sub-shaft speed frequency wave.

The direction of the rotation or whirl of the centre of the rotors was determined from the recorded waveforms. The polarity of the inductive pick-ups being arranged such that when the vertical displacement waveform led the horizontal the rotors "whirled" in a forward direction. Conversely, a reverse "whirl" would be recognised when the horizontal displacement led the vertical. In all the tests carried out the rotors only "whirled" in a forward direction i.e. in the same direction as that of rotation. The whirl motion of the rotors was such that the two rotors moved antiphase to each other. The mode of vibration was considered to be a rigid body mode, brought about, as it was thought at the time, due to the shaft being

supported by the oil spring forces in each bearing, the oil spring being less stiff than the shaft. It can be shown quite easily that in this case, with the two rotors overhung symmetrically from the bearings, the lowest rigid body mode of vibration is one of rocking and not translation. Later it was to be shown that this reasoning was incorrect and that the rigid body vibrations were due to the drive coupling. The coupling prevented any support at one bearing so that the shaft pivots about the other.

Tests were carried out with the bearings set at different centres and in all the tests the above phenomenon occured, there being only a difference in the "jump" speeds and the first resonance.

The "jump" speeds were not exactly whole number multiples of the first resonance, the half shaft speed jump occuring at a speed slightly greater than twice the first. The difference in speed increasing as a higher order sub speed jump occured and being more marked with the longest bearing centres.

Increasing the out-of-balance of either rotor had a most pronounced effect on the generation of these sub-shaft speed "whirls". It was noticed that the first "resonance" appeared (the amplitude was considerably reduced in most cases), with the two rotors moving in anti-phase to each other, no "jump" phenomenon

was produced. Once the first "resonance" had been passed the two rotors moved in phase with each other and the shaft ran quite smoothly until the first forward out-of-balance resonance or critical whirling speed was approached. Here the amplitude increased with increase of speed and the shaft exhibited a normal resonance as the speed was increased past the critical speed, the shaft whirling in the direction of rotation. The measured critical whirling speed agreed very well with theory (see Table 11). However, no second critical speed showed up, the shaft ran with very little vibration up to the maximum speed. The reasons for this anomaly with the theory are thought to be as previously advanced in the case of the natural frequencies of vibration without vibration, remembering that the bearings used in the tests were of large diametral clearance.

The theory also predicted reverse critical whirling speeds, where the shaft whirls in a reverse direction to the rotation, but no reverse whirl was observed. The reason for this is thought to be (in the case of the lower of the critical speeds at least) due to the critical reverse whirling speed being relatively close to the forward critical whirling speed. The out-of-balance forces, rotating in the same direction as the shaft, would tend to excite a resonance at the

forward critical whirling speed rather than at the reverse.

With a reverse whirl, the shaft would undergo stress reversals and these could damp out any vibratory motion of large amplitude, such that a resonance would not be noticed.

The explanation of the sub-shaft speed resonances presented quite a problem. It was thought at the time that the phenonemon was a self excited vibration produced by oil forces within the bearings. Huggins, as mentioned previously in the Historical and Technical review, had shown that with an exciting force (which in this instance would be the rotating out-of - balance force) sub-harmonic resonances could be generated by an oil film. However, with the system under investigation the results did not show exact sub-harmonic resonances insomuch as the resonances did not occur at shaft speeds which were exact whole number multiples of the lowest or fundamental resonance. It was for this reason that the resonances were called sub-shaft speed resonances. Also it was found that when the oil flow to the bearings was increased, in an attempt to clarify the situation as regards the effect of the oil forces, the shaft became unstable and the amplitude of vibration was much greater than with the sub-shaft speed resonances. The frequency of the unstable motion

was exactly half the shaft speed. It was while investigating this latter phenomenon which is described more fully in part two that the answer to the sub-shaft speed resonance appeared.

As part of the investigation the effect of bearing clearances was to be determined. When the shaft ran in bearings of 0.001 in diametral clearance (previous to this the bearing diametral clearance was 0.015 in) it seized and the drive coupling sheared in half. The bearings were enlarged and the coupling replaced with a more flexible one. At no stage after this did the shaft exhibit sub-shaft speed resonances. After the series of tests were completed various measures were taken viz introducing misalignment of the bearings, varying the amount of unbalance, reducing the oil flow, striking the shaft a blow, in an endeavour to repeat the results of the earlier work but all were to no avail.

The only difference between the two series of tests was thus found to be the coupling, all the other variables having been eliminated. However, for sun-shaft speed resonances to occur would require that the external constraint i.e the coupling, have a non-linear spring characteristic. This is so because of the damping effect of the oil in the bearings i.e. a linear system which possesses damping is incapable of

generating sub-harmonics.

Tests were carried out to determine the spring characteristics of the two couplings used in the investigations. In the first instance a coupling of the same rating (Horse Power) and physical size as the coupling which failed was tested. Due to insufficient time it was only possible to measure the coupling spring characteristics in shear for the static case i.e. with no rotation. The tests are described in Appendix IV along with details of how the stiffness of the rotating coupling could be measured. The results of the first test showed the spring characteristics of the coupling in shear to be non-linear. Furthermore the coupling was shown to be a "soft" spring viz. the stiffness descreased with increased displacement.

The spring characteristic of the coupling used in the second part of the investigation was found to be approximately linear, there being a slight deviation from a linear curve at large displacements. A comparison of the spring characteristics of the two couplings is shown in Fig. 10.

From the above reasoning it was concluded that the vibration phenomenon encountered i.e. sub-shaft speed resonances was a direct consequence of out-of-balance forces exciting a non-linear spring system.

The theory evolved in section 3.3. although limited in use in this instance, for reasons given in the discussion of the theory, explains the generation of the sub-shaft speed resonances. By considering the free vibrations in the case chosen in the theory i.e. the coupling had a spring characteristic of the form $k_1x + k_3x^3$ it can be seen that vibrations with the same frequency as the forcing frequency, viz. shaft rotational frequency, start at

$$\omega_n^2 = \frac{k_1 l^2}{(A-C)}$$

while vibrations with the frequency of a third sub-shaft speed start at

$$\omega_n^2 = \frac{9k_1 l^2}{(A-3C)}$$

Thus because of the inertia terms in the denominators of the two expressions a sub-shaft speed resonance should occur at a shaft speed in excess of three times the shaft speed of the synchronous resonance. In general therefore it would be expected that the excess would increase with the increase of the order of the sub-shaft speed resonance e.g. if the third sub-shaft speed resonance occurs at a shaft speed of (3+x) times the shaft speed of the synchronous resonance and the fouth sub-shaft speed resonance occurs at a shaft

speed of(4+y) times the shaft speed of the synchronous resonance, then y will be greater than x. This was verified experimentally.

Experimental results of measured amplitude in horizontal and vertical directions are shown plotted against shaft speed in Figs. 11 to 30. The theoretical natural resonance curves, obtained from the modified rigid body theory (Appendix III) are superimposed on the experimental results and are shown by the continuous curves. It can be seen that for the small bearing centres viz. 4.5 in and 6 in, and shaft speeds up to the third resonance, the experimental points lie close to the theoretical resonance curves. The fourth resonance starts at a shaft speed considerably beyond the predicted value. This is to be expected to some extent because the theoretical natural resonance curves are calculated using the modified theory which does not take into account the polar and diametral moments of inertia of the system. Thus, theoretically, the sub-shaft speed resonances become sub-harmonic resonances viz. the first sub-shaft speed resonance occurs at twice the shaft speed of the first resonance and so on. With the longer bearing spans the discrepancy is seen to increase. An explanation of this is offered as follows:the natural resonance curves were calculated using the spring coefficients obtained from a static

stiffness test on the coupling. With rotation the coupling should become more stiff, thereby increasing the shaft speed at which a resonance occurs. Now, theoretically, increasing the bearing span increases the speed at which a resonance occurs, this agrees with the experimental results, but because of the greater speed, which automatically stiffens the coupling, the experimental results will be excess of the theoretical results.

The results also show that with the longer bearing spans there is a tendency for the experimental resonance curves (shown dotted) to become distorted, especially with the higher orders of sub-shaft speed vibrations. The distortion is thought to be brought about by oil forces within the bearings, stiffening of the coupling, and by the out-of-balance forces. Although the flow of oil to the bearings was restricted there would be a tendency for an oil film to develop. This would lift the shaft in the bearing and so change the equilibrium position and either increase or decrease, depending on the alignment between the coupling and the bearings, the shaft speed at which a resonance occurs. If the equilibrium position is altered so as to approach the zero equilibrium position then the spring stiffness increases and there will be an increase in the shaft speed at which the

the resonance occurs. The forcing level, due to the out-of-balance forces, increases with increase of rotational speed and therefore increases the resonance "bandwidth". Hence an effect may be observed where the amplitude of vibration tends to remain constant. This will be more noticeable with the longer bearing spans because of higher shaft speeds at which the resonances occur.

Generally, the level of the amplitude of vibration varied with each bearing span. This is put down to the damping effect of the oil rather than an effect of varying the bearing span. The oil flow was not measured and could quite easily have been different for each test, thereby producing different degrees of damping.

6. Conclusions.

1. With well balanced rotors the system behaves as a rigid body, rocking on one bearing.
2. When the shaft is driven via a non-linear flexible coupling sub-shaft speed resonance are generated.
3. Agreement between the non-linear theoretical and experimental results is very good at low speeds (up to approximately 80 c/s). At high speeds agreement, as is expected, is not so good.
4. Increase in the bearing span results in an increase

in the shaft rotational speed at which the resonances appear.

5. With large unbalance the shaft exhibits no sub-shaft speed resonances.

6. Agreement between calculated and measured critical whirling speed was only obtained with large unbalance. Only the first forward critical speed resonance appeared.

7. No reverse whirl was detected.

8. Increase of oil flow rendered the shaft unstable at some speed. It would appear therefore that the motion of the shaft can be controlled either by oil forces or coupling forces whichever is predominant. In the investigation, the coupling forces were predominant.

7. Recommendations.

The investigation was initially to determine the behaviour of a two-rotor shaft system supported in two journal bearings, and to this end a test rig was designed. The system was driven through a rubber flexible coupling. Little attention was made to the actual choice of soupling, it was considered that the coupling was sufficiently flexible to allow transverse displacement of the rotor and sufficiently rigid to drive the system. However, the cause of the sub-shaft speed resonances encountered during the investigation

was traced to the coupling. Fortunately or unfortunately therefore, the choice of coupling was wrong, fortunately because it has been shown that the choice of coupling is very important and unfortunately because of the external constraint imposed on the shaft.

The phenomenon is most likely to occur in practice when a light machine is flexibly coupled to a much heavier one and when the oil supply to the bearings is restricted i.e. where the heavier machine forms a rigid attachment for the coupling and, because of the restricted oil flow, the coupling forces predominate and control the vibratory motion of the light machine. It was found that the phenomenon did not occur in the presence of large out-of-balance forces, but this cannot be recommended as a preventive curve if the system is to be run at a speed near or above the critical whirling speed because of the large amplitude of vibration. A more reasonable remedy is to ensure that the spring characteristics of the coupling are linear, so that, because of damping, no sub-shaft speed resonances occur. Although a synchronous resonance will appear, by having a floxible coupling this will occur at a relatively low shaft speed and can be quickly passes through. Also, it is thought with good balancing the amplitude of vibration at the

resonance will not be so excessive as to cause concern.

Because of insufficient time it was not possible to investigate the full significance of the phenomenon and therefore such questions as:

1. To what extent does out-of-balance effect the phenomenon?
2. What is the effect of misalignment of the coupling ?
3. What is the minimum oil flow neccessary before the coupling forces predominate and control the vibratory motion of the shaft.?
4. What types of coupling are liable to produce this phenomenon.?

have not been answered.

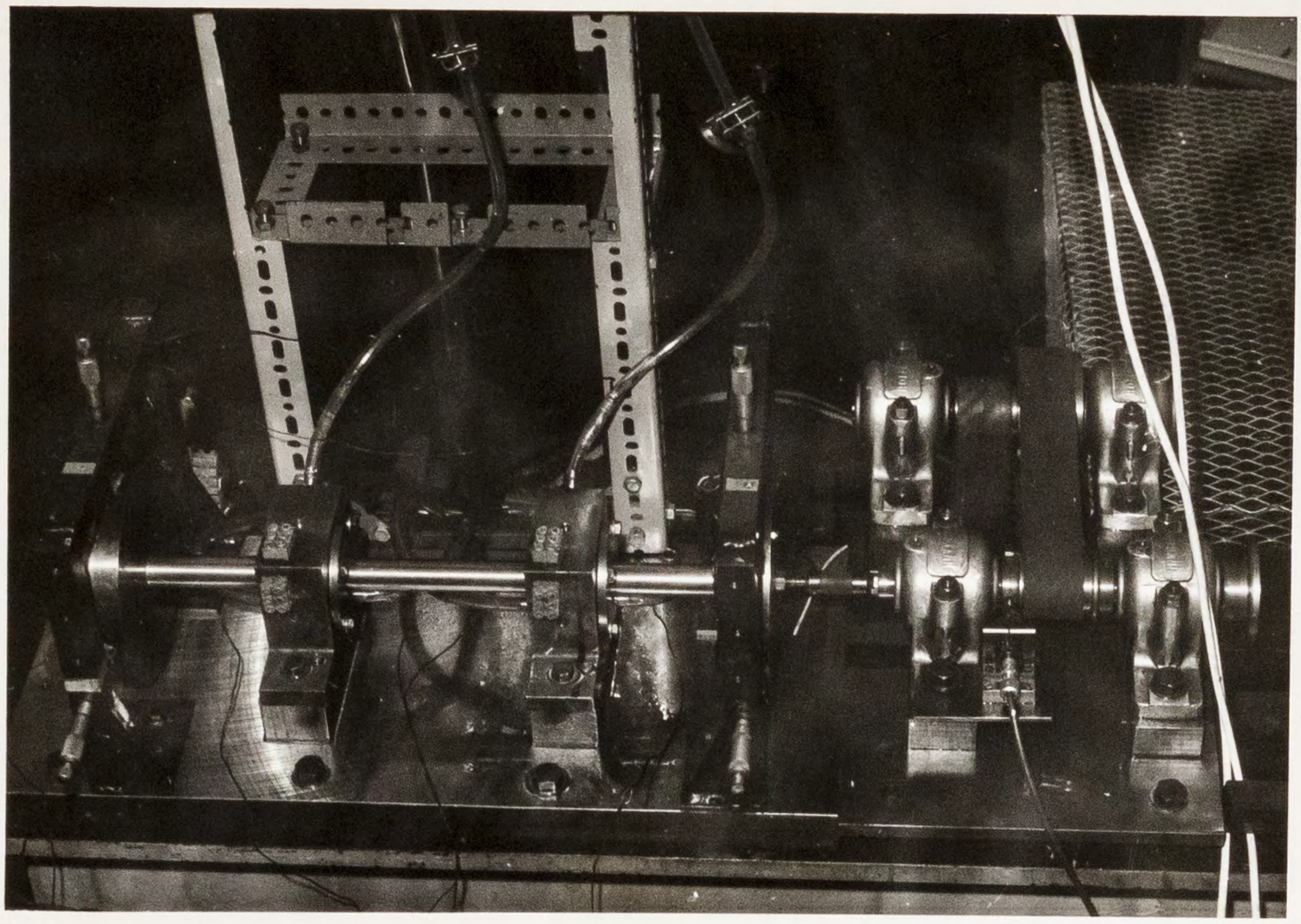

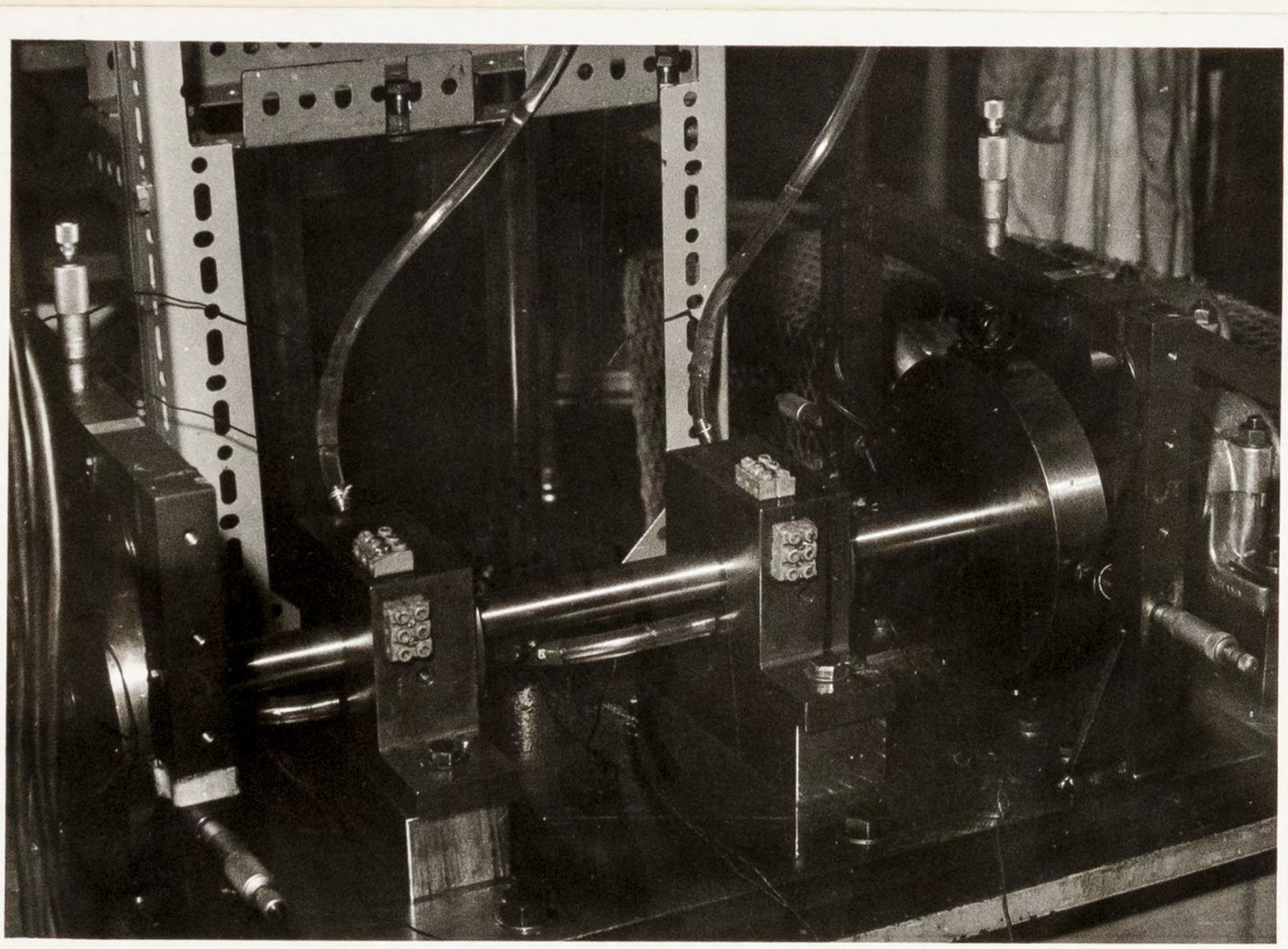

DETAILS OF RIG

FIG 3

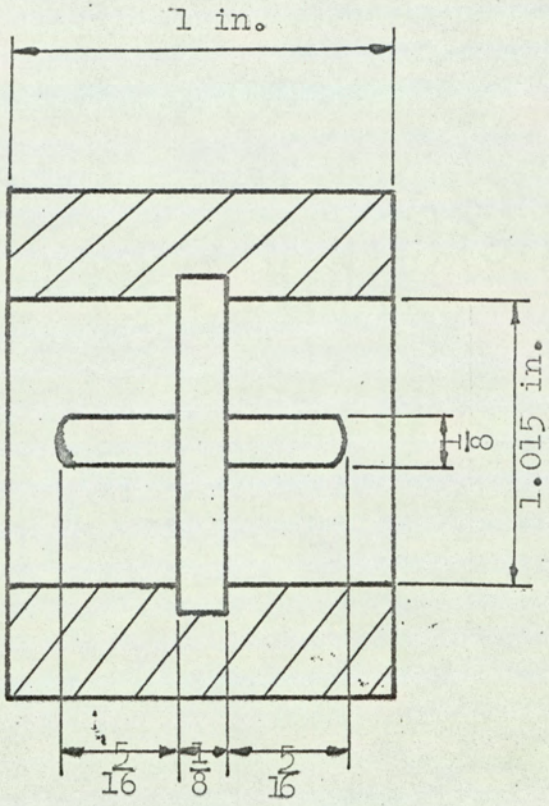

Details of Bearings

FIG. 4

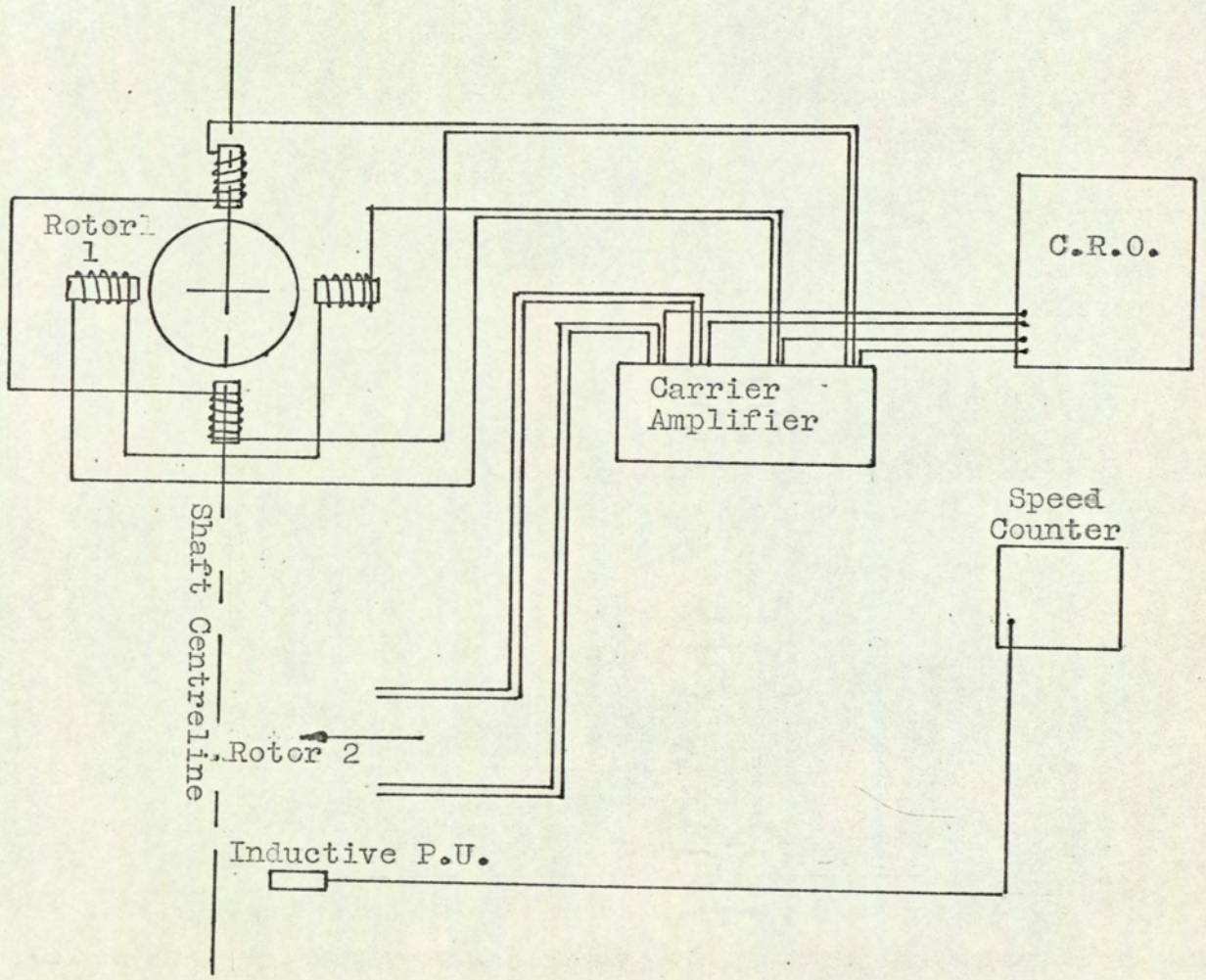

Block Diagram of Electronic Measuring Equipment

FIG. 5

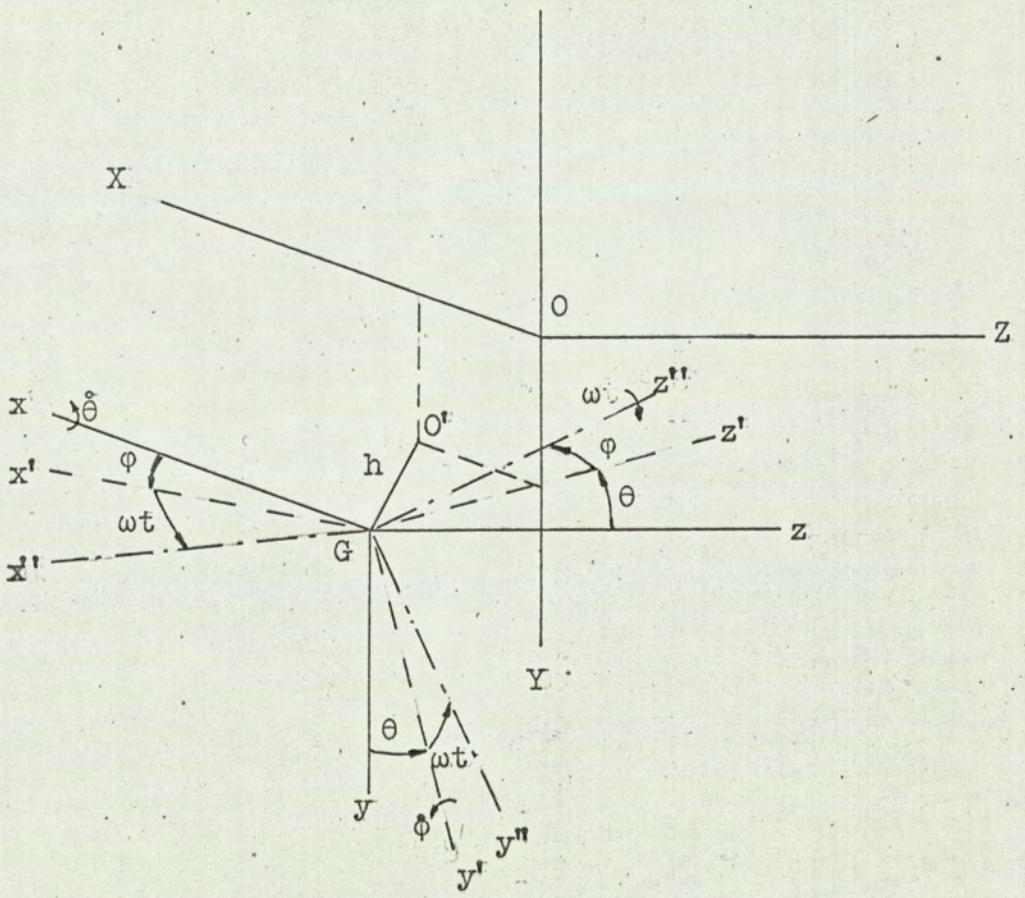

The Whirling Condition

FIG. 6

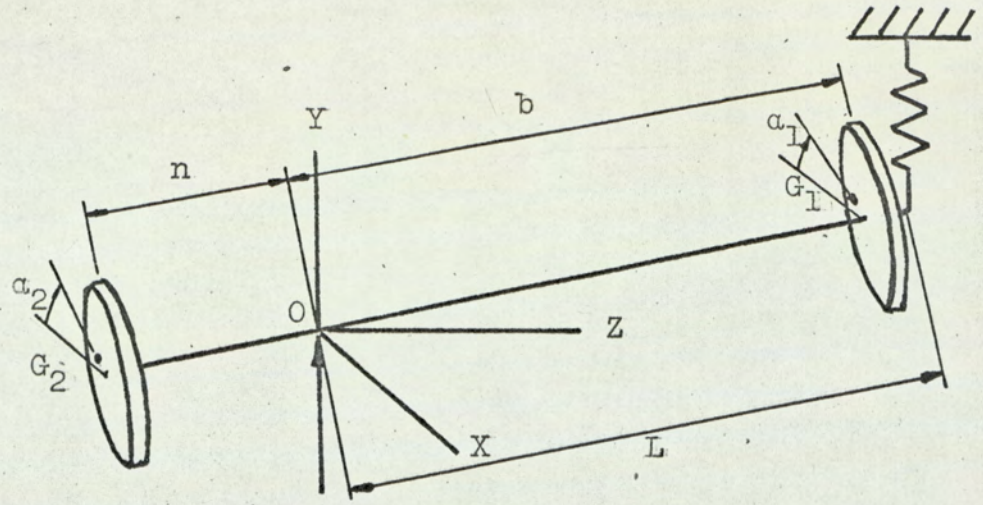

The Rigid Body Condition. FIG. 7a

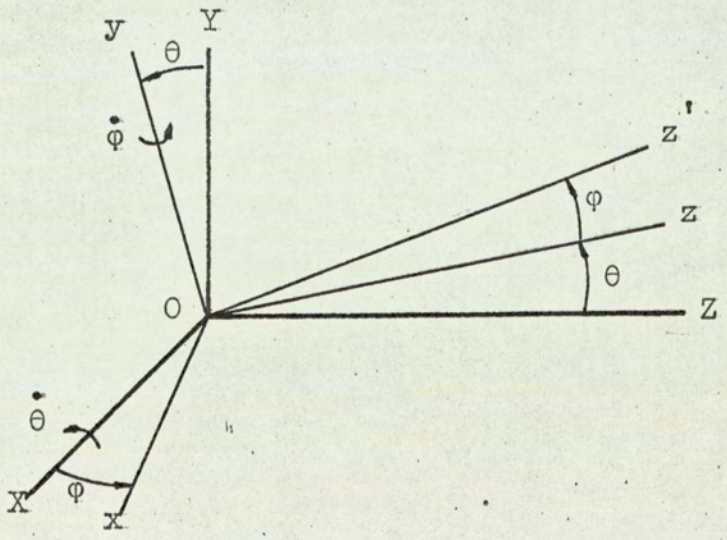

General Displacement of Principal Axese. FIG. 7b

FIG.7

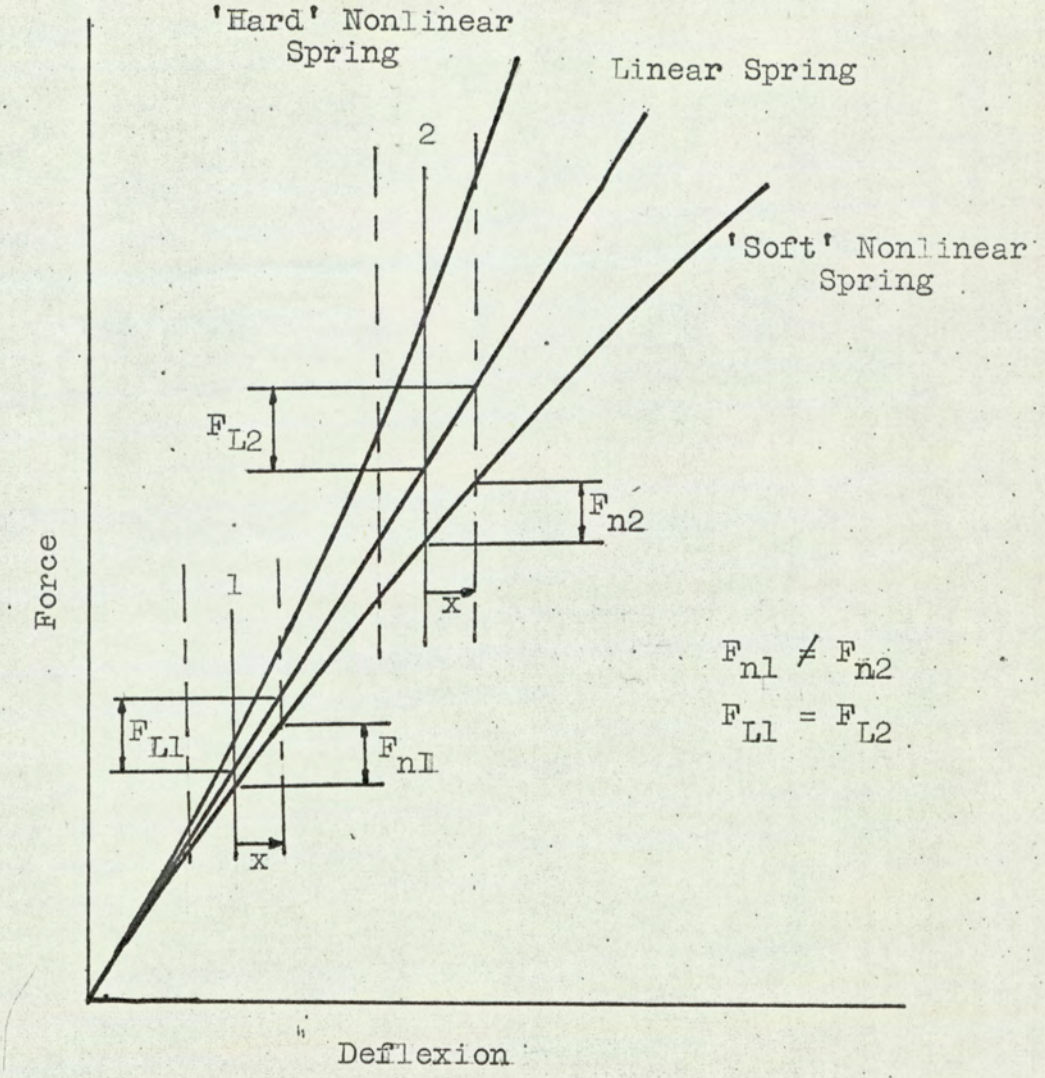

Spring Characteristics.

FIG.8

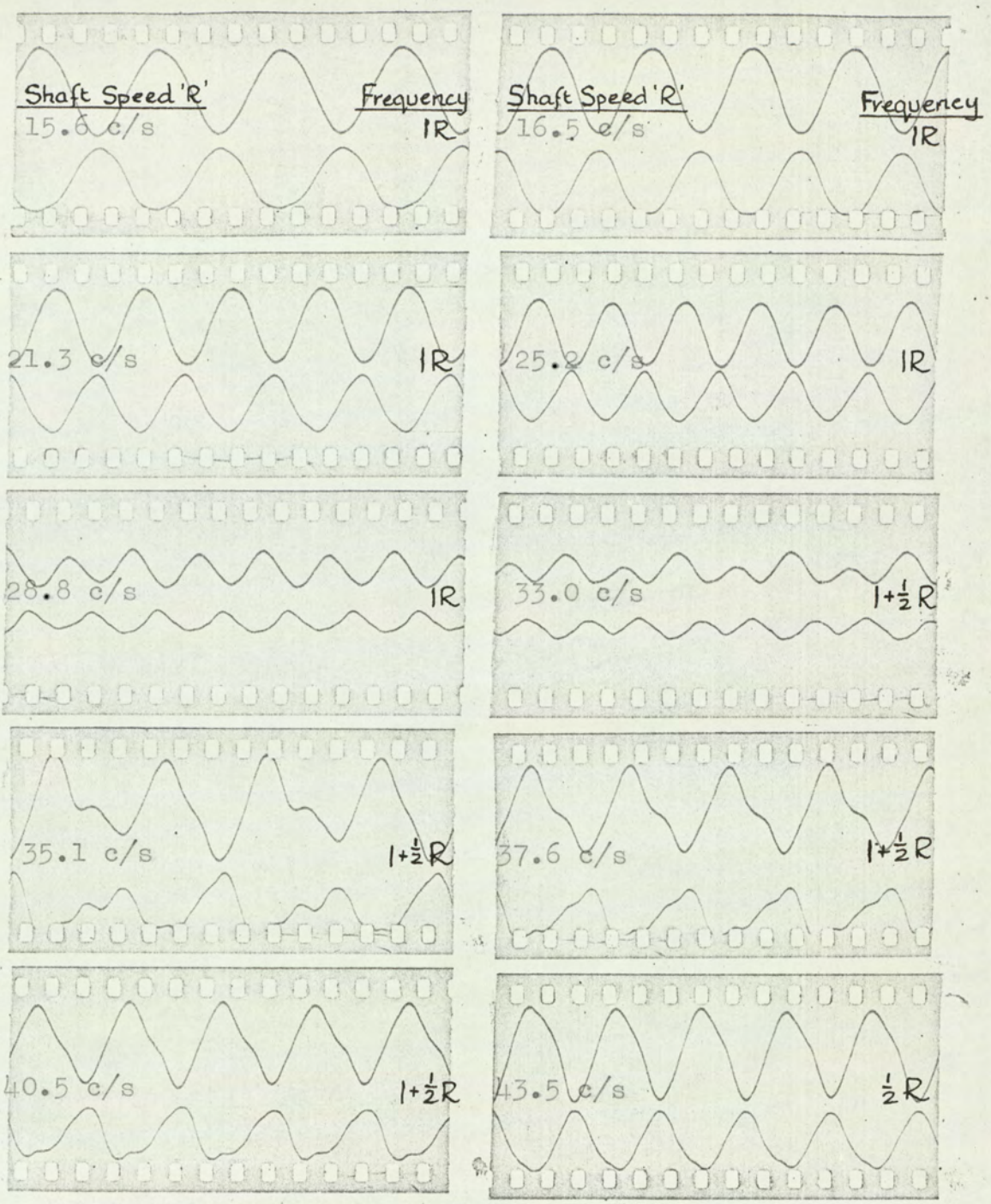

Recorded Waveform of Horizontal Displacements

(Bearings set 6 in. apart)

FIG.9a

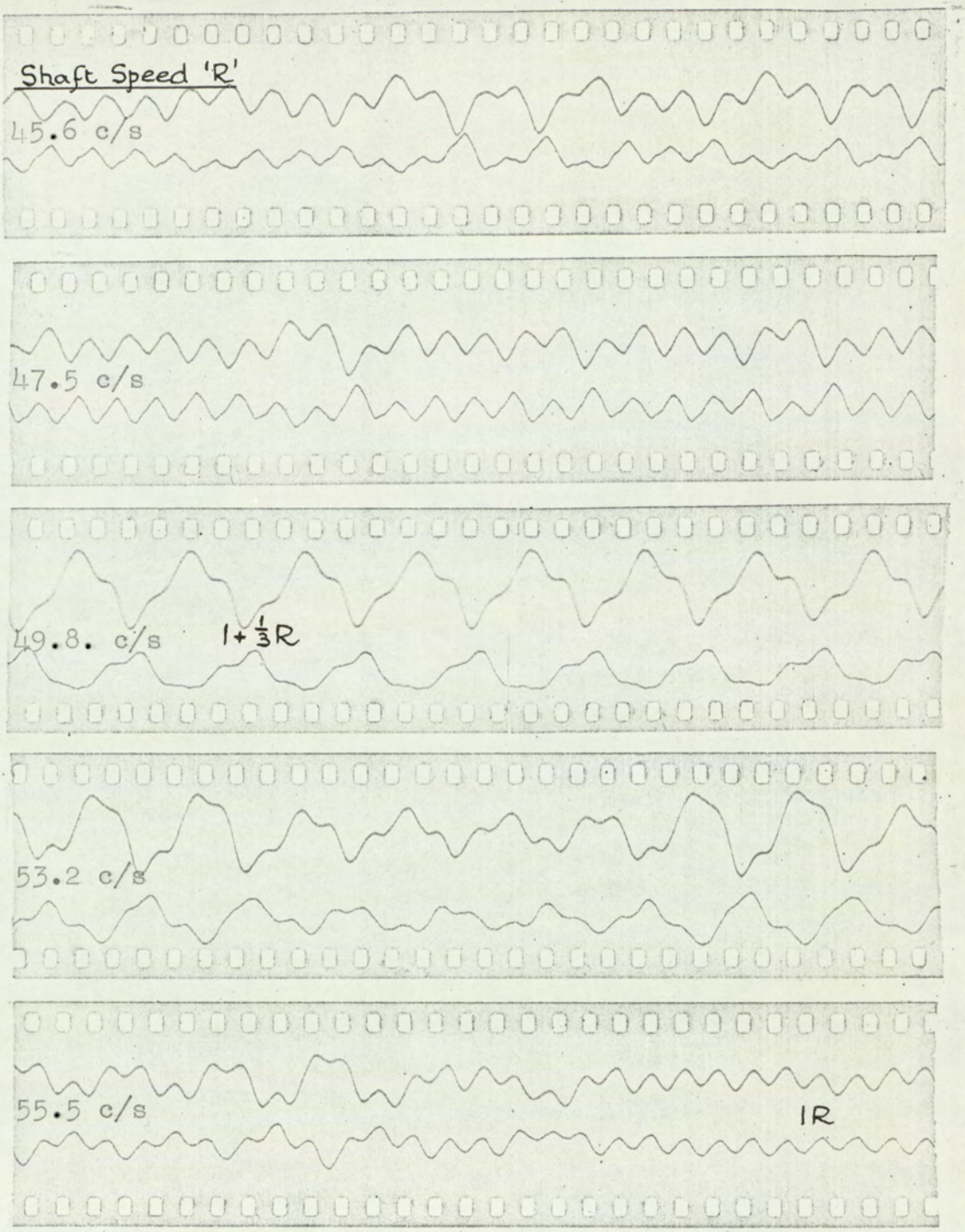

Recorded Waveform of Horizontal Displacements

(Bearings set 6 in. apart)

N.B. amplitudes at 49.8 c/s. and onwards half full size

FIG.9b

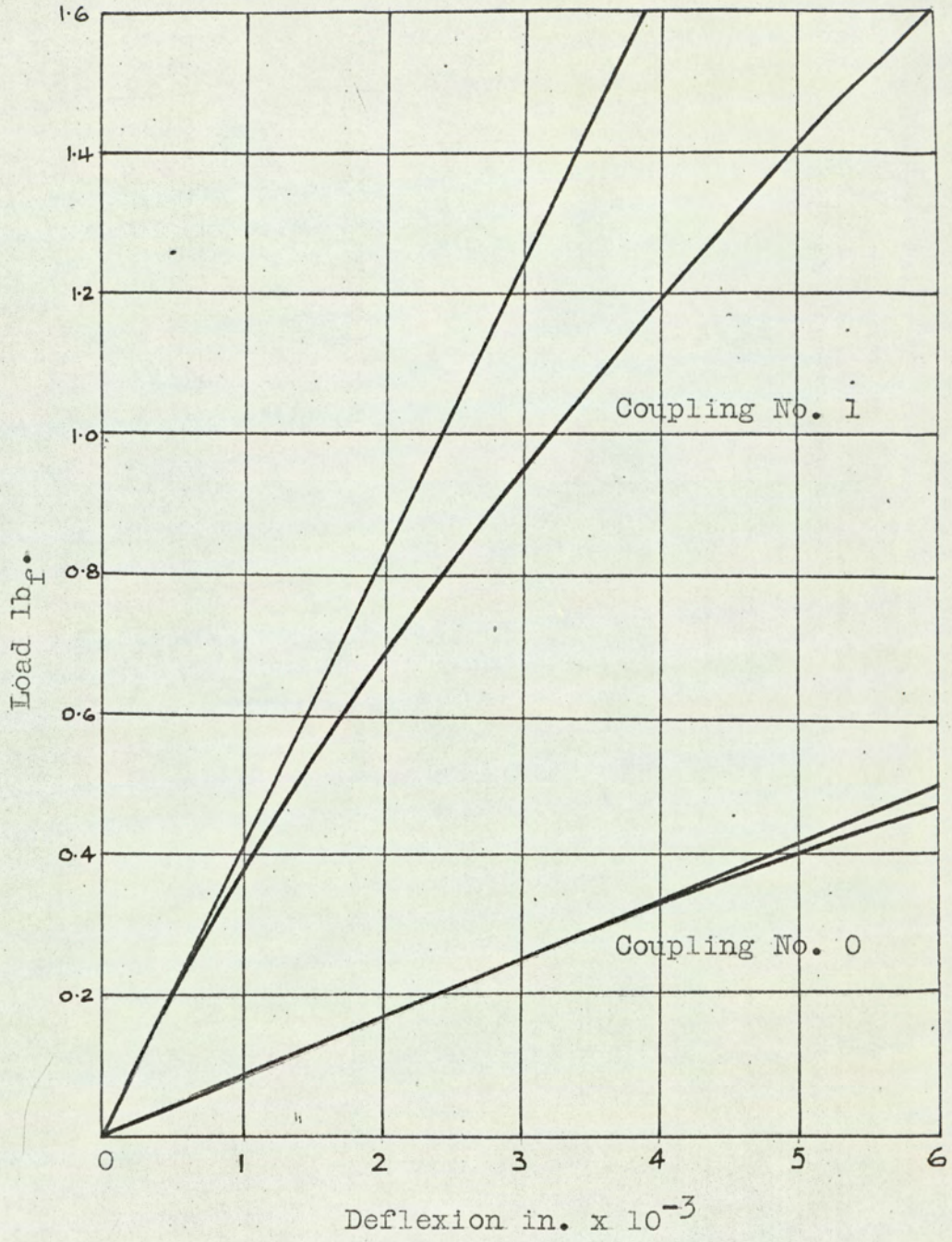

Spring Characteristics of Couplings.

FIG. 10

Vertical Amplitude versus Shaft Speed
Rotor 'A'

FIG 11

Horizontal Amplitude versus Shaft Speed
Rotor 'A'
Amplitude in. x 10^{-3}
6
5
4
3
2
1
0
20
40
60
80
100
120
140
160
180
Shaft Speed C/S
ω_n
$2\omega_n$
$3\omega_n$
$4\omega_n$
4.5in. Brg. Centres.
$\omega_n^2 = 20000 - 238 \times 10^6 A^2$

FIG 12

Vertical Amplitude versus Shaft Speed
Rotor 'B'
Amplitude in. x 10^{-3}
Shaft Speed C/S
4.5 in. Brg. Centres.
$\omega_n^2 = 20000 - 238 \times 10^6 A^2$
ω_n
$2\omega_n$
$3\omega_n$
$4\omega_n$
0
20
40
60
80
100
120
140
160
180
1
2
3
4
5
6

FIG 13

Horizontal Amplitude versus Shaft Speed

Rotor 'B'

FIG 14

Vertical Amplitude versus Shaft Speed
Rotor 'A'

FIG 15

Horizontal Amplitude versus Shaft Speed
Rotor 'A'
Amplitude in. x 10^{-3}
6
5
4
3
2
1
0
20
40
60
80
100
120
140
160
180
Shaft Speed C/S
ω_n
$2\omega_n$
$3\omega_n$
$4\omega_n$
6 in. Brg. Centres.
ω_n^2 23100 - 276 x$10^6 A^2$

FIG 16

Vertical Amplitude versus Shaft Speed

Rotor 'B'

FIG 17

Horizontal Amplitude versus Shaft Speed

Rotor 'B'

FIG 18

Vertical Amplitude versus Shaft Speed.

Rotor 'A'

FIG. 19

Horizontal Amplitude versus Shaft Speed

Rotor 'A'

FIG. 20

Vertical Amplitude versus Shaft Speed

Rotor 'B'.

FIG. 21

Horizontal Amplitude versus Shaft Speed.

Rotor 'B'

FIG. 22

Vertical Amplitude versus Shaft Speed.

Rotor 'A'

FIG. 23

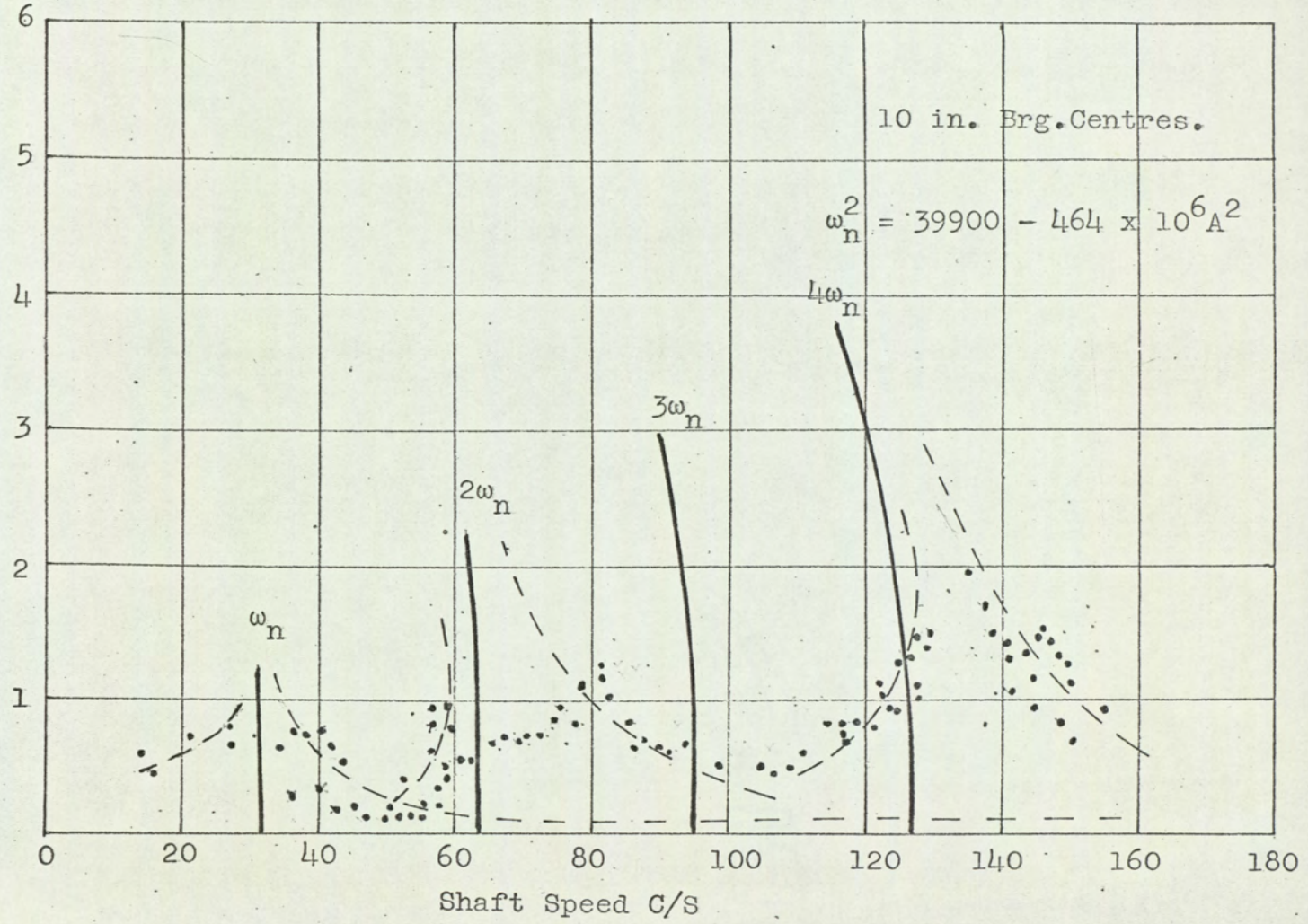
Horizon Amplitude versus Shaft Speed
Rotor 'A'
Amplitude in. x 10^{-3}
Shaft Speed C/S
10 in. Brg.Centres.
$\omega_n^2 = 39900 - 464 \times 10^6 A^2$
ω_n
$2\omega_n$
$3\omega_n$
$4\omega_n$
0
20
40
60
80
100
120
140
160
180
1
2
3
4
5
6

FIG. 24

Vertical Amplitude versus Shaft Speed

Rotor 'B'

FIG. 25

Horizontal Amplitude versus Shaft Speed

Rotor 'B'

FIG. 26

Vertical Amplitude versus Shaft Speed

Rotor 'A'

FIG. 27

Horizontal Amplitude versus Shaft Speed

Rotor 'A'

FIG. 28

Vertical Amplitude versus Shaft Speed

Rotor 'B'

FIG. 29

Horizontal Amplitude versus Shaft Speed

Rotor 'B'

FIG. 30

Table I

Natural Frequencies without Rotation.

Bearing Centres in.	1st. and 2nd. Positive Calculated Natural Freq. without Rotn. c/s		Measured Nat. Frequency Without Rotn. c/s	
	ω_1	ω_2	ω_1'	ω_2'
12	94.3	120	95.0	
10	80.0	113	81.8	
8	72.5	96.1	73.6	
6	67.0	82.0	68.3	
4.5	64.0	76.0	63.5	

Table II

Critical Whirling Speeds.

Bearing Centres in.	Calculated Critical Whirling Speeds c/s				Measured Critical Whirling Speeds c/s			
	Forward		Reverse		Forward		Reverse	
	ω_1	ω_2	ω_3	ω_4	ω_1	ω_2	ω_3	ω_4
12	126·5	196·5	78·0	110·0	–	–	–	–
10	97·3	141·4	70·0	96·0	96·0	–	–	–
8	84·3	115·5	65·0	83·5	85·0	–	–	–
6	74·0	95·5	60·0	75·0	76·2	–	–	–
4.5	67·3	71·8	55·0	66·0	68·3	–	–	–

PART TWO.

Notation

F_1, F_2 Q_1, Q_2	Hydrodyamic oil forces
R	Radius of bearing
$F = 2Mg$	Total external load
n	Eccentricity ratio
c	Radial clearance
ω	Angular velocity
φ	Attitude angle
p	Lubricant film pressure
l	Bearing length
$2b = L$	Length of shaft between bearing centre
A	Diametral moment of inertia of system
C	Polar moment of inertia of system
$\dot{\beta}$	Angular velocity of precession
θ	Arbitrary angle
θ	Precession angle
μ	Viscosity reyns
ρ	Mass density
h	Oil film thickness
h_1, h_2, h_3	Angular momentum
$\omega_1, \omega_2, \omega_3$	Instantaneous angular velocity

PART TWO.

1. Summary.

During the investigation described in part one a phenomenon was observed where, as a result of increasing the oil flow the shaft became unstable.

An investigation of this phenomenon, where the shaft was observed to suddenly whirl in contact with the bearings, the two rotors moving in antiphase at half the shaft rotational speed, is reported. The source of the phenomenon is attributed to a rubber flexible drive coupling which causes the rotors to move in antiphase and the gyroscopic couples to take control of the shaft motion.

When "instability" arose at shaft speeds above the lowest out-of-balance critical whirling speed, two resonances of small amplitude were observed. The first resonance was found to be a reverse whirl and the second a forward whirl. In both cases the resonance occured at shaft speeds in good agreement with the calculated out-of-balance reverse and forward critical whirling speeds.

Neglecting external forces, a theory has been propounded which, provided the lubricant viscosity is known accurately, predicts the shaft speed at the onset of "instability".

2. Description of System and Experimental Technique

2.1. Description of System.

The shaft-rotor assembly and drive system described in section 2.1. of part one is used for the second series of tests. With no restriction on the oil flow tests are carried out to investigate the effect of,

1. bearing clearance.
2. bearing geometry (oil grooving).

and 3. viscosity.

on the shaft behaviour.

Bearings 1 in. long and nominally 1 in. diameter of diametral clearance 0.003 in., 0.005 in. and 0.010 in. are used. The 0.003 in. diametral clearance bearing is machined with a central circumferential oil groove 0.080 in. deep by 0.125 in. wide. Two sets of bearings of 0.005 in. and 0.010 in. diametral clearance are manufactured, one set machined with a single central circumferential groove as with the 0.003 in diametral clearance bearing and the other machined with a single axial groove 3/4 in. long by 0.125 in. wide by 0.080 in. deep along and equal length both sides of the oil inlet hole. The axial groove bearings are manufactured by first boring the inside diameter of the bearings oversize and inserting a sleeve in which a slot (axial groove) is machined. The bearings are then bored to the required

dimension. After tests with these bearings a central circumferential groove was machined in the axial grooved 0.005 in. and 0.010 in. diametral clearance bearings and the tests repeated. The oil inlet hole for all the types of bearings is 0.125 in. diameter and positioned 45° from the vertical on the unloaded portion of the bearing.

Fig 31. shows a plot of the viscosity-temperature relationship of the different oils used in the tests. Oil temperatures are obtained from Chromel-Constaintin thermocouples close to bearing in the inlet and outlet oil pipes. Recordings of the oil temperature in millivolts are taken from a Pye Thermocouple Test Set. These recordings are converted to degrees Centigrade from a temperature millivoltage calibration of the thermocouples.

Measurements of rotor displacements are obtained using the inductive type displacement pick ups described in section 2.1. of part one. Attempts to measure the shaft displacement within the bearings met with failure. Inductive type pick-ups consisting of two coils wound on ferrite dust cores inserted in 3/8 in. B.S.F. screws were made.

The coils were so positioned in the screws as to give maximum sensitivity and to be approximately linear over the small shaft movement within the bearings.

Calibration was performed in situ with the pick-ups screwed into bearings flush with the bore by supporting the shaft and rotating the bearing through 180^{o} on the shaft. This ensured that the pick-ups were subjected to a displacement equivalent to the bearing clearance.

The sensitivity of these pick-ups was considerably less than that of the rotor pick-ups. It was found that a low attenuation of the carrier amplifier was neccessary to obtain a trace of sufficient amplitude for recording purposes.

Because of the low attenuation, balancing (electrical) of the pick-up-bridge system was critical. Fine balancing could not be effected and the waveform of displacements as observed on C.R.O consisted of a trace representing the shaft displacement and superimposed on this, a trace of frequency equal to twice the frequency of the carrier signal from the carrier amplifier. It was neccessary therefore to filter out this high frequency signal. A filter was required which besides reducing the level of the high frequency signal, would not attenuate the signal representing the shaft displacement.

To this end a twin-T filter was considered to be most satisfactory and was accordingly designed (See Appendix VI) for the system.

However when tests were carried out with the pick-ups in position they failed, presumably to shock loading. No further time could be spent on modifications and only rotor displacements were recorded. During tests carried out in part one the time spent on recording and developing film of rotor displacements was found to be excessive. A considerable reduction in time was obtained when the waveforms were recorded with an Ultra Violet Recorder.

2.2. Experimental Techique.

Recordings of the rotor displacement waveform and oil temperature were taken at constant shaft speed settings. The shaft speed was increased in increments, recordings being taken at each increment of speed until the shaft was observed to become unstable. The speed was then increased to determine the speed range, if any, of the unstable motion. The shaft speed at which the stable motion resumed, upon decrease of speed, was also recorded.

Once the general behaviour of the shaft motion had been observed, efforts were concentrated on accurately determining the oil temperature just before the shaft became unstable. The aim being to establish a stability criterion. This involved running the shaft at a speed where it was considered likely to become unstable and taking continuous recordings of

temperature until the shaft became unstable. With the Pye Thermocouple Test Set it was only possible to record one temperature at a time and therefore a temperature difference could arise in the time taken between the first recording and the last, (six temperature recordings were required). However it was considered the method of repeatedly taking temperature recordings would to a large extent obviate this possible source of error.

A technique which enabled a frequency analysis of the rotor displacement to be performed with a wave analyser was to record the signal from the pick-ups on a Tanberg tape recorder and then transfer the signal to a Southern Instruments multi-channel, record-playback loopdeck system. The signal was then fed into a Brüel and Kjær wave analyser, where a frequency analysis was performed automatically.

However, because of the level of the signal voltage required to record a signal on the tape recorder, it was only possible to use this techique with a signal of the unstable motion.

Thus it was more convenient to analyse the waveforms manually from traces obtained with the Ultra Violet recorder. The main issue being in determing the frequency, and direction of whirl of the unstable motion.

3. Analytical Treatment.

3.1. Determination of Oil Film Forces.

The oil forces acting on the journal are determined in two perpendicular directions using Reynolds equation and Ocvirks (39) short bearing approximation.

Reynolds equation, as derived by Shaw and Macks (40) for a journal whose centre position O (see Fig 32) is time dependent is

$$\frac{1\partial}{R\partial\theta}\left(\frac{h^3\partial p}{R\partial\theta}\right) + \frac{\partial}{\partial z}\left(h^3\frac{\partial p}{\partial z}\right) = 6\mu(\omega-2\dot{\varphi})\frac{\partial h}{\partial\theta} + 12\mu c\dot{n}\cos\theta$$

3.1.(1)

where it is assumed the lubricant viscosity is constant throughout the oil film.

As a first step towards obtaining the oil forces, it is neccessary to determine the pressure distribution in the oil film. Equation 3.1.(1) is insoluble for p in closed form and therefore cannot be used directly. For short bearings i.e. whose length to diameter ratio is 1 or less, Ockvirk has shown reliable results may be obtained by ignoring the first term of the left hand side of equation This approximation is based on the assumption that if the effect of the oil flow due to the relative motion

of the surfaces is considered large relative to that due to the action of the pressure gradient, the neglect of the latter is justified.

Equation 3.1.(1) thus becomes for short bearings

$$\frac{\partial}{\partial z}\left(h^3\frac{\partial p}{\partial z}\right) = 6\mu(\omega-2\dot{\phi})\frac{\partial h}{\partial \theta} + 12\mu c\dot{n}\cos\theta \qquad 3.1.(2)$$

Integrating twice with respect to z and putting p=0 at z=0 and at z=1 gives,

$$p = \frac{z(z-1)(12\mu c\dot{n}\cos\theta - 6\mu(\omega-2\dot{\phi})cn\sin\theta)}{2c^3(1+n\cos\theta)^3} \qquad 3.1.(3)$$

use having been made of the substitution $h = c(1+n\cos\theta)$

A double integration of equation 3.1.(3), with the appropriate limits will give the force exerted on the journal by oil film. However a difficulty arises here as to the extent of the oil film. Integrating between the limits $\theta=0$ and $\theta=\pi$ i.e. assuming the bearing clearance to be completely filled with lubricant, gives rise to a pressure distribution which is positive over the converging region (shown shaded in Fig.32) and negative over the diverging region. Experiments tend to show for a plain journal bearing having no pressurized oil supply, that although oil

may exist in the diverging region it will be discontinuous, air having segregated from solution or been entrained due to the existence of sub-atmospheric pressure.

Ocvirk has demonstrated that for a stable journal centre a convenient and reliable simplification is to assume that no oil exists over the diverging region.

Hence, assuming the oil film pressure to be positive and exist only over the converging region i.e. $\theta=0$ to $\theta=\pi$, by resolving parallel to the displacement of the bearing centre (F_1) and perpendicular to the former (F_2) the oil forces are obtained as follows.

$$F_1 = R\int_0^l\int_0^\pi p\cos\theta \, d\theta dz \qquad 3.1.(4)$$

$$F_2 = R\int_0^l\int_0^\pi p\sin\theta \, d\theta dz \qquad 3.1.(5)$$

Consider equation 3.1.(4), integrating by parts gives,

$$F_1 = R\int_0^l (p\sin\theta)_0^\pi \, dz - R\int_0^l\int_0^\pi \frac{dp}{d\theta}\sin\theta \, d\theta dz$$

Now

$$p = 0 \text{ at } \theta = 0 \text{ and } \theta = \pi$$

therefore

$$F_1 = -R\int_0^l\int_0^\pi \frac{dp}{d\theta}\sin\theta \, d\theta dz$$

Differentiating equation 3.1.(3) gives,

$$\frac{dp}{d\theta} = \frac{6\mu z(z-1) -(2c\dot{n}\sin\theta - (\omega-2\dot{\varphi})cn\cos\theta)}{2c^3(1 + n\cos\theta)^3}$$

$$+\frac{6\mu z(z-1)(c\dot{n}\cos\theta - (\omega-2\dot{\varphi})cn\sin\theta)3n\sin\theta)}{2c^3(1 + n\cos\theta)^4} \qquad 3.1.(6)$$

Hence

$$F_1 = -R\int_0^1\int_0^{\pi} \frac{6\mu z(z-1)}{2c^3}\left[\frac{-(2c\dot{n}\sin\theta + (\omega-2\dot{\varphi})cn\cos\theta)}{(1+n\cos\theta)^3}\right.$$

$$\left. + \frac{(2c\dot{n}\cos\theta-(\omega-2\dot{\varphi})cn\sin\theta)3n\sin\theta}{(1+n\cos\theta)^4}\right]\sin\theta d\theta dz$$

3.1.(7)

Use is now made of the Sommerfeld substitution (see Barwell(40))

$$\cos\varphi = \frac{n + \cos\theta}{1 + n\cos\theta}$$

Substitution in equation 3.1.(7) gives upon performing the first integration

$$F_1 = -\frac{\mu R1^3}{2c^2}\int_0^{\pi}\left(-2\dot{n}\left(\frac{n-\cos\varphi}{1-n\cos\varphi}\right) + \left(\frac{(\omega-2\dot{\varphi})n\sqrt{(1-n^2)(1-\cos^2\varphi)}}{1-n\cos\varphi}\right)\right.$$

$$\left. \times \frac{3n(1-n^2)(1-\cos^2\varphi)(1-n^2)^{1/2}}{(1-n\cos\varphi)^2(1-n\cos\varphi)}\right) d\varphi$$

$$+\frac{\mu R1^3}{2c^2}\int_0^{\pi}\left(-\frac{2\dot{n}\sqrt{(1-n^2)(1-\cos^2\varphi)}}{1-n\cos\varphi} - \left(\frac{(\omega-2\dot{\varphi})n(n-\cos\varphi)}{1-n\cos\varphi}\right)\right.$$

$$\left. \times \frac{\sqrt{(1-n^2)(1-\cos^2\varphi)}(1-n^2)^{1/2}}{(1-n\cos\varphi)^2}\right) d\varphi \qquad 3.1.(8)$$

Upon integration, equation 3.1.(8) becomes,

$$F_1 = -\frac{\mu R l^3}{2c^2}\left\{\frac{2n^2(\omega-2\dot{\varphi})}{(1-n^2)^2} + \frac{\pi(1+2n^2)\dot{n}}{(1-n^2)^{5/2}}\right\} \qquad 3.1.(9)$$

Similarly it may be shown

$$F_2 = \frac{\mu R l^3}{2c^2}\left\{\frac{\pi n(\omega-2\dot{\varphi})}{2(1-n^2)^{3/2}} + \frac{4n\dot{n}}{(1-n^2)^2}\right\} \qquad 3.1.(10)$$

Equations 3.1.(9) and 3.1.(10) are the same as those deduced by Holmes (33) and Huggins (35).

The assumptions made in arriving at these oil forces are,

1. The bearings are sufficiently short to allow the first term of the left hand side of equation 3.1.(1) to be neglected.
2. There is no pressurized oil supply to the bearings.
3. The viscosity is constant throughout the lubricant film.
4. The lubricant film is of 180° arc.
5. The inertia force of the lubricant may be neglected.
6. The oil film thickness is small and the effect of the film curvature may be neglected.
7. The variation of pressure across the film

thickness is negligible.

8. The oil flow in the bearing is laminar.
9. Oil forces due to viscous drag are negligible compared with the pressure forces.
10. The lubricant is incompressible.

Of the assumptions, numbers 3,5, and 8 are most likely to suffer from practical considerations.

It is unlikely that the lubricant viscosity is constant throughout the lubricart film. Under test conditions it is possible to allow the bearing to reach a steady running temperature, but even so the temperature (and thus viscosity) of the lubricant in the bearing will vary along the arc of the lubricant film. However the assumption is neccessary in order that Reynolds equation may be formulated.

Attempts have been made therefore to obtain an expression for the effective viscosity (constant) of the film lubricant in terms of the lubricant temperature. One such expression, propounded by Cameron, which gives reliable results is,

$$T_{Eff} = Ti + 0.8\ (T_o - T_i)$$

where

T_{Eff} = effective temperature of lubricant.

T_i = inlet temperature of lubricant to the bearing

T_o = outlet temperature of lubricant from the bearing.

It is usual engineering practice to use bearings whose diametral clearance is calculated as being 0.001 in./in. diameter of the journal. With modern day turbo-generator sets, journal diameters of 20 in. are not unusual. This would normally mean using bearings with a diametral clearance of 0.020 in. The inertia forces arising in such an oil film of such a bearing could be appreciable (the magnitude depending largely on the rotational speed) and could invalidate assumption No.5.

The rotational speed range for laminor flow is determined from Taylors (41) criterion viz.

$$R_e = \frac{\rho V c}{\mu}$$

where

ρ = density of lubricant.

μ = viscosity of lubricant.

V = relative velocity of journal to bearing

R_e = critical Reynolds number.

c = radial clearance.

However, because of bearing geometry (oil grooving etc) it is possible that the speed range of the laminar flow regime will be considerably reduced.

Thus the design running speed of a particular machine could be in the turbulent regime if this is the case the theory will not hold true.

For this investigation all the assumptions are considered to be valid. Treatments on the effect of inertia forces can be found by Barlow (39) and of a journal operating in the turbulent regime by Constantinescu. (40).

Rigid Body Theory-Steady Uniform Precession.

Consider the case where the shaft takes up the position shown in Fig.33a. The only external forces are those due to the oil film, i.e. the shaft-rotor assembly is considered to be perfectly balanced, any spring force arising from the drive coupling is assumed to be negligible compared with the oil forces. Also the shaft is assumed to be rigid and the two rotors to move in antiphase to each other.

Fixed axes OXYZ are set up at midspan, 'O' being at the centre of the shaft and OZ drawn parallel to the centreline of the bearings.

The positions of three mutually perpendicular axes in a general displacement of the system (see Fig 33b) are represented by Ox, Oy' and Oz' and are determined by imagining first a rotation β' in YX plane about the Z axis and then a rotation θ' in the yZ plane about the displaced x axis. The shaft is then assumed

to rotate about the z' axis with angular velocity ω. These axes are principal axes because of the geometric symmetry of the rotors and move so that Oz is always coincident with Oz' and Ox remains in the plane ZOz.

The component angular velocities about the axes Ox, Oy' and Oz' represented by ω_1, ω_2 and ω_3 are

$$\omega_1 = \dot{\theta}' \qquad \omega_2 = \dot{\beta}'\sin\theta \qquad \omega_3 = \dot{\beta}'\cos\theta$$

The component angular momentum about these axes, represented by h_1, h_2 and h_3, are

$$h_1 = A\omega_1 \qquad h_2 = A\omega_2 \qquad h_3 = C\,(\omega_3 + \omega\,)$$

The external moments about 'O' arise from oil forces only. About the Oy' axis the moments are

$$-(Q_2\cos\varphi_2 + Q_1\sin\varphi_2)b + (F_2\cos\varphi_1 + F_1\sin\varphi_1)b$$

and about the Ox axis the moments are

$$-(Q_2\sin\varphi_2 + Q_1\cos\varphi_2)b + (F_1\cos\varphi_1 + F_2\sin\varphi_1)b$$

About the Oz' axis the moments are zero.

The momentum equations are thus,

$$A\ddot{\theta} - (A-C)\dot{\beta}^2\sin\theta\cos\theta + C\omega\dot{\beta}\sin\theta = -(Q_2\sin\varphi_2 + Q_1\cos\varphi_2)b + (F_1\cos\varphi_1 + F_2\sin\varphi_1)b \qquad 3.2.(1)$$

$$-A\ddot{\beta}\sin\theta - (2A-C)\dot{\beta}\dot{\theta}\cos\theta + C\omega\dot{\theta} = -(Q_2\cos\varphi_2 + Q_1\sin\varphi_2)b + (F_2\cos\varphi_1 + F_1\sin\varphi_1)b \qquad 3.2.(2)$$

$$C(\dot{\omega} - \dot{\beta}\dot{\theta}\sin\theta + \ddot{\beta}\cos\theta) = 0 \qquad 3.2.(3)$$

If the angular velocity ω is constant and the shaft is assumed to perform steady uniform precession then $\dot{\beta}$ and $\dot{\theta}$ are also constant. Thus equations 3.2.(1)and 3.2.(2) become,

$$\ddot{\theta} - (A-C)\dot{\beta}^2\sin\theta\cos\theta + C\omega\dot{\beta}\sin\theta = -(Q_2\sin\varphi_2 + Q_1\cos\varphi_2)b + (F_1\cos\varphi_1 + F_2\sin\varphi_1)b \qquad 3.2.(4)$$

and

$$0 = -(Q_1\sin\varphi_2 + Q_2\cos\varphi_2)b + (F_2\cos\varphi_1 + F_1\sin\varphi_1)b \qquad 3.2.(5)$$

Consider equation 3.2.(5).

At some stage during the shaft motion see Fig. 34

$$\varphi_2 = \varphi_1 = \varphi_o$$

Hence

$$0 = (F_1-Q_1)b\sin\varphi_o - (Q_2-F_2)b\cos\varphi_o \qquad 3.2.(6)$$

Therefore

$$\tan\varphi_o = \frac{Q_2 - F_2}{F_1 - Q_1}$$

Now when $\varphi_o = 45^o$

$$\tan\varphi_o = 1$$

Hence equation 3.2.(6) becomes,

$$F_1 + F_2 = Q_1 + Q_2 \qquad 3.2.(7)$$

Substituting for F_1, F_2, Q_1 and Q_2 gives,

$$\left[\frac{2n_1^2(\omega-2\dot{\varphi}_o)}{(1-n_1^2)^2} + \frac{\pi(1+2n_1^2)\dot{n}_1}{(1-n_1^2)^{5/2}}\right] + \left[\frac{\pi n_1(\omega-2\dot{\varphi}_o)}{2(1-n_1^2)^{3/2}} + \frac{4n_1\dot{n}_1}{(1-n_1^2)^2}\right]$$

$$= \left[\frac{2n_2^2(\omega-2\dot{\varphi}_o)}{(1-n_2^2)^2} + \frac{\pi(1+2n_1^2)\dot{n}_2}{(1-n_2^2)^{5/2}}\right] + \left[\frac{\pi n_2(\omega-2\dot{\varphi}_o)}{2(1-n_2^2)^{3/2}} + \frac{4n_2\dot{n}_2}{(1-n_2^2)^2}\right] \qquad 3.2.(8)$$

from which

$$\omega = 2\dot{\varphi}_o \text{ and } \dot{n}_2 = \dot{n}_1 = 0$$

Thus the shaft must whirl (precess) about the bearing centreline at half the rotational speed since $\dot{\varphi}_o = \dot{\beta}$ i.e. the equilibrium position lies along the bearing centres.

The amplitude of the precessional motion θ can be found by substituting

$$\omega = 2\dot{\varphi}_o \text{ and } \dot{n}_2 = \dot{n}_1 = 0$$

in equation 3.2.(4)

$$-(A-C)\dot{\beta}^2\sin\theta\cos\theta + C\omega\dot{\beta}\sin\theta = 0$$

Also $\omega = 2\dot{\beta}$

Therefore $$\cos\theta = \frac{2C\omega\dot{\beta}}{(A-C)\dot{\beta}^2}$$

Hence

$$\cos\theta = \frac{2C}{A-C} \qquad 3.2.(9)$$

3.3. The Equilibrium Position.

By equating the static load upon the journal, F and the static parts of the oil reactions F_1 and F_2

$$F^2 = F_1'^2 + F_2'^2$$

where

$$F_1' = -\frac{\mu R l^3 (2\omega n_o^2)}{2c^2(1-n_o^2)^2}$$

and

$$F_2' = \frac{\mu R l^3 (\pi\omega n_o)}{2c^2 2(1-n_o^2)^{3/2}}$$

hence

$$F = \frac{\mu R l^3 \omega n_o (\pi^2 - (\pi^2-16)n_o^2)^{1/2}}{2c^2(1-n_o^2)^2}$$

also

$$\tan\varphi_o = \frac{F_2'}{F_1}$$

$$= \frac{\pi(1-n_o^2)^{1/2}}{4n_o} \qquad 3.3.(1)$$

3.4. Calculated Results for the Experimental System.

3.4.1. Critical Speed.

The static eccentricity ratio n_o is first calculated from equation 3.1.(4) appropriate to the case when $\varphi_o = 45^o$ viz.

when

$$\varphi_o = 45^o \quad n_o = 0.618$$

The shaft speed is then calculated from equation 3.2.(10) with the substitution for n_o viz.

$$F = 2Mg = \frac{1.41\mu Rl^3\omega}{c^2}$$

or

$$\omega = \frac{2Mgc^2}{1.41\mu Rl^3} \qquad 3.4.1.(1)$$

Equation 3.4.1.(1) gives the shaft speed at which the shaft precesses at half the shaft speed.

3.4.2. Amplitude of Precessional Motion.

The amplitude is calculated from equation 3.2.(9), which for the system under consideration gives

$$\cos\theta = \frac{\pm 2R_r^2}{(L^2 - R_r^2)}$$

where

R_r = radius of rotor = 3.5 in.

L = length of centre of rotor to midspan of shaft

= 10 in.

hence

$$\cos\theta = 0.2794$$

whence

$$\theta = 73^{\circ}\ 50'$$

The amplitude at the rotor is thus given by $b\theta$.

4. Discussion of Theory.

The theory has been propounded assuming the shaft to perform steady uniform precession. Half shaft speed precession is predicted for a static eccentricity ratio of 0.618 which corresponds to a shaft speed of

$$\omega = \frac{2Mgc^2}{1.41\mu Rl^3}$$

The amplitude of the motion is given by $b\theta$ where $b=10$ in. and $\theta=73^{\circ}50'$. For the system under investigation this implies that the shaft will make contact with the bearings such that the theoretical amplitude will never be realized. Thus once the half speed precession is initated the shaft can be considered as being unstable i.e. at all shaft speeds above the 'critical' speed the shaft will precess at half the shaft speed and remain in contact with the bearings.

If it is assumed that each variable can be varied alone e.g. increase of bearing clearance does not alter

the lubricant viscosity, then equation 3.4.1.(1) predicts the stable range can be increased by,

1. Decrease of lubricant viscosity.
2. Decrease of bearing length.
3. Decrease of bearing radius.
4. Increasing the bearing load.
5. Increasing the radial clearance.

5. Discussion of Results.

Figs (35 and 36) show plots of amplitude and frequency of vibrations versus shaft speed for bearings of 0.005 in. and 0.010 in. diametral clearance respectively. The amplitude is representative of vibrations in both the vertical and horizontal directions. It can be seen that as the shaft speed is increased the amplitude of vibration remains approximately constant until a speed of frequency 65 c/s is approached, where a resonance appears. From an analysis of the waveforms (see Fig 37) at this speed, it was concluded that the shaft whirled in a reverse direction to that of the rotation, at shaft speed i.e. the vibrations in the horizontal direction led those in the vertical direction. The shaft speed at which the amplitude of the whirl is maximum agrees very well with the calculated speed (See Table II Part One).

Further increase of shaft speed shows a resonance

to occur at a speed of frequency 85 c/s. An examination of the waveform (see Fig 38) showed this to be a forward whirl. Agreement between the observed and the calculated forward critical speed (see Table II Part One) is very good.

The fact that the amplitude at the reverse and forward critical speed (of the order 0.0015 in.) is small is indicative of a well balanced shaft-rotor system.

As the speed is increased beyond the forward critical speed the amplitude decreases and then at a shaft speed of 110 c/s for the 0.005 in. diametral clearance bearings and 117.c/s for the 0.010 in. diametral clearance bearings the shaft becomes unstable, the amplitude being limited by the bearings. At these 'critical' speeds the frequency of vibration changed from that of shaft speed frequency to a half shaft speed.

Further increase of speed showed the amplitude to remain approximately constant and the frequency to remain at exactly half the shaft speed frequency. Upon decreasing the speed the amplitude of vibration decreases slightly until a speed of 72 c/s is reached where the amplitude drops suddenly to a much smaller level and the frequency of vibration changes from a half shaft speed to shaft speed frequency.

Results from all the tests showed that the shaft speed at the onset of "instability" was always greater

than the shaft speed at which the shaft became stable again. The speed range between the speed of onset of instability and stability was found to vary with the "depth" of instability i.e. the speed range would be small (of approxinately 5 c/s) if the shaft speed was reduced immediately the shaft became unstable while if the shaft speed was increased further after the instability, or allowed to remain constant for a time at the speed of onset of instability, the speed range would be considerable (See Fig.35 and 39). This phenomenon appears to be similar to the "inertia" effect described by Pinkus and Hori. The explanation offered here is;

For a given set of bearing conditions the speed of onset of instability is dependent on the viscosity of the lubricant. Now, once the shaft has become unstable the oil temperature increases (the viscosity decreases) because of the reduced oil flow when the shaft whirls around the bearing and therefore the speed must be reduced, bringing about an increase in the oil flow, until the viscosity is such that the shaft becomes stable. Increasing the shaft speed beyond the speed of onset of instability reduced the oil flow further and increased the "depth" of the instability. Hence in this case the shaft speed must be reduced considerably below speed of the onset of

instability before the shaft becomes stable.

In the majority of the tests the shaft became unstable at shaft speeds below the first calculated forward critical whirling speed, see Table III, it being only possible to exceed this speed by slowly increasing the shaft speed. This indicates that lower viscosity gives a higher stable operating region since the oil temperature will increase more rapidly the slower the increase in speed.

Table III shows a comparison between the measured and calculated critical (onset of instabilty) speed for the different types of bearings used. The effect of the different type of grooving appears merely to regulate the oil flow. Bearings with a single central groove were found to give the least oil flow, while bearings with the axial and circumferential grooves the greatest. This is shown by the value of the viscosity of the lubricant.

The effect of increase in the bearing diametral clearance is diguised to a large extent by the corresponding increase in oil flow which enables the bearings to run cooler, thereby decreasing the viscosity of the lubricant. Thus no comparison can be made directly between tests with bearings of different clearance. In some instances the onset of instability with larger bearing clearance occured at a lower shaft

speed than the onset speed with the smaller bearing clearance and vice versa. Generally though, where the viscosity of the lubricant is approximately the same for both types of bearing the onset speed is greater with the larger clearance bearings.

Agreement between the measured and the calculated speed of onset of instability is very good, considering that errors can arise in the measurement and determination of the effective viscosity of the lubricant. Temperature measurements were taken "just before" the shaft became unstable and because of the technique (see Experimental Technique) it is most likely for there to be a difference between the measured oil temperature and the actual oil temperature.

It was observed with large unbalance that no half shaft speed vibration (precession) occured below the out-of-balance critical speed. No records were taken with large unbalance for the amplitude of vibration was so great as the critical speed was approached that the system was shut down for safety.

Table IV shows the speed of onset of instability when the shaft was run in bearings of different diametral clearance. Good agreement was obtained with the results calculated for the larger bearing (i.e. the bearing with the higher lubricant viscosity). It would appear therefore that viscosity has the major influence

on the instability speed. Hence, with different clearance bearings an accurate knowledge of the lubricant viscosity of the two bearings is required before the instability speed can be predicted.

A frequency analysis of a recorded waveform during instability is shown in Fig 40 . A shaft speed frequency component has been analysed, which in this instance is expected as the shaft speed is close to the lowest critical whirling speed, although the waveform consisted mainly of half shaft speed frequency. The amplitude of the half order harmonic is approximately 3.2. times the amplitude of the harmonic component.

Fig 41 shows a film record of the whirling motion during instability at a shaft speed of 60 c/s. It can be seen to consist of one frequency only, namely half shaft speed frequency.

6. Conclusions.

1. With well balanced rotors the system is capable of performing uniform precession at half the shaft speed.
2. When the shaft precesses it becomes unstable
3. The shaft speed at the onset of instability can be predicated quite accurately from theoretical considerations based on the :

assumption that the shaft is perfectly balanced and supported by short journal bearings.

4. The stable operating region can be increased by i. increasing the bearing clearance

ii. decreasing the lubricant viscosity.

These findings agree with theoretical predictions and therefore it is reasonable to assume that the stable region can also be increased by

i. increasing the load on the bearings.

ii. decreasing the bearing length.

and iii. decreasing the bearing radius.

5. When instability arose at shaft speeds above the lowest calculated forward critical whirling speed the shaft would exhibit resonances at the calculated lowest reverse and forward critical whirling speed.

6. With large unbalance the shaft exhibited no half shaft speed precessional motion. Unbalance forces therefore, if of sufficient magnitude, tend to give stability, although it was found in the investigation that the amplitude of vibration was excessive as the critical forward whirling speed was approached.

7. Recommendations.

The theory propounded was based on the assumption that the shaft performed uniform precession. The precessional motion was thought to be instigated by the flexible drive coupling viz. when the hydrodynamic oil forces become zero the shaft should be supported by the bearings, the hydrostatic oil forces which would normally support the shaft are in this case negligible, but because of the coupling support the shaft is inclined to the horizontal axis so that gyroscopic couples which arise because of the inclination take control of the motion and the shaft precesses. The amplitude of the precessional motion was found to be excessive, the shaft behaved as though it was unstable. The reason for this was because of the relationship between the moment of inertia about a diameter at the midspan of the shaft (A) and the polar moment of inertia (C) of the system. For the system under investigation, with the two rotors overhung from the bearings. 'A' was much greater than 'C' and, as the theory predicted, this tends for a large precessional angle. Hence for a system such as the one investigated the choice of the coupling is extremely important.

According to the theory and verified experimentally, this phenomenon occurs only with an eccentricity ratio

of 0.618 and therefore it is essential to prevent the shaft from taking up this position if the phenomenon is to be avoided.

It has been shown the main contributory factor in preventing this type of "instability", or rather, extending the stable region, was lubricant viscosity; the lower the viscosity the greater is the stable operating region. Also it was observed that unbalance forces can prevent the system from becoming unstable although the amplitude at the critical speed could be excessive.

In designing a shaft-rotor system where it is neccessary for the rotor to be overhung from the bearings e.g. a turbo-charger, it is recommended

1. the shaft length between the bearings should be as small as is practicable.
2. the length of the overhung shaft should be as small as is practicable.
3. the radius of the rotors should be large.
4. the bearings should be narrow.
5. the radius of the bearing should be small.
6. the diametral bearing clearance should be large.
7. A low viscosity lubricant should be used.

Recommendations 1,2, and 3 will ensure that the ratio of the diametral moment of inertia to the polar moment of inertia is low and so reduce the amplitude of any

precessional motion. Recommendations 4 and 5 will, besides increasing the stable region effect an increase in the journal load which will also tend for stability. Recommendations 6 and 7 will give a greater stable operating region although it was found in the investigation that a large bearing clearance tended for high viscosity, because of the corresponding greater oil flow, and hence a reduction in the stable region.

The system under investigation was analogous to a turbo-charger, which in practice would experience a considerable difference in temperature between the turbine and compressor stages. Thus one bearing would run much cooler than the other. This effect has been investigated to some extent by running the system in two bearings of different diametral clearance. It was observed that the viscosity of the oil in one bearing was much greater than in the other, which would be expected in the practical case of a turbo-charger. It was found that the speed of onset of instabilty could be calculated from the bearing with the higher viscosity. Hence in a system where a temperture difference between two bearings is expected it is advisable to ensure that the cooler bearing has a high stable operating region.

Due to insufficient time it was not possible to investigate the signifiance of the effect of varying

the length of the bearings. It is considered however, that this is an important factor as, theoretically, the speed of onset of instability is proporational to $1/(\text{bearing length})^3$ and therefore should have a considerable influence on the stable operating region.

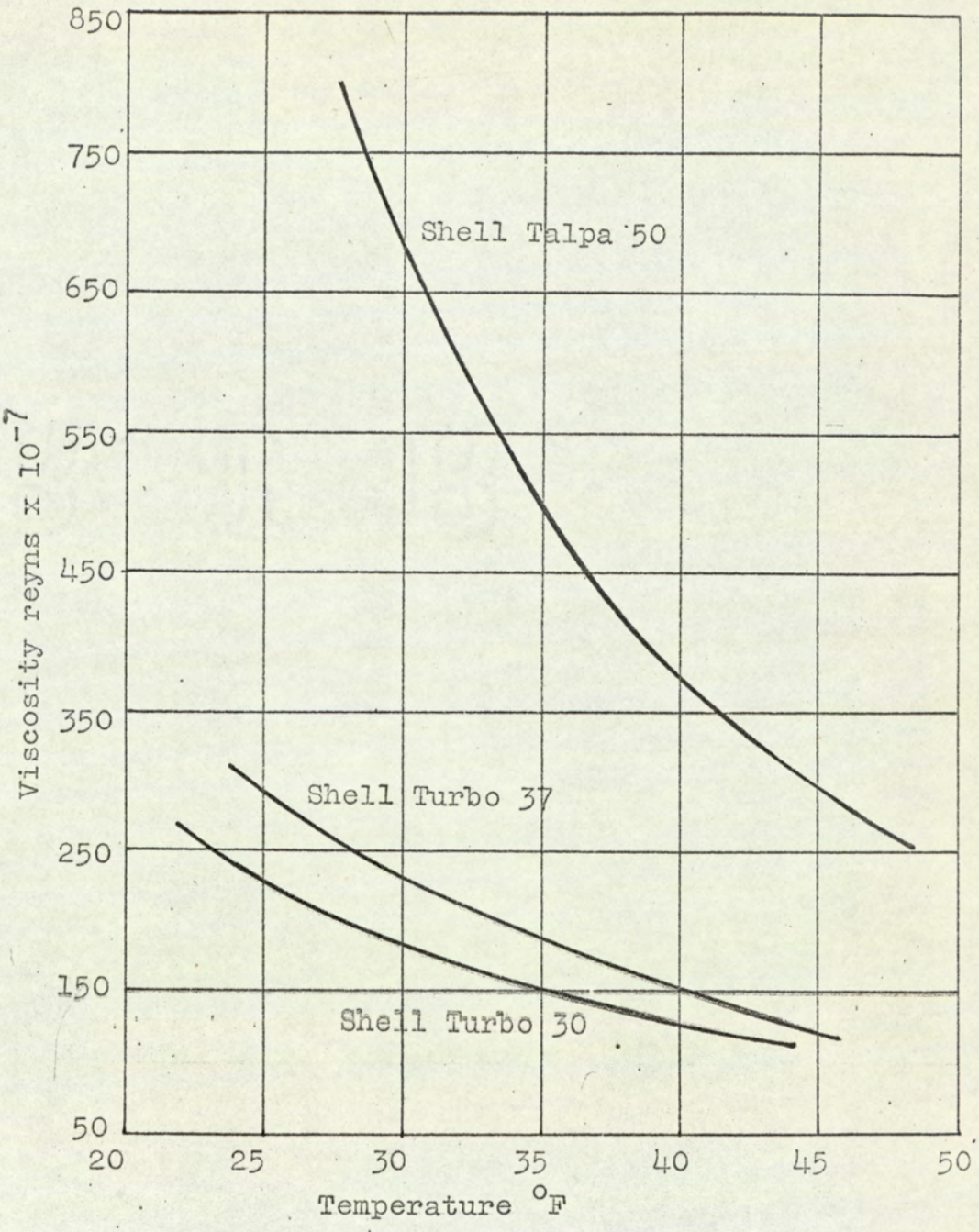
850
750
650
550
450
350
250
150
50
Viscosity reyns x 10^{-7}
Shell Talpa 50
Shell Turbo 37
Shell Turbo 30
20
25
30
35
40
45
50
Temperature °F

FIG. 31

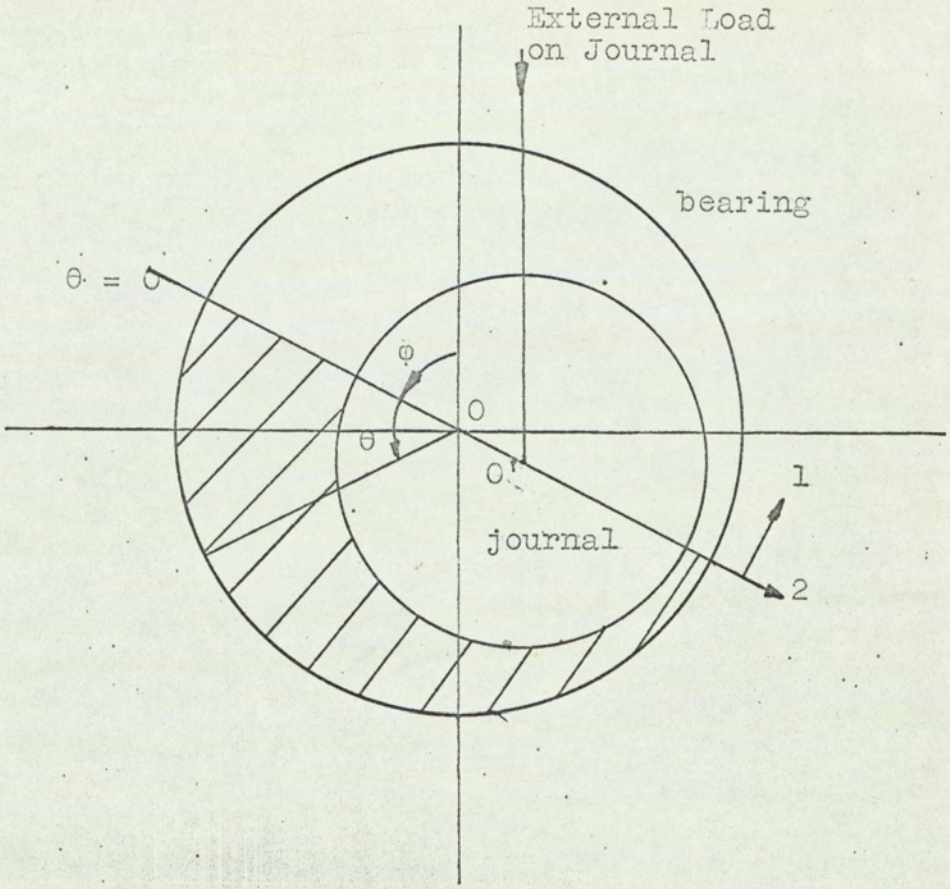

O represents the bearing centre

O' represents the journal centre

FIG. 32

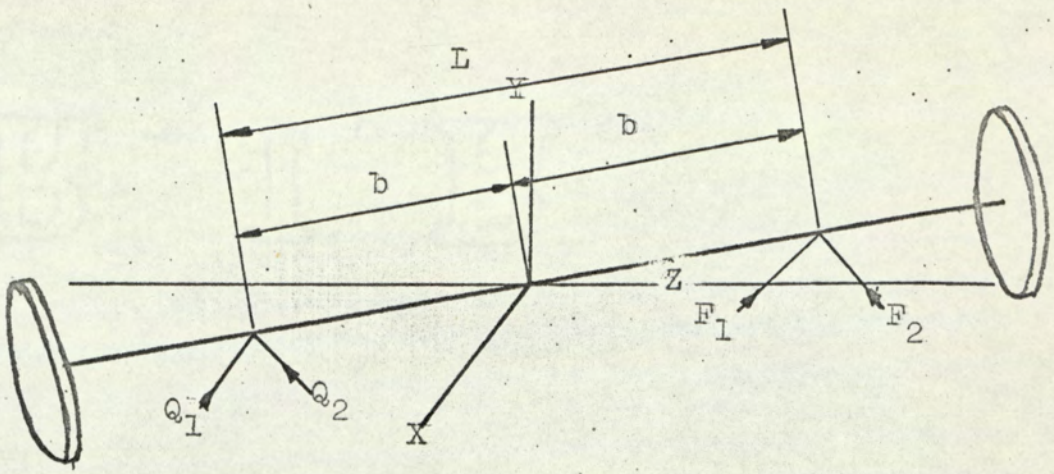

The Rigid Body Condition. FIG. 33a

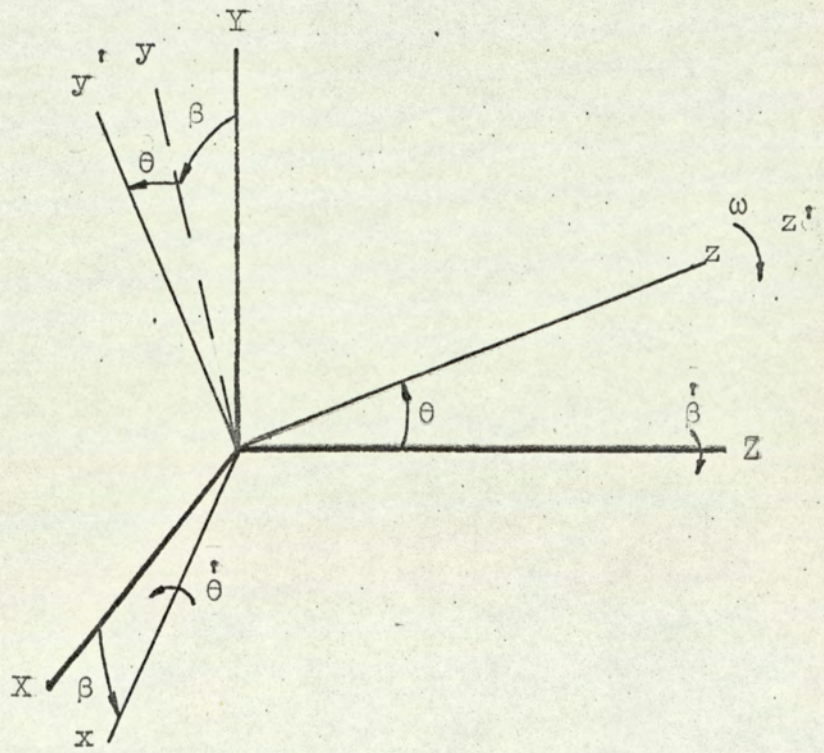

General Displacement of Principal Axes. FIG.33b

FIG. 33

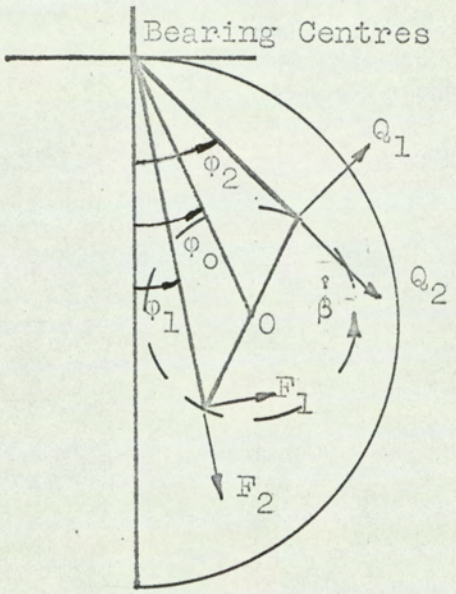

Shaft Describing Precessional Motion

Rotors Anti-Phase

FIG. 34

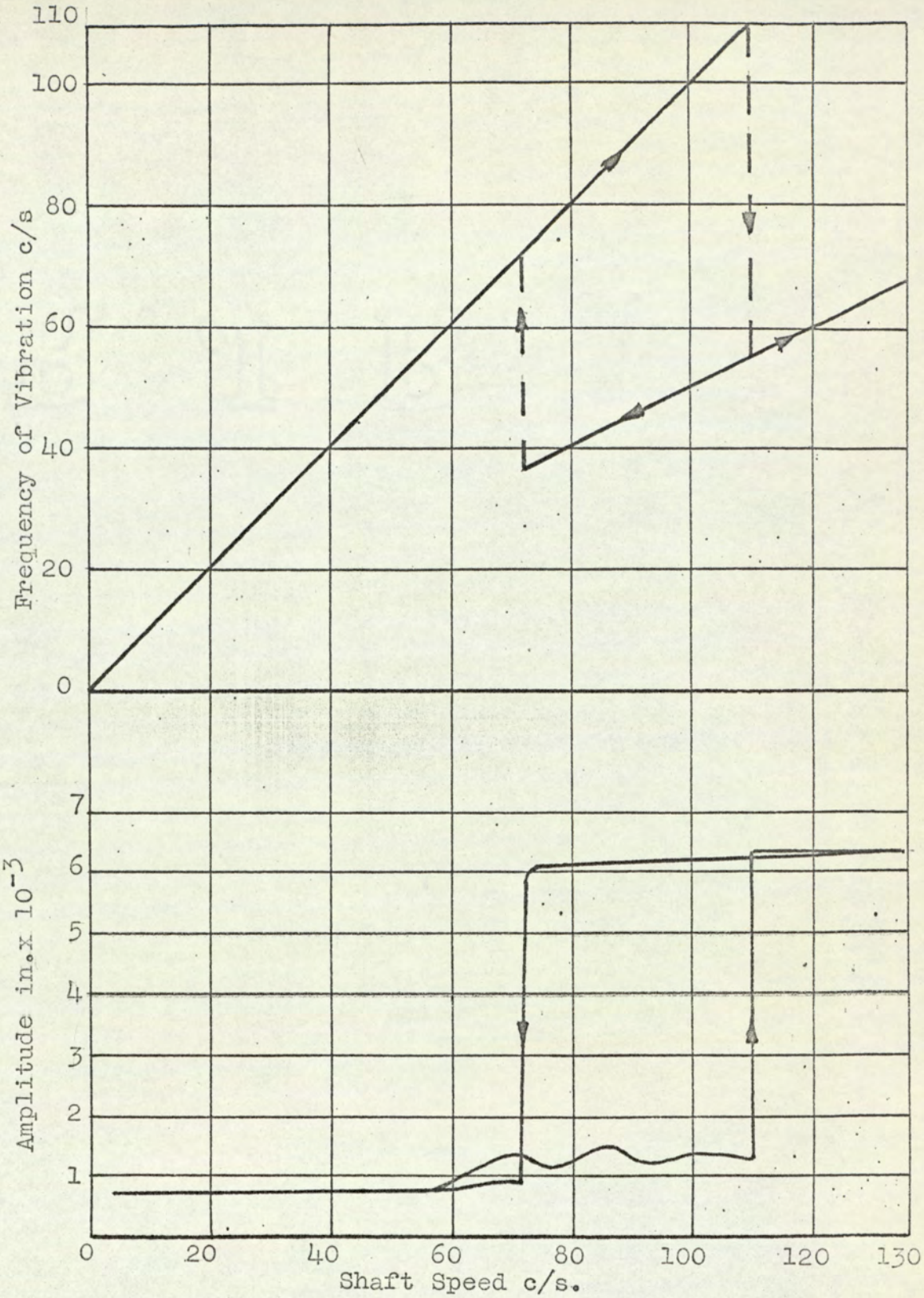

Amplitude and Frequency versus Shaft Speed
0.005 in. Diametral Clearance Bearing

FIG.35

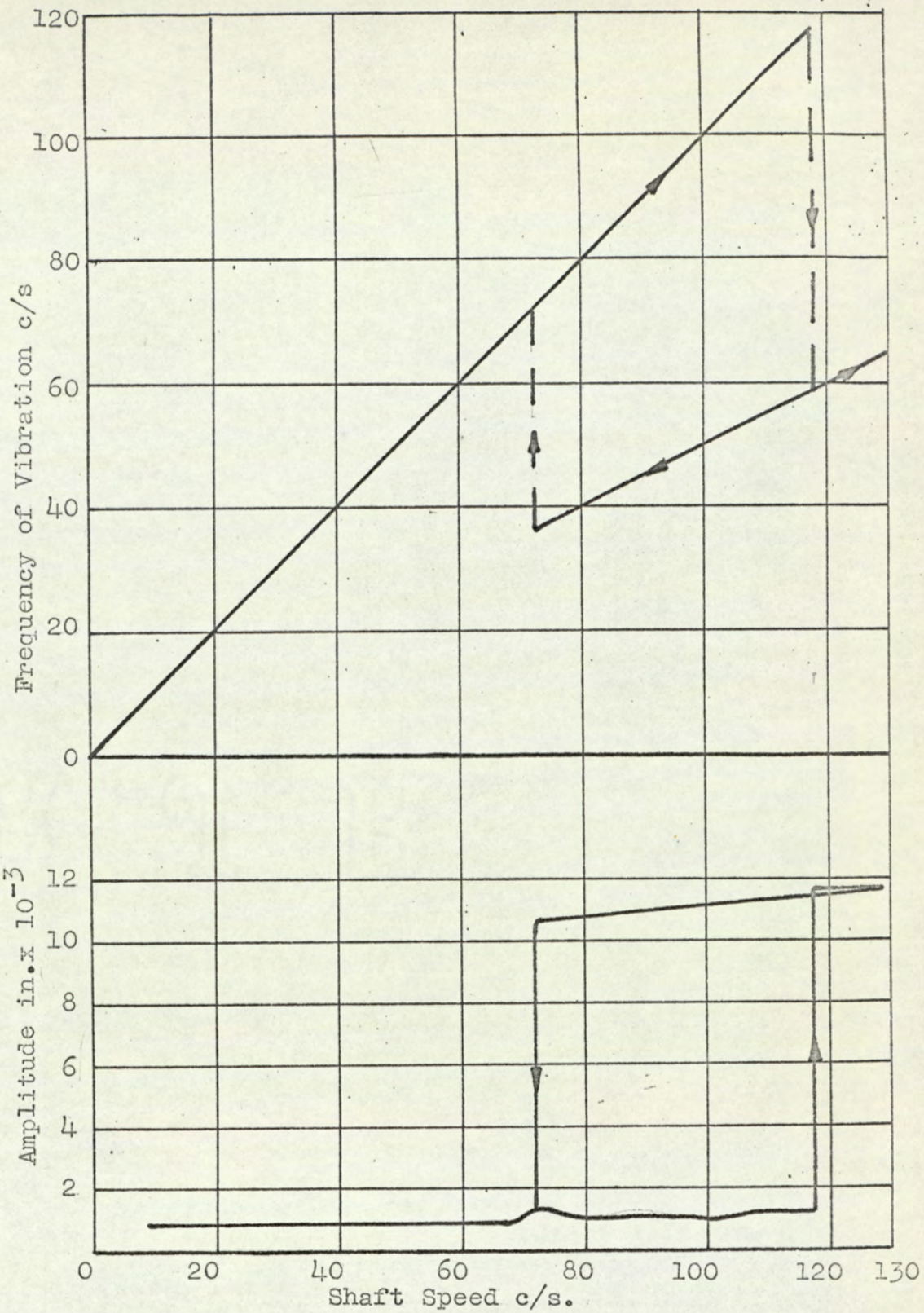

Amplitude and Frequency versus Shaft Speed

0.010 in. Diametral Clearance Bearing

FIG.36

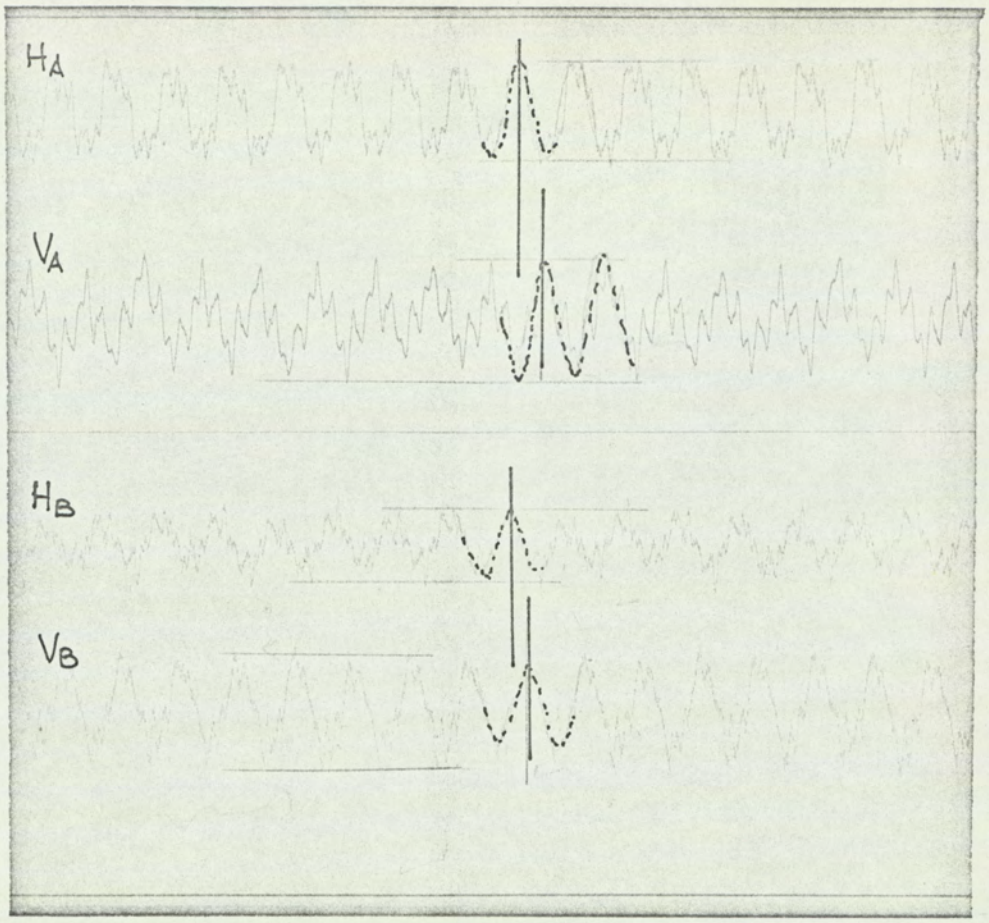

Waveforms Showing Reverse Whirl at 65 c/s.

FIG. 37

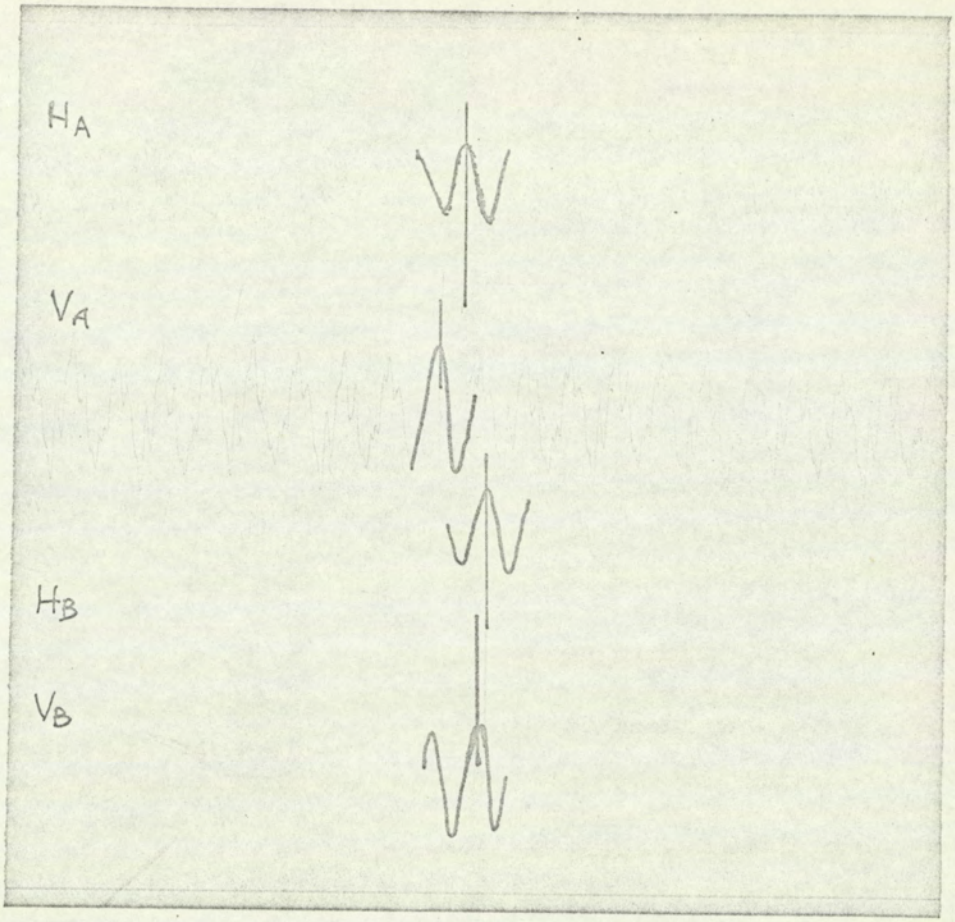

Waveforms Showing Forward Whirl at 85 c/s.

FIG. 38

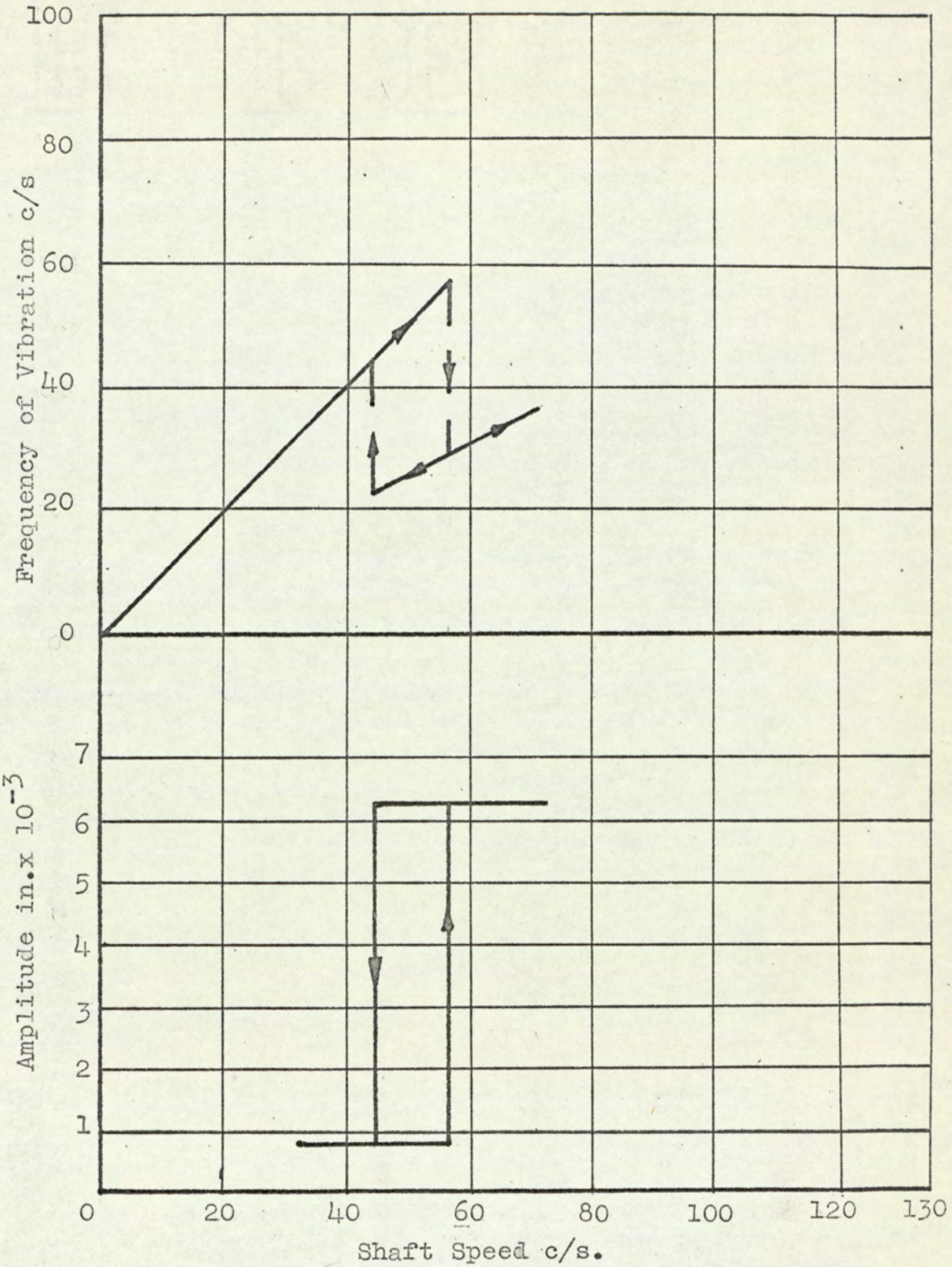

Amplitude and Frequency versus Shaft Speed
0.005 in. Diametral Clearance Bearing

FIG.39

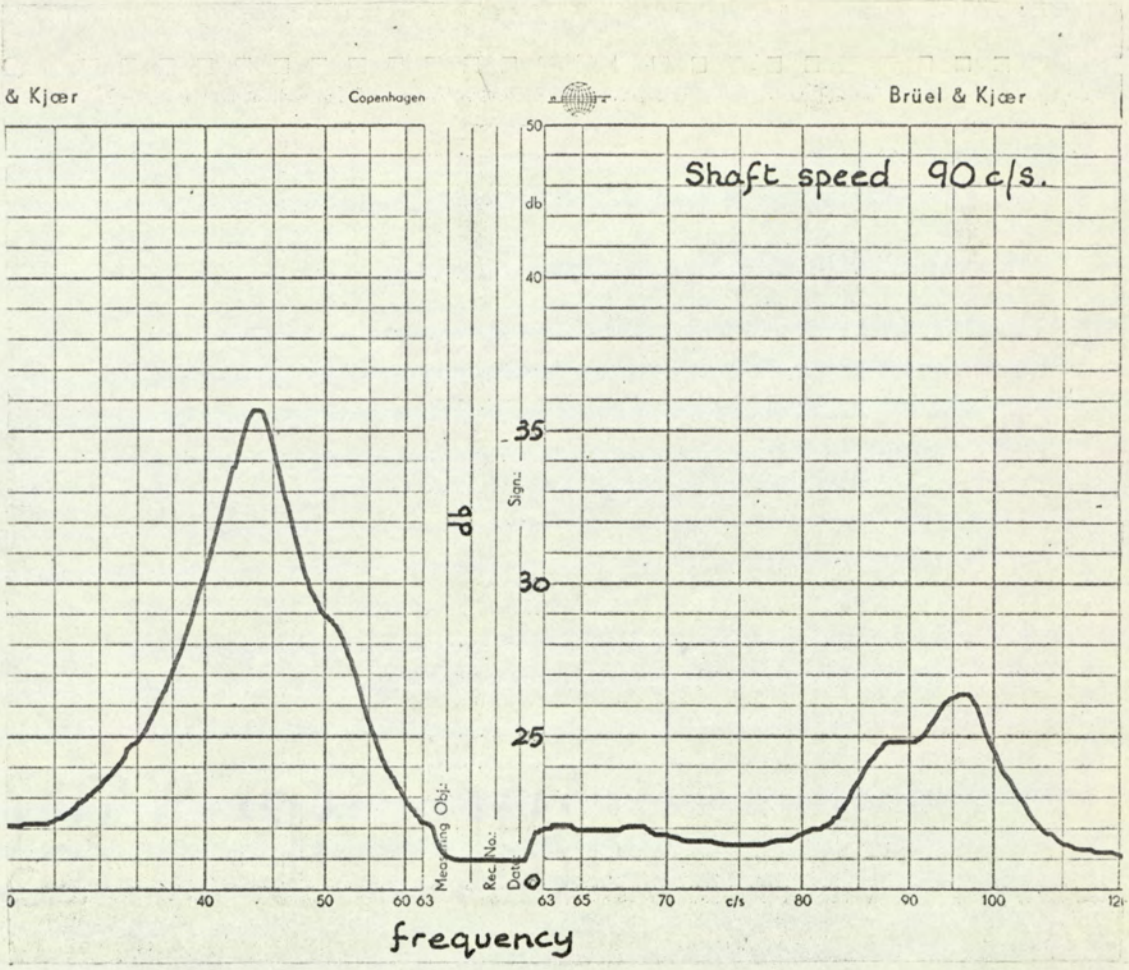

Frequency Analysis from Wave Analyser

FIG.40

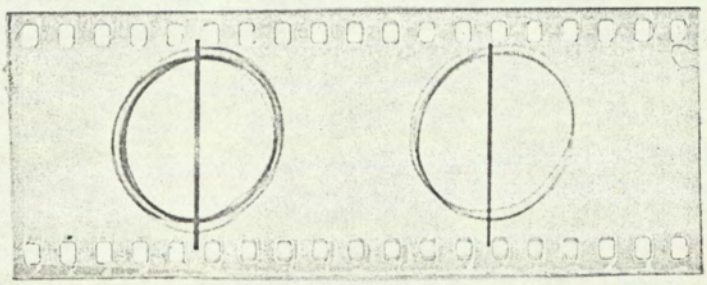

Rotor A

Rotor B

Whirling Motion of Rotor During Instability

(Shaft Speed 60 c/s.)

FIG. 41

Table III

Critical Speeds.

Brg. Clearance Diametral in.	Viscosity Reyns $x10^{-7}$		Measured Speed of Onset of Instability c/s	Calculated Speed of Onset of Instability c/s
	Brg. 1	Brg. 2		
0.003	50	53	64	60.6
0.005	75	78	110	112.6
	116	112	72.1	68.5
	108	117	71.2	69.4
	120	120	70.4	67.6
	142	140	64.5	62
	130	137	63.9	64.6
	180	165	49.2	50.3
0.010	276	290	117	122
	350	360	91.3	97.0
	412	448	76.9	80.0
	500	535	61.2	66.7
	640	680	50.4	52.5

Table IV

0.010	568		62.1	60.8
0.005		390		

APPENDICES.

Appendix I

The calculation of equivalent Weight of Shaft.

The energy method.

In this method an equivalent system is calculated having the same kinetic energy when vibrating transversely as the shaft-rotor system under consideration.

Let v be the transverse velocity at a given instant at the free ends of the shaft, and assume that the shape of the curve into which the vibrating shaft deflects, is the same as the static deflection curve of the shaft loaded at each end.

At a distance x from one end, the velocity is given by

$$V_{(x)} = V.\frac{y}{\delta} \qquad (1)$$

where y = deflection of shaft at position x

and δ = deflection of the shaft at the free ends.

The kinetic energy of an element of length dx is

$$K.E. = \frac{1wdx(v.y}{2g\ (\delta}\Big)^2 \qquad (w = \text{wt./ unit length}) \qquad (2)$$

and for the whole shaft the total kinetic energy is

$$K.E. = \frac{2wv^2}{2g\delta^2}\int_0^c y^2dx + \frac{wv^2}{2g\delta^2}\int_c^{l+c} y^2dx \qquad (3)$$

where 'c' represents the length of the overhung portion and 'l' represents the length between the supports.

From strength of materials

$$y = \frac{W}{6EI}\left(-x^3 + (x-c)^3 + (x-l-c)^3 + 3c(x+l) - c^2(3l+2c)\right)$$

and

$$\delta = -\frac{W}{6EI}\, c^2(3l+2c)$$

Upon substitution into and integration of equation (3) the total kinetic energy of the shaft becomes

$$K.E. = \frac{Wv^2}{2g.350(9l^2 + 12cl + 4c^2)}\, 2c(330c^2 + 33.35cl + 3.350l^2) + \frac{Wv^2}{2g.350(9l^2 + 12cl + 4c^2)}\, \frac{3.350l^5}{10c^2} \qquad (4)$$

The kinetic energy of a light shaft loaded at the free ends is

$$K.E. = \frac{2w}{2g} v^2 \qquad (5)$$

Equating equations (4) and (5) gives

$$W = w\, \frac{c\left(\frac{33}{35} c^2 + \frac{33}{10} l.c. + 3l^2\right) + \frac{3l^5}{20c^2}}{(9l^2 + 12cl + 4c^2)} \qquad (6)$$

= equivalent weight of shaft.

It should be noted that equation (6) is only applicable for a symmetrically supported shaft.

2. The Dunkerley Method.

Another method which is often easier to apply with relatively good results, is an extension of the Dunkerley empirical formula for a shaft carrying a number of loads.

Dunkerley's empirical formula is

$$\frac{1}{\omega^2} = \frac{1}{\omega_1^2} + \frac{1}{\omega_2^2} + - - - - - \qquad (1)$$

Applying this to the uniform beam shown in section 1 of this appendix, gives for a section distance x from the origin, width dx

$$\frac{1}{\omega_x^2} = \frac{w}{g} y_{xx}\, dx \qquad (2)$$

Where y_{xx} = deflection at x due to unit load there.
The natural frequency of the shaft is therefore given by

$$\frac{1}{\omega^2} = \frac{2W}{3EIg}\int_o^c x^2 (1+x)\, dx + \frac{W}{3EIg}\int_o^l x^2 (1-x)^2\, dx. \qquad (3)$$

the last term of R.H.S. of equation (3) is obtained by treating the centre span alone as a simply supported beam. Integrating equation (3) gives

$$\frac{1}{\omega^2} = \frac{2Wc^3}{36EIg}(4l + 3c) + \frac{Wl^4}{90EIg} \qquad (4)$$

For a massless shaft carrying an equal load at each end Dunkerley's formula gives as the natural frequency.

$$\frac{1}{\omega^2} = \frac{2W}{3EIg} c^2 (1+c) \qquad (5)$$

Equating equations (4) and (5) gives

$$W = \frac{W\ (c^3(41 + 3c)/\ 12 + l^4/60)}{c^2\ (1+c)}$$

A comparision between the equivalent weights obtained by the two methods is show in Fig. 42 Also shown are the equivalent tip loads treating the overhung portion as a cantilever beam and the equivalent central load when only the length of shaft between the bearings is considered. It is interesting to note that with the bearings set less than 8 in. apart, the equivalent tip load for the two rotor system lies close to the tip load calculated assuming the overhung portion to exist as a cantilever only. Above 8 in. bearing span the two curves deviate as the length of shaft between the bearings becomes more important and the overhung portion less so.

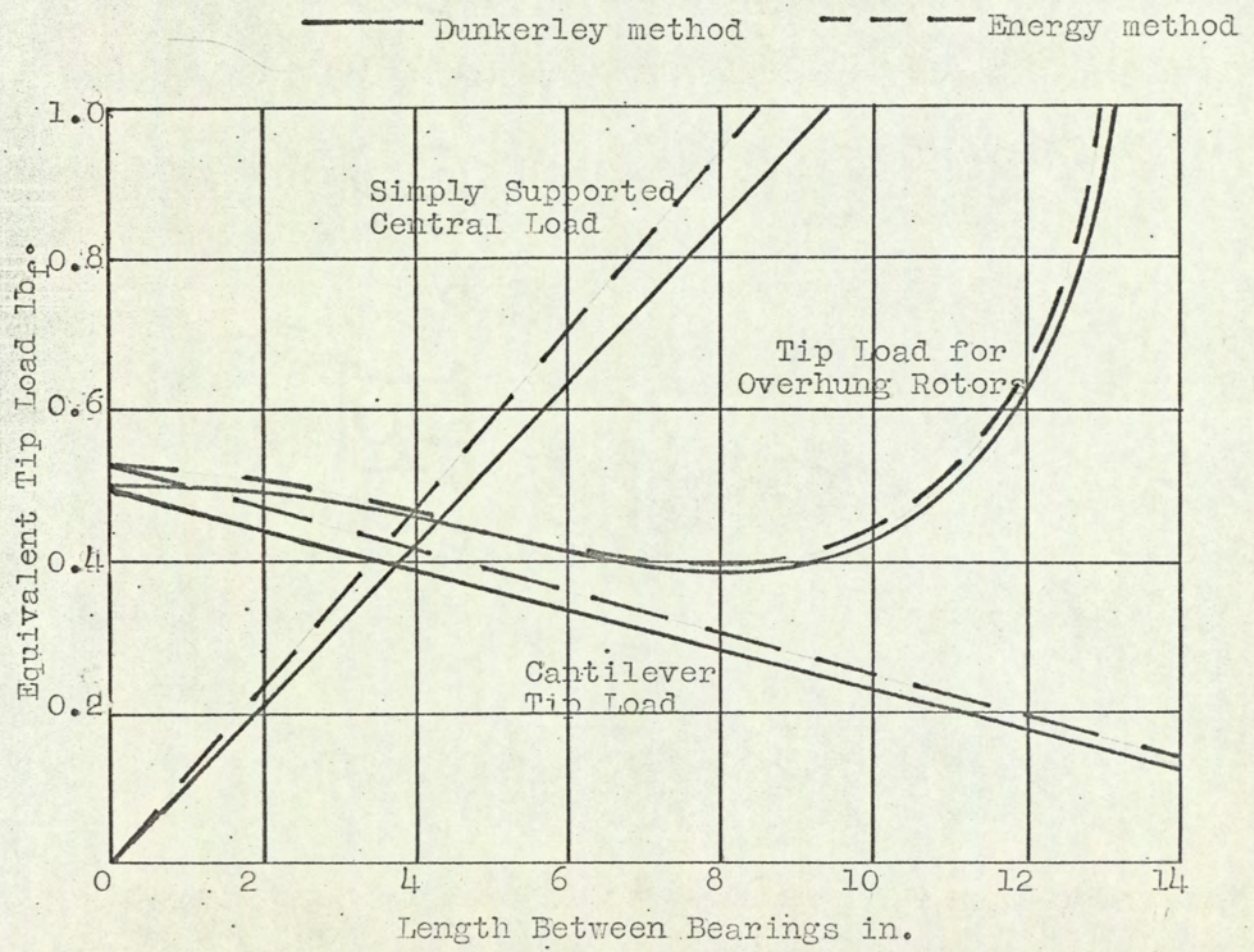

Equivalent Tip Load versus Bearing Span

FIG. 42

Appendix II

Details of Experimental Rig.

Length of Shaft	= 21.25 in.
Diameter of Shaft	= 1 in.
Weight of Shaft	= 4.375 lb_f
Diameter of Rotor	= 7 in.
Thickness of Rotor	= 1.25 in.
Weight of Rotor	= 13.375 lb_f
Length of Bearing	= 1 in.
Diameter of Bearing (Nominal)	= 1 in.

Deflexion Coefficients.

l = length between bearing centres.

c = length of overhang.

E = Youngs Modulus (30×10^6 lb_f/in^2).

I = Second Moment of Area.

$$y_{11} = y_{22} = c^2(c+l)/3EI$$
$$\Phi_{11} = \Phi_{22} = l+3c/3EI$$
$$z_{11} = z_{22} = c(2l+3c)/6EI$$
$$y_{12} = y_{21} = lc^2/6EI$$
$$\Phi_{12} = -\Phi_{21} = -l/6EI$$
$$z_{12} = -z_{21} = lc/6EI$$

Using appendix I and II the family of resonance curves Fig. 43 is plotted.

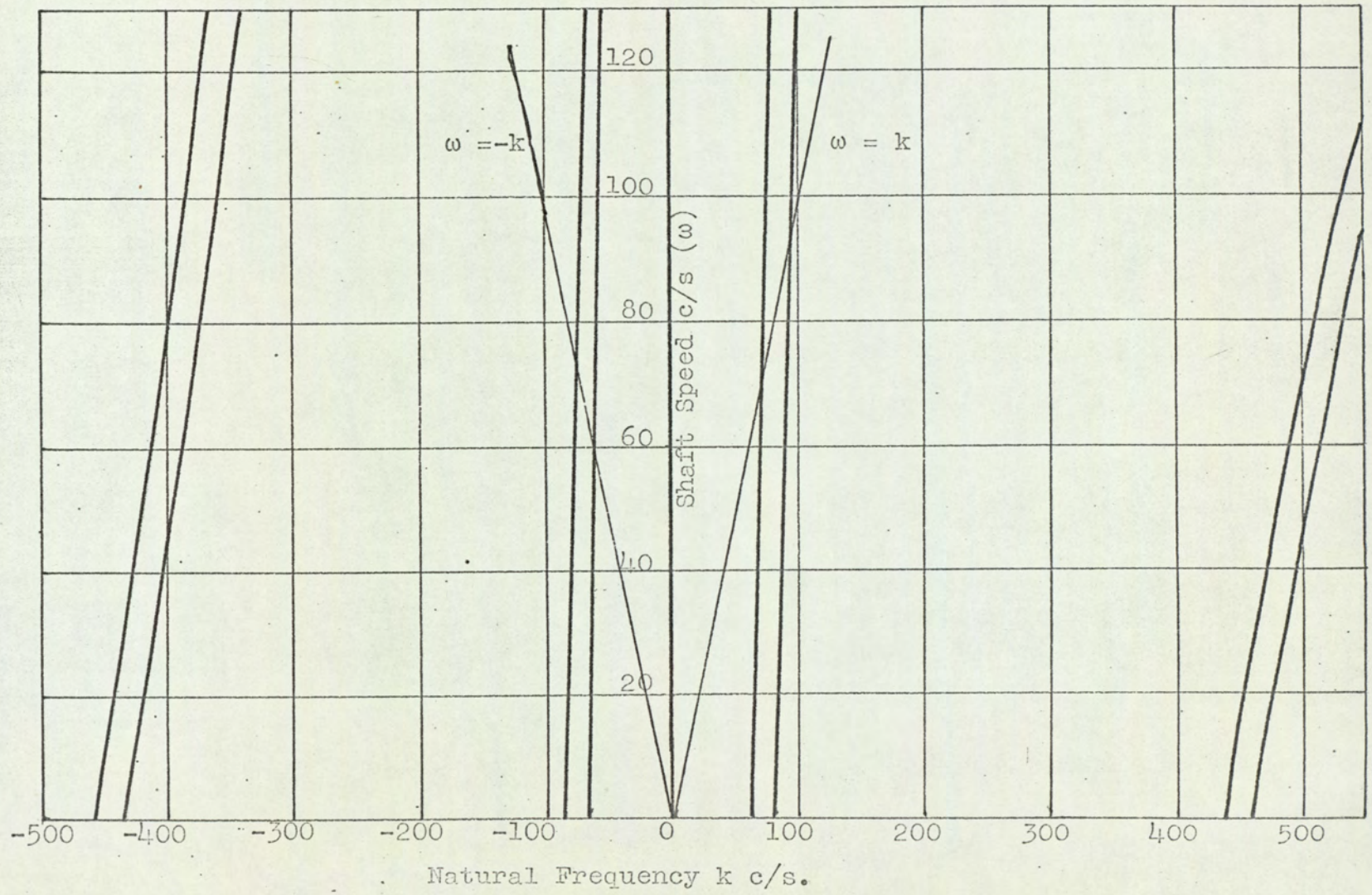

Shaft Speed versus Natural Frequency

FIG.43

Appendix III

Approximate Method of Determining Natural Resonance Curves of the Rigid Body Theory.

Because of the difficulty of obtaining representative resonance curves (as mentioned in Discussion of Rigid Body Theory) it was decided to represent the experimental system as an equivalent mass-spring system.

The equation of motion was determined, using the coupling spring coefficients found in Appendix IV, as

$$m\ddot{x} + k_1x - k_2x^2 - k_3x^3 + k_4x^4 = F \sin \omega t \qquad (1)$$

where F sin ωt represents the out-of-balance forcing function. The frequency-amplitude relationship of equation (1) of the harmonic natural free vibrations is

$$\omega^2 = \frac{k_1}{m} - \frac{4k_3}{3m} x^2 \qquad (2)$$

Using equation (2), the equivalent mass m was calculated from the experimental results for each bearing span, by inserting the value of the frequency of rotation of the first resonance when x=0 i.e.

$$m = \frac{k_1}{\omega^2} \qquad (3)$$

The frequency-amplitude relationship was then obtained for the harmonic resonance by calculating the values of

ω for given values of amplitude x from equation (2). Resonance curves for the sub-harmonic vibrations which are represented by an equation of the form

$$\left(\frac{\omega}{n}\right)^2 = \frac{k_1}{m} - \frac{4k_3x^2}{3m}$$

Where n is the order of the sub-harmonic vibration, were obtained by multiplying the frequencies of the harmonic resonance by the order of the sub-harmonic i.e.

$$\omega_2 = 2\omega_1$$

where ω_1 is the frequency of the harmonic resonance and ω_2 = frequency of half order sub-harmonic resonance. A family of resonance curves thus obtained is shown in Fig. 44

Family of Resonance Curves for 6 in. Bearing Centres.

FIG. 44

Appendix IV

Determination of the Coupling Spring Coefficients.

1. Without Rotation.

A photograph of the jig designed to enable the stiffness of the couplings to be measured is shown in Fig.(45). The two end plates are constrained to move parallel to each other so that the coupling only deflects due to shear forces. One plate is clamped to a solid foundation while the other is used as a means of loading the coupling. Weights are added to the plate in small increments and the deflection for each increment and the deflection for each increment of load noted. Tets were performed with the coupling in different angular position i.e. after one test the coupling was rotated and another test performed, to check for stiffness assymetry.

Fig.(10) shows the average curve or spring characteristic obtained by plotting load against deflexion.

By applying a curve fitting technique to the stiffness curve of coupling A used in Part One, a spring characteristic of form

$$k_1 x - k_2 x^2 - k_3 x^3 + k_4 x^4$$

was obtained, where

$$k_1 = 414 \text{ lb}_f/\text{in.}$$

$$k_2 = 2.618 \times 10^4 \text{ lb}_f/\text{in.}$$

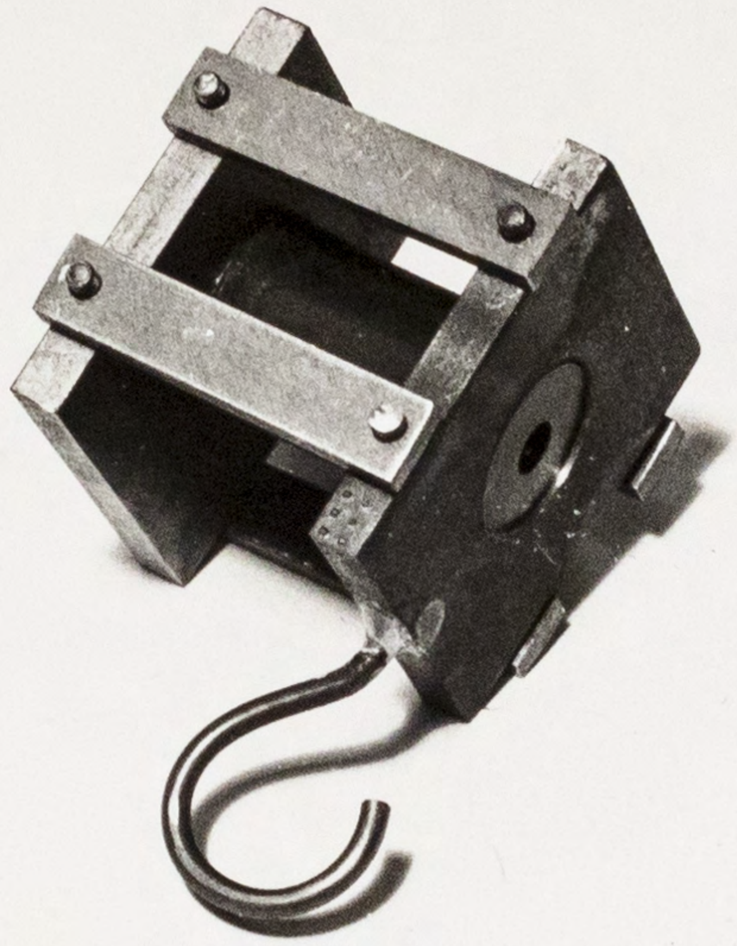

Jig for Stiffness Measurement of Couplings

FIG. 45

$$k_3 = 6.59 \times 10^6 \text{ lb}_f/\text{in.}$$
$$k_4 = 9.42 \times 10^9 \text{ lb}_f/\text{in.}$$

2. With Rotation.

Due to insufficient time it was not possible to determine the spring characteristics of the couplings when rotating. It was thought, that the characteristics obtained for the static case would suffice for qualitive explanation of the generation of sub-shaft speed resonances.

A method which at first sight seems suitable to determine the spring characteristics of the rotating couplings is to arrange for the coupling to be attached to an end of a drive shaft. The free end of the coupling is then supported by a spring balance attached to the outer race of a ball bearing, the inner race of which is fitted over the end of the coupling. The coupling can be loaded by weights, also attached to the outer race of the bearing, the deflection of which can be determined from a clock gauge. Two difficulties which could arise are,

1. Unbalance causing the coupling to vibrate, making accurate readings difficult to obtain.

and 2. Ensuring the free end of the coupling to deflect parallel to the fixed end.

APPENDIX V

Details of the Couplings

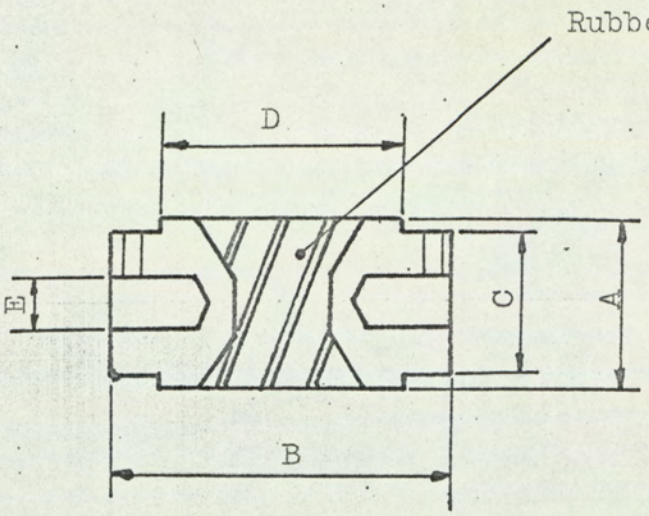

Coupling No.	A in.	B in.	C in.	D in.	E in.	H.P.@ 1500 R.P.M.
I	$\frac{15}{16}$	$1\frac{3}{4}$	$\frac{13}{16}$	$1\frac{1}{8}$	$\frac{1}{4}$	0.12
O	$\frac{3}{4}$	$1\frac{3}{4}$	$\frac{23}{32}$	$1\frac{1}{8}$	$\frac{1}{4}$	0.06

Appendix VI

Limiting Rotational Speed of System.

The bursting speed of the rotors are first calculated using a theory propounded for rotating thin disks and applying Tresca's yield criterion (see later) for failure of the rotors. A safety factor of 3 is applied to the bursting speed to give a speed which is considered to be the limiting speed of operation.

From the rotating thin disk theory, see page 286 of "Strength of Materials" by Ryder, the radial and hoop stresses at some arbitrary radius are:

radial stress $$p = \frac{\rho\omega^2}{8g} (3+\Delta) (R^2 - r^2)$$

hoop stress $$\delta = \frac{\rho\omega^2}{8g} R^2 (3+\Delta) - r^2(1+3\Delta)$$

where ρ = mass density lb/in^3.

ω = rotative speed rad/sec

R = outside radius of rotor in.

r = radius of section considered from axis of rotation in.

Δ = Poisson's ratio

g = 32.2 lb in/sec^2.

For a solid disk the maximum stresses occur at the centre i.e. r=0. Thus

$$\hat{p} = \frac{\rho\omega^2}{8g} (3+\Delta) R^2$$

$$\hat{\delta} = \frac{\rho\omega^2}{8g} (3+\Delta) R^2$$

A criterion of failure which gives good agreement with ductile materials, the rotors being of mild steel, is that due to Tresca. Now Tresca's yield criterion implies that failure will occur when the maximum shear stress 'q' in a complex system reaches the value of the maximum shear in simple tension at the elastic limit, i.e.

$$q = \frac{1}{2} (f_2 - f_1) = \frac{1}{2} f$$

where f_1, f_2 are the principal stresses
and f is the tensile stress at the elastic limited in simple tension.

Applying this criterion gives

$$f = \hat{p} = \hat{\delta}$$

thus $$f = \frac{\rho\omega^2 (3+\Delta) R^2}{8g}$$

Which upon inserting a value of 0.3 for Poisson's ratio and rearranging, leads to the following equation for the bursting speed,

$$N = \frac{84}{R} \sqrt{\frac{f}{\rho}} \qquad \text{R.P.M.}$$

Introducing the appropriate values for R, f and ρ gives

$$N = 28{,}800 \text{ R.P.M.}$$

The limiting speed is thus set at

$$N_L = \frac{28{,}800}{3} = 9600 \text{ R.P.M. or } 180 \text{ c/s}$$

Appendix VII

Design of Twin - T Filter

A twin - T, RC network is designed to filter a frequency of twice the frequency of a carrier signal viz. 6Kc/s. Using data given in a paper by D.R.Bocast (41) the following design was reached,

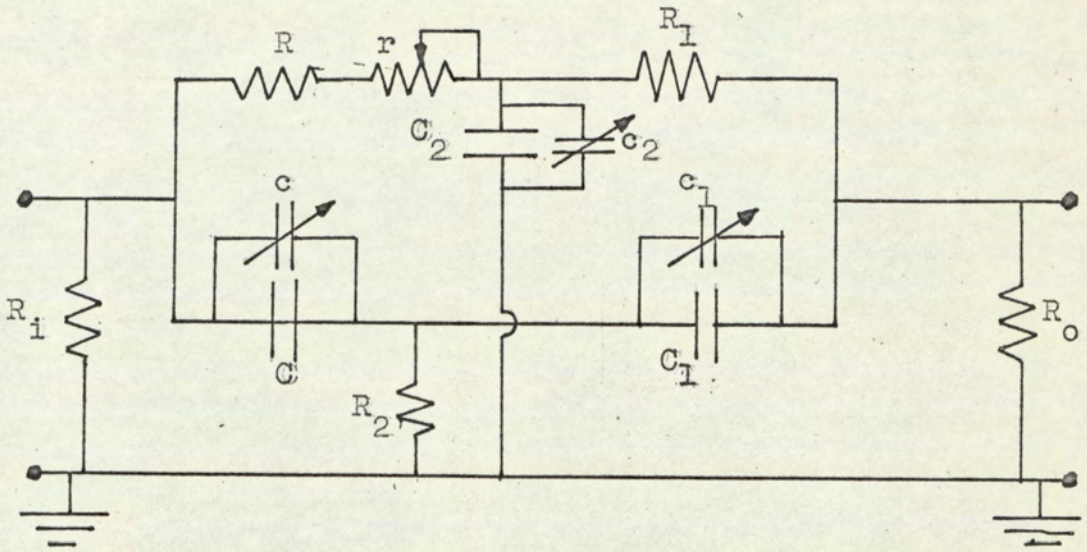

where	R_i = 100 KΩ	R_o = 1 MΩ
	R = 330 KΩ	r = 0 - 100 KΩ
	R_1 = 2.2 MΩ	R_2 = 43 KΩ
	C = 180 pF	c = 60 pF
	C_1 = 30 pF	c_1 = 15 pF
	C_2 = 60 pF	c_2 = 15 pF

The above filter was adjusted to give an attenuation of 66db at the rejection frequency.

Appendix VIIII

List of References.

No.	Author.	Title etc.
1	H.H. Jeffcott	"The Lateral Vibration of loaded shafts in the neighbourhood of a Whirling Speed. The Effect of Want of Balance". Phil.Mag.Vol.XXXVII March,1919.
2	Greenhill	"On the Stability of a Rotating Shaft Subject to Thrust and Twisting". Proc.I.Mech.E.April,1883.
3	C.Chree	"The Whirling and Transverse Vibrations of Rotating Shafts". Phil.Mag.Vol.7,1904.
4	S. Dunkerley	"On the Whirling and Vibration of Shafts". Phil.Trans. June,1897.
5	J.Morris	"The Strength of Shafts in Vibration". Crosby, Lockwood 1929.

No.	Author.	Title etc.
6	E.Downham	"Theory of Shaft Whirling" The Engineer., Nos.1, II, III, IV 1957
7	E.H. Hull	"Shaft Whirling as Influenced by Stiffness Asymmetry" Trans.A.S.M.E. May 1961.
8	J.G.Baker	"Self-Induced Vibrations" Trans.A.S.M.E. Vol.55 1933
9	C.A. Ludeke	"Predomintly Subharmonic Oscillations" Jour.App.Physics.Vol.22.No.11 November, 1951.
10	J.J. Stoker	"Nonlinear Vibrations" Interscience Publishers, Inc. New York.
11	A. Stodola	"Steam and Gas Turbines" McGraw-Hill Book Co., New York, 1927.

No.	Author.	Title etc.
12	J.P. Den Hartog	"Mechanical Vibrations" McGraw-Hill Book Co.,Inc. New York 1947. (3rd Edition)
13	R.B. Green	"Gyroscopic Effects on the Critical Speeds of Flexible Rotors". Trans. A.S.M.E. December, 1948
14	C.A. Schulte and R.A. Riester	"Effects of Mass Distribution on Critical Speeds."
15	A.Kimball Jr.	"Internal Friction Theory of Shaft Whirling". General Electic Review, April, 1924.
16	A.Kimball Jr.	"Measurement of Internal Friction in a Revolving Deflected Shaft" General Electric Review. Vol. XXVIII No 8. Aug.1925.

No.	Author.	Title etc.
17	D. Robertson	"Hysteretic Influences on the Whirling of Rotors"
18	B.L. Newkirk	"Shaft Whipping" General Electric Review, March, 1924.
19	E.Downham	"Theory of Shaft Whirling" The Engineer No II Oct,18 1957.
20	R L.Newkirk and Taylor	"Shaft Whipping Due to Oil Action in Journal Bearings" General Electric Review Vol. XXVIII, No.8. Aug.1925
21	D. Robertson	"Whirling of a Journal in a Sleeve Bearing". Phil.Mag.Vol.15,No.93, Jan.1933.
22	E.M.Simons	"The Hydrodynamic Lubrication of Cyclically Loaded Bearings". Trans.A.S.M.E. Vol.70,1950

No.	Author.	Title etc.
23	A.C.Hagg	"The Influence of Oil-Film Journal Bearings on the Stability of Rotating Machines". Jour. App. Mech. Trans.A.S.M.E. September, 1946.
24	A.C. Hagg and P.C. Warner	"Oil Whip of Flexible Rotors" Trans.A.S.M.E. October, 1953.
25	A.C. Hagg and Sankey	"Some Dynamic Properties of Oil-Film Journal Bearings with Reference to the Unbalance Vibration of Rotors" Jour.App.Mech.Trans.A.S.M.E. June, 1956.
26	D.F.Miller	"Forced Lateral Vibrations of Beams on Damped Flexible End Supports" Jour.App.Mech.Trans.A.S.M.E. Vol.75. 1953.

No.	Author.	Title etc.
27	H.Poritsky	"Contribution to the Theory of Oil Whip" Trans.A.S.M.E., Vol.75.1953
28	B.L. Newkirk	"Varieties of Shaft Disturbance Due to Fluid Films in Journal Bearings". Trans.A.S.M.E. July, 1956
29	O.Pinkus	"Experimental Investigation of Resonant Whip". Trans.A.S.M.E. Vol.78, 1956.
30	B.L.Newkirk and J.F. Lewis	"Oil-Film Whirl-An Investigation of Disturbances Due to Oil-Film in Journal Bearings. Trans A.S.M. Vol.78.1956
31	C. Hummel	"Kritische Drehzahlen als Folge der Nachgliebigkeit des Schmiemittels im Lager V.D.I."

No.	Author.	Title etc.
32	Y.Hori	"A Theory of Oil Whip" Jour.App.Mech. Trans.A.S.M.E. Vol. 81, 1959.
33	R. Holmes	"The Vibration of a Rigid Shaft on Short Sleeve Bearings". Jour.Mech.Eng.Science.Vol.2.
34	D. Morrison	"Influence of Plain Journal Bearings on the Whirling Action of an Elastic Rotor". Proc.Instn. Mech. Engrs. Vol. 76.No.22. 1962.
35	N.J. Huggins	"Non-Linear Modes of Vibration of a Rigid Rotor in Short Journal Bearings". Proc.Instn. Mech.Engrs.Vol.178 Pt.3N. 1964
36	C.C. Kennedy and C.D.P. Pancu	" Use of Vectors in Vibration Measurement and Analysis Jour. Aero. Science. Vol. 14, 1947

No.	Author.	Title etc.
37	R.E.D. Bishop and J.W. Pendered	"Note on Resonance Testing" Journ. Mech. Engrg. Science Vol.5 No. 4 1963.
38	D.D. Fuller and B. Sternlicht	"Preliminary Investigation of Minimum Oil-Feed Rates for Fluid-Film Conditions in Journal Bearings". Trans. A.S.M.E. Aug. 1956.
39	G.B. Dubois and F.W. Ocvirk	"Short Bearing Approximation for Plain Journal Bearings" Trans. A.S.M.E. Nov. 1955.
40	M.C. Shaw and E.F. Macks.	"Analysis and Lubrication of Bearings" McGraw Hill Book Co., New York 1949.
41	G.I. Taylor	"Stability of a Viscous Liquid Contained between Two Rotating Cylinders". Phil. Trans. series A, Vol. 223, 1923.

No.	Author.	Title etc
42	Barlow	"Lubrication of Bearings" Butterworth's Scientific Publications."
43	V.N. Constantinescu	"Analysis of Bearings Operating in Turbulent Regime". Jour. Basic Engrg. March, 1962.
44	D.R. Bocast	"Graphical Solution for Twin-T Networks" Electronics, June 17,1960.